



HAL
open science

Multimodal study of the interactions between the hepatitis B virus and the cyclic GMP-AMP synthase cGAS

Seung-Ae Yim

► **To cite this version:**

Seung-Ae Yim. Multimodal study of the interactions between the hepatitis B virus and the cyclic GMP-AMP synthase cGAS. *Virology*. Université de Strasbourg, 2017. English. NNT : 2017STRAJ041 . tel-02003380

HAL Id: tel-02003380

<https://theses.hal.science/tel-02003380v1>

Submitted on 1 Feb 2019

HAL is a multi-disciplinary open access archive for the deposit and dissemination of scientific research documents, whether they are published or not. The documents may come from teaching and research institutions in France or abroad, or from public or private research centers.

L'archive ouverte pluridisciplinaire **HAL**, est destinée au dépôt et à la diffusion de documents scientifiques de niveau recherche, publiés ou non, émanant des établissements d'enseignement et de recherche français ou étrangers, des laboratoires publics ou privés.

Ecole Doctorale des Sciences de la Vie et de la Santé ED414

UMR_S1110

Institut de recherche sur les maladies virales et hépatiques

THÈSE présentée par :

Seung-Ae YIM

Soutenue le : 12 Septembre 2017

Pour obtenir le grade de : **Docteur de l'Université de Strasbourg**

Discipline: Sciences de la Vie et de la Santé

Spécialité: Aspects Moléculaires et Cellulaires de la Biologie

Option: Virologie

**Multimodal study of the interactions between
the hepatitis B virus
and the cyclic GMP-AMP synthase cGAS**

THÈSE dirigée par :

Directeurs de thèse : Prof. Thomas F. BAUMERT, PU-PH, Université de Strasbourg, France

Dr. Catherine SCHUSTER, DR Inserm, Université de Strasbourg, France

RAPPORTEURS :

Rapporteur externe : Prof. Stéphane CHEVALIEZ, PU-PH, Université Paris-Est, France

Rapporteur externe : RN Dr. Ivan HIRSCH, DR CNRS, Charles University, République Tchèque

AUTRES MEMBRES DU JURY :

Examineur : Dr. Evelynne SCHAEFFER, CR CNRS, Université de Strasbourg, France

Examineur : Privatdozent Dr. Christoph NEUMANN-HAEFELIN, Freiburg University,
Allemagne

Acknowledgement

First of all, I am deeply grateful to my thesis supervisor, Prof. Thomas F. Baumert of the Université de Strasbourg, Inserm U1110 for guidance and support for my PhD study and research. He provided a lot of critical advice and suggested many important additions. It has been a greatly enriching experience to me to work under his guidance. I've learned a lot from his enthusiasm for science, encouragement of research, and hard-working attitude.

I also would like to express the deepest appreciation to my thesis co-supervisor, Dr. Catherine Schuster of Inserm U1110, for the continuous support of my PhD study and research. Her lot of detailed guidance helped me all the time for research and writing of manuscripts too. The door to Catherine's office was always open whenever I ran into a trouble or had questions not only about research but also about life. I appreciated all her contributions of time, ideas, and advice.

Many thanks to my thesis committee member, Prof. Stéphane Chevaliez, Dr. Ivan Hirsch, Dr. Christoph Neumann-Haefelin, and Dr. Evelyne Schaeffer, who give their precious time to participate in my thesis defense.

In regards to the project, I would like to offer my special thanks to Eloi Verrier. He not only gave me a lot of guidance for the experiments but also made contributions to the project and writing of the manuscript. I acknowledge Laura Heydmann, Charlotte Bach, Christine Thumann, and Laurent Mailly for doing experiments and providing technical supporting for my projects.

I would like to acknowledge honorary team members Emilie Crouchet, Carla Eller, Marie Parnot, Clara Ponsolles, and Vincent Turon-Lagot. I gave my special thanks to Hussein El Saghire, Nourdine Hamdane, Che Colpitts, Catherine Corbel, and Olga Koutsopoulos for their help and support. We were not only able to support each other by deliberating over our problem and finding, but also happily by talking about things other than just our work.

It is my pleasure to express my thanks to all colleagues at U1110 Vanesa Ayala-Nunez, Camille Clément, Cristina Dorobantu, Sarah Durand, Raphaël Gaudin, Katharina Herzog, Emilie Heuillard, Frank Jühling, Dominique Lecestre, Vincent Lucansky, Joachim Lupberger, Laurent Mailly, Marine Oudot, Andres Roca, Antonio Saviano, Sigismond Sliwinski, Patricia Wechlser, Florian Wrensch, and Anne Zeter for the friendship and support. I also thanks my previous colleague Antonina Fedorova who helped me to adapt to the lab although she has now left the lab.

My time here was made enjoyable in large part due to the colleagues that became a part of my life. Words are not enough to express my thanks to all colleagues and friends, who supported me without any conditions. And I also would like to thank Inserm, the University of Strasbourg, the LabEx HepSys and Région Alsace for providing me scholarships and excellent research environment.

Finally, I must express my very profound gratitude to my parents, my boyfriend, and to all my friends for supporting me and continuous encouragement through my years of study. Thank you very much, everyone! This accomplishment would not have been possible without you.

Table of contents

List of figures	7
List of tables	9
Abbreviations	10
I. INTRODUCTION.....	12
1. Pathophysiology of Hepatitis B virus infection.....	12
1.1. Liver disease and pathology of Hepatitis B virus.....	12
1.2. HBV infection worldwide	12
1.3. Pathogenesis of hepatitis B	13
1.4. Diagnosis of HBV infection	15
1.5. Therapy of chronic HBV infection.....	16
1.6. Vaccines against HBV infection	19
2. HBV molecular biology.....	20
2.1. HBV molecular virology.....	20
2.2. The hepatitis B virus	20
2.3. The HBV viral genome	21
2.4. The HBV transcripts.....	23
2.5. Function and characterization of HBV viral proteins.....	23
2.5.1. HBV envelope proteins, HBsAg	23
2.5.2. HBV core or capsid protein, HBcAg	24
2.5.3. HBV e antigen, HBeAg.....	25
2.5.4. HBV polymerase.....	26
2.5.5. HBV X protein, HBx.....	27
2.6. The viral replication cycle	28
2.6.1. HBV attachment and entry	29
2.6.2. cccDNA formation in the nucleus	30
2.6.3. Transcription of viral RNA	30
2.6.4. HBV pgRNA packaging and encapsidation.....	30
2.6.5. Production of viral particles	33
3. Host response to viral infection.....	33
3.1. Pattern recognition receptors	34

3.2. Nucleic acid sensing by TLRs.....	36
3.3. Cytosolic RNA sensing.....	38
3.4. Cytosolic DNA sensing.....	40
3.5. Identification and characterization of the cGAS-STING pathway.....	42
3.5.1. 2'3'-cyclic GMP-AMP synthase, cGAS.....	43
3.5.2. 2'3'-cGAMP.....	44
3.5.3. Role of the cGAS-STING pathway in pathogen infection.....	45
4. HBV experimental models.....	48
4.1. Primate models for the study of HBV infection.....	49
4.2. Mouse models for the study of HBV infection.....	49
4.3. Cell-based experimental model.....	51
4.3.1. Hepatoma-derived cell lines.....	51
4.3.2. NTCP-overexpressing cell lines.....	52
III. MATERIALS AND METHODS.....	56
1. Human-derived materials.....	56
2. Maintenance of cell lines and human hepatocytes.....	56
3. Reagents and plasmids.....	56
4. Small interfering RNAs for functional studies.....	57
5. Lentivirus production.....	57
6. Establishment of HepG2-NTCP-cGAS overexpressing cells.....	57
7. sgRNA design for CRISPR/Cas9.....	58
8. Validation of sgRNA by the Surveyor assay.....	58
9. Generation of <i>MB21D1</i> knock-out cells using CRISPR/Cas9.....	59
10. Analysis of gene expression using qRT-PCR.....	60
11. Protein expression.....	60
12. HBV purification and infection.....	61
13. Extraction of HBV rcDNA from HBV infectious particles.....	62
14. HBV cccDNA detection by Southern blot.....	62
15. Transcriptomic analysis using nCounter NanoString.....	63
16. HBV infection of human liver chimeric mice.....	66
17. Statistical Analysis.....	66
IV. RESULTS.....	67
1. cGAS expression in different cell types.....	67

2. Validation of the HepG2-NTCP cells as a model to study innate immune responses.....	68
3. Decrease in cGAS-, STING-, and TBK1 expression leads to an increase in HBV infection.....	69
4. Validation of sgRNA using Surveyor assay.....	71
5. Selection of cGAS KO cells generated by co-expressing plasmid system.....	72
6. Establishment of cGAS KO cell lines using the lentivirus transduction.....	73
7. Confirmation of the role of cGAS in the regulation of HBV infection.....	75
8. HBV infection fails to induce cGAS-related innate immune responses at early time points.....	78
9. HBV rcDNA is sensed by cGAS.....	80
10. HBV infection down-regulates cGAS-expression in cell culture.....	83
11. HBV infection represses the expression of cGAS-STING pathway related genes <i>in vivo</i>	85
V. DISCUSSION.....	89
VI. Résumé en français.....	95
VII. REFERENCES.....	105
ANNEX.....	125

List of figures

Figure 1. Countries with moderated and high endemicity for HBV infection	13
Figure 2. Natural history of chronic HBV infection	14
Figure 3. Typical serological courses of acute and chronic hepatitis B	16
Figure 4. The efficacy of approved anti-HBV drugs	18
Figure 5. Schematic representation of the different types of HBV infectious and noninfectious particles produced by HBV infected cells	21
Figure 6. Genetic organization of the HBV genome (genotype ayw)	22
Figure 7. Domain structure of HBV surface proteins	24
Figure 8. HBV core protein dimers depend on their activity	25
Figure 9. The crystal structure of HBeAg	26
Figure 10. The four domains of the HBV polymerase (genotype D)	26
Figure 11. The 3D structural model of HBV polymerase	27
Figure 12. HBV replication cycle	28
Figure 13. Model of HBV reverse transcription	32
Figure 14. Cellular PRRs	35
Figure 15. Endosomal Toll-like receptors specialized for RNA and DNA binding	37
Figure 16. Intracellular RNA sensing by RLRs	39
Figure 17. Pathways of type I interferon induction by intracellular DNA sensors and receptor signaling	42
Figure 18. cGAS-STING pathway for sensing of cytosolic DNA	43
Figure 19. The crystal structure of human cGAS	45
Figure 20. Development of HBV experimental models	48
Figure 21. HepG2, HepG2-NTCP cells, and PHH express cGAS	68
Figure 22. HepG2-NTCP cells express cGAS and induce <i>IFNB1</i> expression	69
Figure 23. The silencing of cGAS-related gene expression increases HBV infection	70
Figure 24. Representative gel image showing a typical Surveyor nuclease assay	71
Figure 25. Validation of cGAS KO cells generated by co-expressing plasmid system	72
Figure 26. Validation of pool cGAS KO cell lines	74
Figure 27. Validation of clonal cGAS KO cell lines	74
Figure 28. cGAS expression alters HBV infection	75
Figure 29. Detection of HBV cccDNA by Southern blot	77

Figure 30. HBV infection is associated with a very weak or absent innate immune response in cell culture ...	79
Figure 31. HBV genome exposure induce a cGAS-mediated innate immune response	81
Figure 32. Assembly-defective HBV mutants and <i>IFNB1</i> expression.....	83
Figure 33. HBV infection reduces cGAS-STING expression in infected HepG2-NTCP cells	84
Figure 34. Expression of cGAS-related genes is impaired by HBV infection <i>in vivo</i>	86
Figure 35. The expression of cGAS-related genes was quantified using the nCounter NanoString Technology and analyzed by GSEA	87

List of tables

Table 1. Hepatitis B virus infection serological markers, and their interpretation	15
Table 2. Approved drugs for treatment of hepatitis B; from reference (23)	17
Table 3. Innate immune signaling pathways suggested to be interfered by HBV viral proteins	38
Table 4. Viruses and intracellular DNA sensors	46
Table 5. Characterization of HBV infection in primary hepatocytes from different species expressing human NTCP	50
Table 6. Summary of current cell culture models for study HBV	53
Table 7. Selected sgRNA targeting <i>MB21D1</i>	58
Table 8. PCR primer list for Surveyor assay	59
Table 9. The list of probes to detect HBV cccDNA and mitochondrial DNA.....	62
Table 10. Specific probes for a set of cGAS-related genes	65
Table 11. cGAS expression in HBV infected human liver chimeric mice	88

Abbreviations

Anti-HBc	Antibodies to Hepatitis B virus core antigen
Anti-HBs	Antibodies to Hepatitis B virus surface antigen
CHB	Chronic hepatitis B
cccDNA	Covalently closed circular DNA
cGAMP	cyclic GMP-AMP
cGAS	cGAMP synthase
CRISPR	Clustered Regularly Interspaced Short Palindromic Repeats
CT-DNA	Calf thymus DNA
Ctrl	Control
DDX	DEAD/H box helicase protein
DIG	Digoxigenin
DNA	Deoxyribonucleic acid
dpi	day post-inoculation
ds	double-stranded
FDR	False Discovery Rate
HBeAg	Hepatitis B envelope antigen
HBsAg	Hepatitis B surface antigen
HBV	Hepatitis B virus
HCC	Hepatocellular carcinoma
HCMV	Human cytomegalovirus
NTCP	sodium/taurocholate cotransporting peptide
IFI16	Gamma-interferon-inducible protein 16
IFN	Interferon
ISGs	Interferon stimulated genes
kb	kilobase pairs
KO	Knock-out
KSHV	Kaposi sarcoma-associated virus herpesvirus
MDA5	Melanoma differentiation-associated protein 5
nd	non detectable
ORF	Open reading frame

PAMPs	Pathogen-associated molecular patterns
PCR	Polymerase chain reaction
pgRNA	pre-genomic RNA
PHH	Primary human hepatocyte
qRT-PCR	quantitative real-time polymerase chain reaction
RIG-I	Retinoic acid-inducible gene I
RNA	Ribonucleic acid
sgRNA	single-guide RNAs
siRNA	small interfering RNA
ss	single-stranded
STING	Stimulatory of interferon genes
TBK 1	TANK Binding Kinase 1
TLRs	Toll-like receptors

I. INTRODUCTION

1. Pathophysiology of Hepatitis B virus infection

1.1. Liver disease and pathology of Hepatitis B virus

The liver is a key organ within the human body by, playing many crucial roles, including detoxification and metabolism of proteins, lipids, and carbohydrates. Hepatitis or inflammation of the liver, can be caused by infection of hepatotropic viruses, such as hepatitis A, hepatitis B, hepatitis C, hepatitis D, and hepatitis E viruses. While many of these virus infections are acute and self-limiting, hepatitis B and hepatitis C virus infection can lead to chronic hepatitis and cause severe liver disease, including cirrhosis and hepatocellular carcinoma (HCC) (1, 2). Among these viruses, hepatitis B virus (HBV) is a DNA virus belonging to the *Hepadnaviridae* family. The classification is based on the small size of the viral genome, the unique viral replication strategy differing from other known viruses (1).

1.2. HBV infection worldwide

Approximately, two hundred fifty seven million people are chronically infected by HBV worldwide (3, 4). HBV infection results in either acute or chronic hepatitis (1). While 95% of HBV-infected adults will spontaneously resolve infection, 80-90% of neonates infected with HBV develop chronic infection (5). Progression of chronic HBV infection (CHB) can lead to end-stage liver disease such as liver cirrhosis and/or hepatocellular carcinoma (6, 7). CHB is defined as the detection of hepatitis B surface antigen (HBsAg) in serum for 6 month following infection. Although a highly effective vaccine has been established (8), HBV infection still remains a major health problem worldwide.

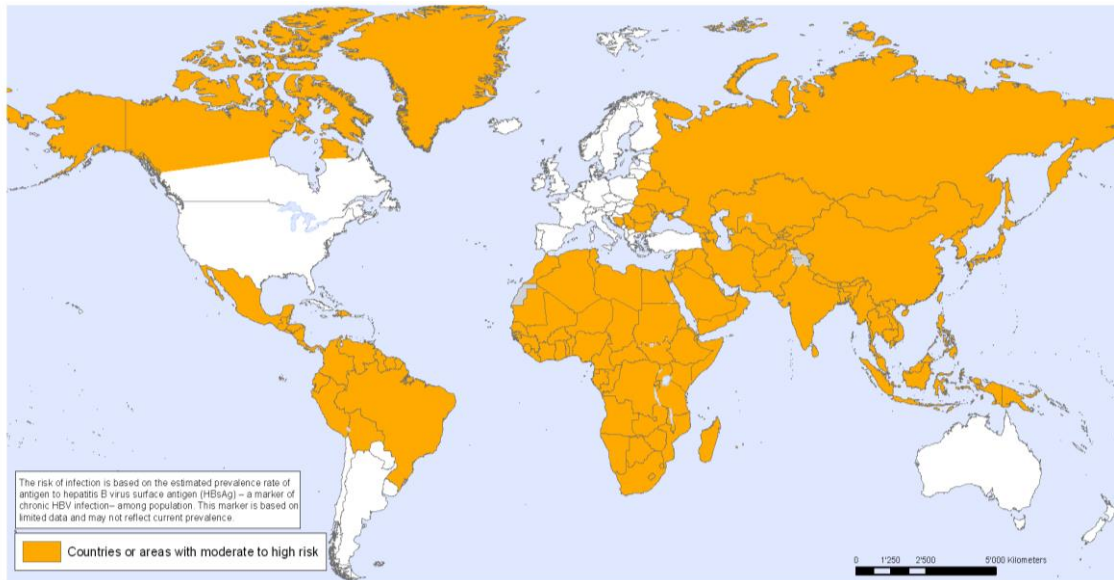


Figure 1. Countries with moderated and high endemicity for HBV infection

(Downloaded from [Oxford Medicine Online](http://gamapserv.who.int/mapLibrary/Files/Maps/Global_HepB_ITHRiskMap.png). Reproduced with permission from World Health Organization, *Hepatitis B, Countries or Areas at Risk*, Copyright © WHO 2012, Non-estimated area marked as gray color. http://gamapserv.who.int/mapLibrary/Files/Maps/Global_HepB_ITHRiskMap.png)

1.3. Pathogenesis of hepatitis B

HBV infects essentially the human liver. It is transmitted horizontally by exposure to infectious blood or body fluids i.e. saliva, menstrual, vaginal, and seminal fluids. However, perinatal vertical transmission is the major route of HBV transmission to neonates in the world (2).

The incubation period of HBV infection varies from 3 to 18 days. Acute infection can be associated with jaundice and several symptoms such as loss of appetite, joint and muscle pain, low-grade fever, and possible stomach pain (2). The vast majority of acute HBV infected patients will resolve infection within six months. After six months, the risk to develop CHB is highly increased. CHB is mainly asymptomatic.

After HBV ingress into the body it reaches the liver, where it infects hepatocytes. Recognition of HBV infection by Kupffer cells in the liver has been shown to activate NF-κB and proinflammatory cytokine production (9). In contrast to other viral infections, the innate immune response is not strongly triggered by HBV infection (10-12). In the infected adults, the adaptive

immune response contributes to viral clearance and prevention of viral spread during HBV infection (10). In contrast, impaired cellular immune responses such as, immunological tolerance, mutational inactivation of B-cell and T-cell epitopes, or incomplete down-regulation of viral replication and infection in immunologically privileged tissues are observed in chronic infection (13).

The natural history of CHB infection consists of four phases, the immune tolerant phase is characterized by the presence of hepatitis e antigen (HBeAg), accompanied by a high level of HBV DNA (> 2,000 IU/ml) but normal level of alanine aminotransferase (ALT) in patient serum (1). Most of patients in this phase have minimal liver injury and slow risk of developing HCC. The immune clearance phase has a similar pattern as the immune tolerant phase. However, ALT levels are intermittently increased and inflammation is activated in the liver. The inactive (carrier) phase is characterized by the absence of HBeAg, but the presence of anti-HBe antibodies. The level of ALT is normal and HBV DNA level is low or undetectable in serum. The reactive phase (also known as HBeAg-negative CHB) is defined by the absence of HBeAg, the presence of anti-HBe, intermittently or persistently elevated serum HBV DNA and ALT levels, and active inflammation in the liver (14, 15). Most of patients in this phase are older and have more advanced liver disease (8).

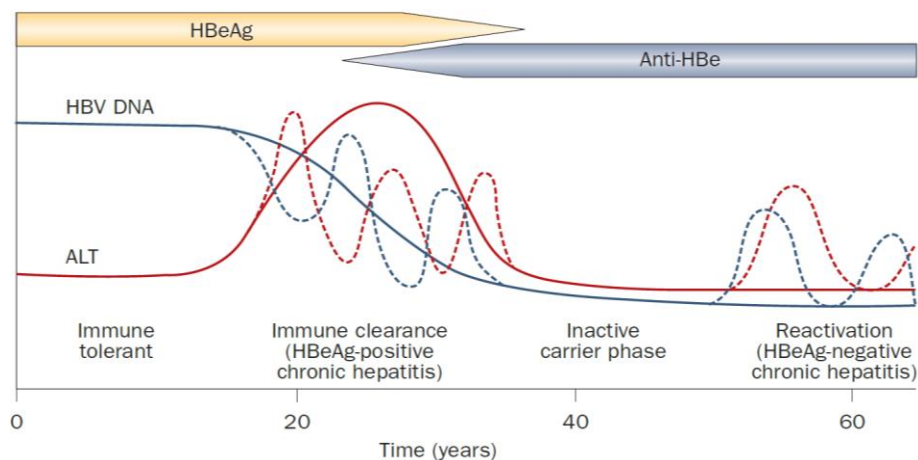


Figure 2. Natural history of chronic HBV infection

The profile of natural CHB infection in patients consists of four phases: the immune tolerant phase, the immune clearance phase, the inactive (carrier) phase, and the reactivation phase. See text for more details (14).

1.4. Diagnosis of HBV infection

The diagnosis of HBV infection is accomplished by evaluating clinical, biochemical and serological markers. **Table 1** gives an overview of the serological markers used in diagnosis of HBV and their interpretation.

Table 1. Hepatitis B virus infection serological markers, and their interpretation

HBsAg	HBeAg	HBcAg IgM	HBcAg IgG	Anti-HBe	Anti-HBs	Interpretation
POS	NEG	NEG	NEG	NEG	NEG	Incubation period
POS	POS	POS	POS	NEG	NEG	Acute infection
POS	NEG	NEG	POS	NEG	NEG	HBV infection (acute or chronic HBV infection)
POS	NEG	NEG	POS	NEG/POS	NEG	Chronic HBV infection or end of recent infection
NEG	NEG	POS	POS	NEG	NEG	Recent HBV infection. Beginning of the convalescence period
NEG	NEG	NEG	POS	NEG	NEG	Past HBV infection (immunological window)
NEG	NEG	NEG	POS	POS	POS	Immune, recent past infection
NEG	NEG	NEG	POS	NEG	POS	Immune, past infection (old infection)
NEG	NEG	NEG	NEG	NEG	POS	Immune, contact HBsAg, vaccine response
NEG	NEG	NEG	NEG	NEG	NEG	Susceptible individual. Never had contact with HBV

Abbreviations used in this table: POS, positive; NEG, negative; from reference (16)

HBsAg is the first serological marker HBV infection. The detection of HBsAg correlates with active viral replication. Thus, it usually drops to an undetectable level in patients who clear the virus and persists in chronically infected patients (17). Other markers including hepatitis B e antigen (HBeAg) and IgM antibody to hepatitis B core antigen (anti-HBc) are also routinely detected in acute and chronic infected patients. HBeAg is detected in the early phase of HBV infection and is a marker of active viral replication. Clearance of HBeAg and appearance of anti-HBeAg, known as e seroconversion, is related to decline of viremia and viral clearance. Persistence of HBeAg is observed in patients who develop CHB (18). The level of IgM anti-HBcAg gradually declines, often becoming undetectable within 6 months (19, 20). Meanwhile, the serum ALT and aspartate aminotransferase (AST) level can be elevated after the acute infection phase.

Chronic infection exhibits a similar serological profile as acute infection during the first weeks following infection. However, it is considered when HBsAg persists longer than six months and detectable viral DNA in patient's serum (18). The serological profile of progression to acute (A) and chronic (B) HBV infection is shown in **Figure 3**.

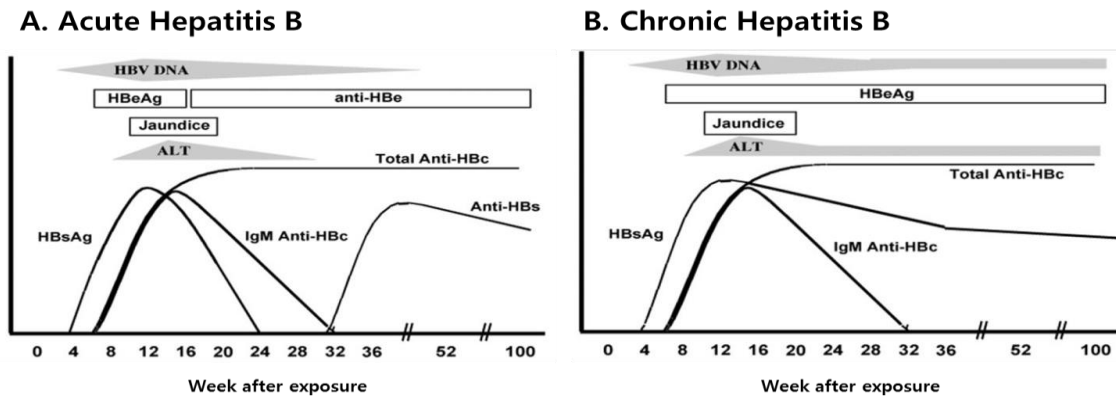


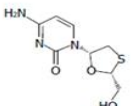
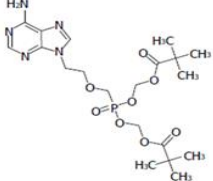
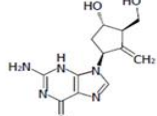
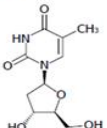
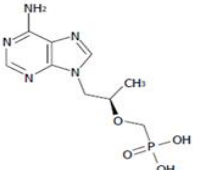
Figure 3. Typical serological courses of acute and chronic hepatitis B

(A) Typical serologic course of acute HBV infection. **(B)** Typical serologic course of acute infection with development to chronic HBV infection (21).

1.5. Therapy of chronic HBV infection

Clinically approved treatments for CHB infection include nucleos(t)ide analogues (NAs) and interferon alpha (IFN α) based combination therapies (22, 23). NAs consists of three structural groups: L-nucleosides (lamivudine) and alkyl phosphonates (telbivudine, adefovir and tenofovir), and D-cyclopentanes (entecavir) (24). The first treatment of CHB infection was IFN α -based treatment, which has both antiviral activity and immune-stimulatory properties (23). In individuals with HBV infection, pegylated-IFN α treatment is more effective than standard treatment of IFN α due to improved pharmacokinetic properties. Furthermore, combination treatment of pegylated-IFN α with NAs improves serological responses compared with monotherapy (23). However, these treatments do not provide complete cure since the virus persists in the nucleus of the infected cells. Moreover, these treatments have limitations, such as multiple side effects, drug resistance, and high cost for treatments of chronically infected patients (14, 24, 25). Thus, new strategies for efficient virus eradication and cure are urgently needed. An improved understanding of the viral life cycle and virus-host interactions may allow for such novel strategies to be developed. The clinically approved anti-HBV drugs are shown in **Table 2**.

Table 2. Approved drugs for treatment of hepatitis B; from reference (23)

Name	Trade name	Strong points	Weak points	Approved	Chemical structure
Interferon alpha-2b and pegylated interferon 2a	Intron A Pegasys	Finite duration of treatment Durable response post-treatment No known resistance	Needle injection High cost 65%-70% fail to respond Significant side effects	1991 2005	Human leukocyte clone
Lamivudine	Epivir (Zeffix)	Oral Safe with negligible side effects Effective and safe in pregnancy Least expensive	Long term treatment is necessary High incidence of resistance	1998	
Adefovir dipivoxil	Hepsera	Oral Low resistance	Long term treatment is necessary Long term treatment renal toxicity Less potent than other treatments	2002	
Entecavir	Baraclude	Oral Potent viral suppression Safe with negligible side effects Low resistance	Long term treatment is necessary High cost	2005	
Telbivudine	Tyzeka	Oral Potent viral suppression Effective and safe in pregnancy	Long term treatment is necessary High incidence of resistance	2006	
Tenofovir	Viread	Oral Potent viral suppression Safe with negligible side effects No known resistance for 6 years' study Effective and safe in pregnancy	Associated with osteopenia Long term treatment is necessary	2008	

As shown **Figure 4**, most NAs effectively suppress HBV replication through inhibition of HBV DNA polymerase activity. Thus, antiviral therapy with NAs is the first-line of treatment for CHB patients. However, resistance to NAs treatments appears following discontinuation of treatment and/or long-term use of NAs. For instance, HBV polymerase mutations in the YMDD motif, cause resistance to lamivudine treatment (23, 26). Moreover, current NAs do not directly target cccDNA (27), resulting in cccDNA persistence in the nucleus of the infected cell. Therefore, not only design correct combination therapies to prevent the progression of liver disease by HBV infection but also development of new therapeutic targets to prevent resistance are required.

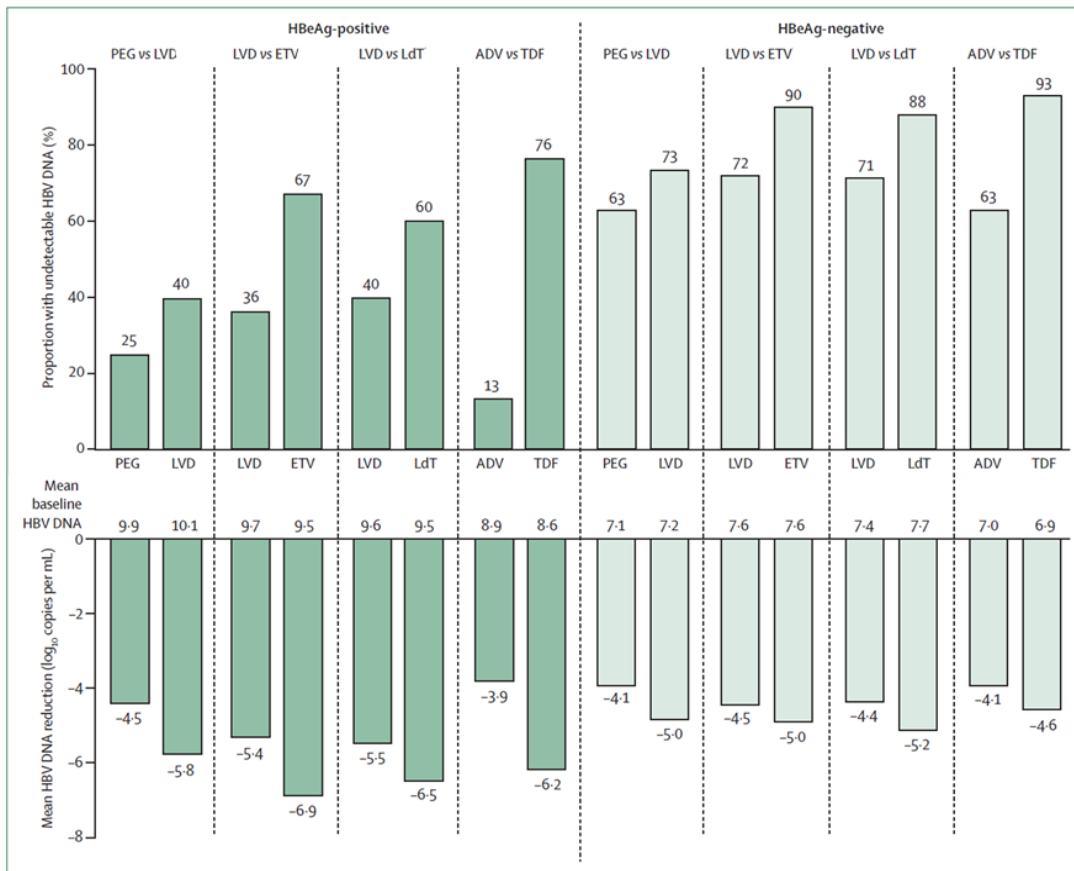


Figure 4. The efficacy of approved anti-HBV drugs

Comparison of rates of viral suppression and mean baseline hepatitis B virus DNA levels (log₁₀ copies per mL) at 1 year from clinical studies of pegylated IFN α -2a, lamivudine, adefovir, telbivudine, tenofovir, and entecavir that enrolled nucleos(t)ide-analogue-naïve HBeAg-positive and HBeAg-negative patients; from reference (24). *Abbreviations for this figure: PEG, pegylated interferon alfa-2a; LVD, lamivudine; ETV, entecavir; ADV, adefovir; LdT, telbivudine; TDF; tenofovir.*

An end stage therapeutic option for HBV-induced cirrhosis and cancer is liver transplantation. In general, patients awaiting liver transplantation will be treated with NAs to reduce progression of disease and to prevent potential flares of hepatitis. After liver transplantation, reinfection of the graft is systematic. Indeed, complete eradication of HBV is extremely rare because HBV persist in blood (28-30). Thus, new lifelong antiviral therapy and immunosuppressive treatments are needed for preventing recurrent hepatic flares.

Hepatitis B immune globulin (HBIG), a pool of human immunoglobulins, efficiently prevents HBV infection after liver transplantation. It has been reported that recurrence rate in HBsAg positive patients undergoing liver transplantation with treatment of HBIG was significantly reduced compared with non-treated patients (31). However, its costs for regular injection, and mutation of viral epitope occurs can lead to immune escape (32). Treatment of NAs reduces the recurrence rate after liver transplantation (33, 34). However, transplanted patients presented a higher rate (up to 70%) of drug resistance after 5 years in therapy (35, 36).

1.6. Vaccines against HBV infection

Vaccination is the most effective method for preventing new HBV infection, and it is widely used in the world. Although HBV is transmitted at a high rate by parenteral, percutaneous and sexual contact, HBV vaccine effectively prevents against HBV infection. The WHO recommended that all countries introduce universal hepatitis B vaccination. Consequently, many countries have shown a decrease in the HBV carrier rate and HCC incidence after the introduction of immunization campaigns (37).

The first clinical trials for plasma-derived HBV vaccine were conducted in 1982, when purified serum derived particles were used after viral inactivation by urea, pepsin, and heat (38). Thereafter, recombinant HBV vaccines were developed by overexpressing the HBV surface antigen in yeast. This vaccine is still widely used today. Third generation of vaccines are based on a mammalian cell-derived recombinant system overexpressing the viral preS region, which is important for viral binding on the cell surface. This vaccine should be more efficient than previous vaccines, but it is not widely used. Despite the global high efficacy of HBV vaccination, universal vaccination (UV) programs have not been adopted yet in several countries. It has been reported that approximately 10% of vaccinated people fail to mount an efficient immune response after completing vaccination (39). Moreover, one risk persists, since HBV in vaccinated subjects may develop mutations, allowing escape from immune responses induced by vaccination (39).

2. HBV molecular biology

2.1. HBV molecular virology

The *Hepadnaviridae* family includes DNA viruses causing hepatitis in a various number of hosts. The family includes two genera, avihepadnaviruses and orthohepadnaviruses (40). Their host range is restricted to either birds or mammals, respectively (1). Whereas, the avihepadnaviruses are transmitted by vertical routes, orthohepadnaviruses spread by horizontal transmission. The genome size of orthohepadnavirus is bigger than that of the avihepadnavirus. In general, these viruses have narrow host ranges, and infection leads to variable outcomes (1).

Avihepadnaviruses exclusively infect birds (41); these include duck hepatitis B virus (DHBV) and heron hepatitis B virus (HHBV). Recently, parrot hepatitis B virus (PHBV) (42) was identified as an avihepadnavirus. Orthohepadnaviruses infect mammals (43, 44), including humans, bats, rodents, and primates. Notable examples include, HBV, woodchuck hepatitis virus (WHV), ground squirrel hepatitis virus (GSHV) and woolly monkey hepatitis virus (WMHV). 1 genotypes have been described for HBV.

2.2. The hepatitis B virus

HBV is one of the smallest human DNA viruses. It is a 42-47 nm enveloped virus also called Dane particles (45) (**Figure 5**). Dane particles are actual infectious particles which contain the partial double-stranded (ds) HBV genome and the viral polymerase (46, 47). The basic unit of the capsid is formed by dimerization of two core proteins. HBV capsids present an icosahedral symmetry formed of 120 dimers. The capsid is surrounded by the viral envelope from reticulum endoplasmic origin, in which are embedded the three viral envelop proteins HBsAg, i.e. the small (S), middle (M) and the large (L) HBsAg. These transmembrane proteins share the C-terminal domain corresponding to the S protein, but differ in their N-terminal domains. The N-terminal domain of L-HBsAg is called preS1, while the N-terminal domain of M is called the preS2 domain. The preS1 domain is involved in HBV binding to the surface of the human hepatocyte (48, 49). In addition HBeAg is present between the viral envelop and the capsid.

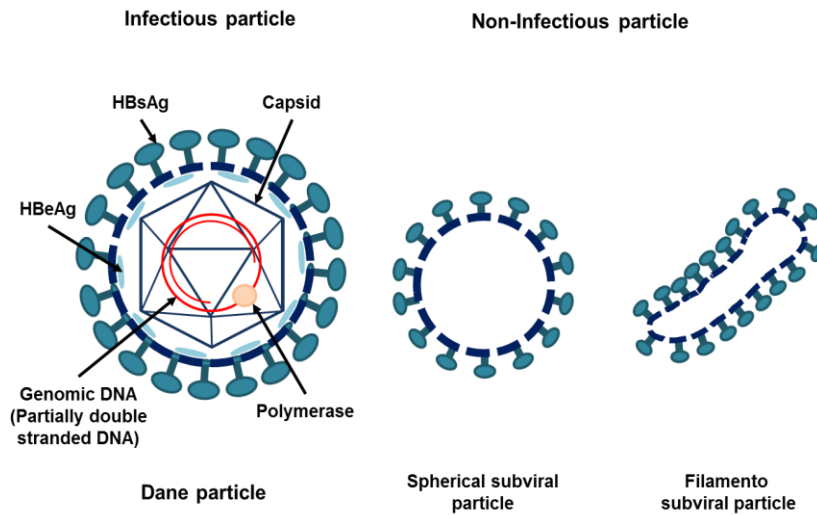


Figure 5. Schematic representation of the different types of HBV infectious and noninfectious particles produced by HBV infected cells

The infectious HBV particle also known as Dane particle (left). The genome consists of a partially dsDNA genome bound to the viral polymerase encapsulated in the capsid. Two different forms of subviral particles lacking the nucleocapsid are presented (right). Figure not according to the scale. *Abbreviations used in this figure: HBeAg, HBV envelop antigen; HBsAg, HBV surface antigen.*

Unlike other viruses, HBV virus-infected cells produce noninfectious subviral particles (SVPs) (**Figure 5**). These empty spherical or filamentous SVPs, composed only of a lipid membrane and HBsAg, are approximately 22 nm in diameter but differ in their length (50). SVPs differ from infectious viral particles by their ratio of L-, M- and S-HBsAg (51). The 22 nm of spherical particles are produced in excess, more than the Dane particle. Due to lack of the nucleocapsid containing viral genome and polymerase, they thus are noninfectious particles (52).

2.3. The HBV viral genome

The genome of HBV consists of approximately 3.2 kb of partially circular dsDNA (known as relaxed circular, rcDNA) with the non-ligated minus-strand covalently linked to the viral DNA polymerase (53). This compact genome encodes 4 open reading frames (ORFs) that are partially overlapping. This allows the virus to replicate autonomously with minimal genome information. The complete minus-strand is the template for transcription. The incomplete plus-strand will be

completed in the infected cells to form the cccDNA. It is about two-thirds complete for HBV, almost complete for DHBV (47, 54).

The genomic sequence presents at the 5' terminus of each strand, direct repeat (DR) sequences that are complementary and help to maintain the configuration as a circular DNA (55). DRs are important for priming viral replication (56).

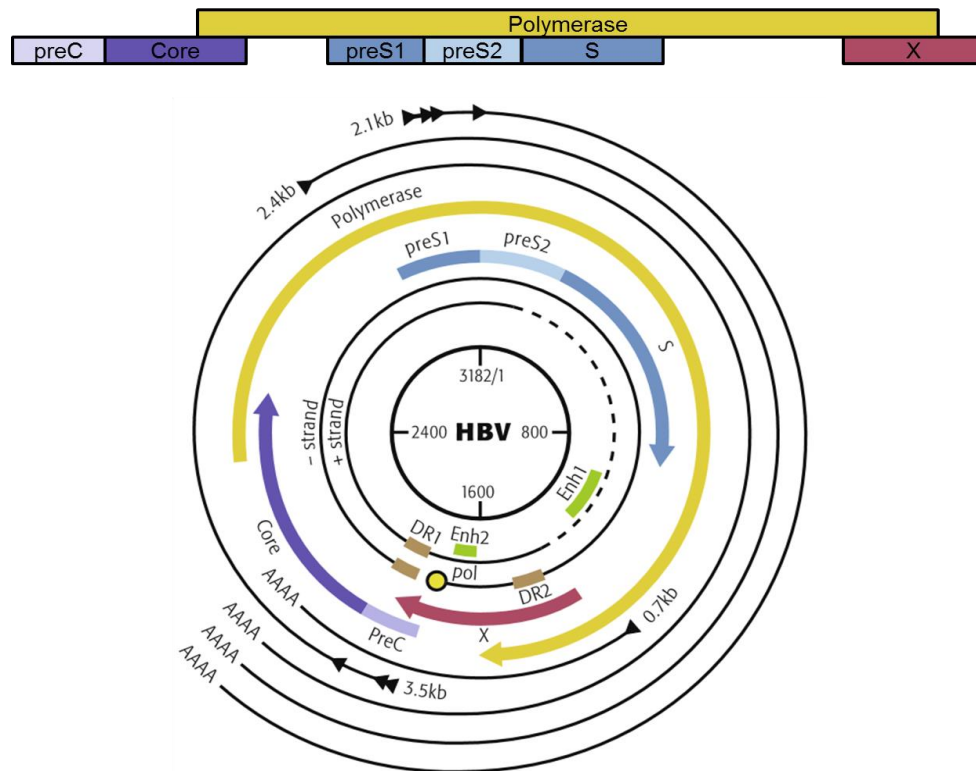


Figure 6. Genetic organization of the HBV genome (genotype ayw)

The internal black circle represents genomic position. Partially double-stranded genome shows the four encoded ORFs reading by different colored lines. The genome consists of a circular, partially double-stranded genome. It is known rcDNA, repaired into cccDNA. cccDNA serves as a template for viral transcription. The Enh1, Enh2, DR1, and DR2 are indicated by different colors. The outer black circles represent the viral transcripts with polyadenylation tails. The core and polymerase ORF are in the same orientation and on the same bicistronic transcript, the S translational reading frame overlaps the polymerase reading frame (57). The black arrowheads present the position of different initiation sites on each ORF; cartoon from reference (58). *Abbreviations used in this figure: rcDNA, relaxed circular DNA (rcDNA); cccDNA, covalently closed circular DNA; Enh, enhancers; DR, direct repeats.*

2.4. The HBV transcripts

HBV transcription and replication process is highly complex and unique for Hepadnaviruses. HBV transcription is controlled by four promoters (the core, preS1, pre S2/S, and X promoters) and two enhancer regions (Enh1 and Enh2) (52), generating viral capped and polyadenylated mRNAs that are 3.5, 2.4, 2.1, and 0.7 kb in size (58). The 3.5 kb mRNA known as pre-core mRNA serves as template for precore/core, HBeAg and capsid protein respectively, and viral polymerase synthesis. Alternatively, the pgRNA constitutes also the template for viral replication. The 2.4 kb (known as preS1 mRNA) is the template for the translation of L-HBsAg and 2.1 kb transcripts (known as pre S2/S mRNA) are used for the translation of the M-HBsAg and S-HBsAg. The smallest 0.7 kb transcript encodes the X protein (58). HBx might be produced immediately after formation of the cccDNA minichromosome resulting in activation of the other three promoters by direct or indirect mechanisms (59).

2.5. Function and characterization of HBV viral proteins

HBV transcripts contain multiple start codons to generate distinct proteins from overlapping ORFs.

2.5.1. HBV envelope proteins, HBsAg

Three different HBV envelope proteins are expressed from the preS1 (2.4 kb) and preS2/S (2.1 kb) transcripts. Envelope proteins are synthesized and immediately embedded in the endoplasmic reticulum membrane. The major function of these proteins is to form the HBV envelop allowing the viral particles to bind to susceptible cells. The preS1 domain is crucial for viral entry. The S-HBsAg (21 kD) is the smallest surface antigen, sharing the same C-terminal region with the two larger surface antigens. The M-HBsAg (31 kD) overlaps the S gene and has additional sequences known as preS2. The L-HBsAg (39 kD) is the largest surface antigen, containing S, preS2 and additional amino acids forming the preS1 domain, which interacts with the HBV entry receptor, human sodium/taurocholate cotransporting peptide (hNTCP/*SLC10A1*, referred to as NTCP in this study) (48, 49, 60). Each HBV envelop protein contains glycosylation sites and the preS1 domain in L-HBsAg is myristoylated. Of note the myristoylated preS1 domain is the Myrcludex B, an antiviral peptide that blocks specifically HBV entry into hepatocytes (48).

HBV envelope proteins are highly immunogenic and are used as immunogen for the preparation of HBV vaccines (61).

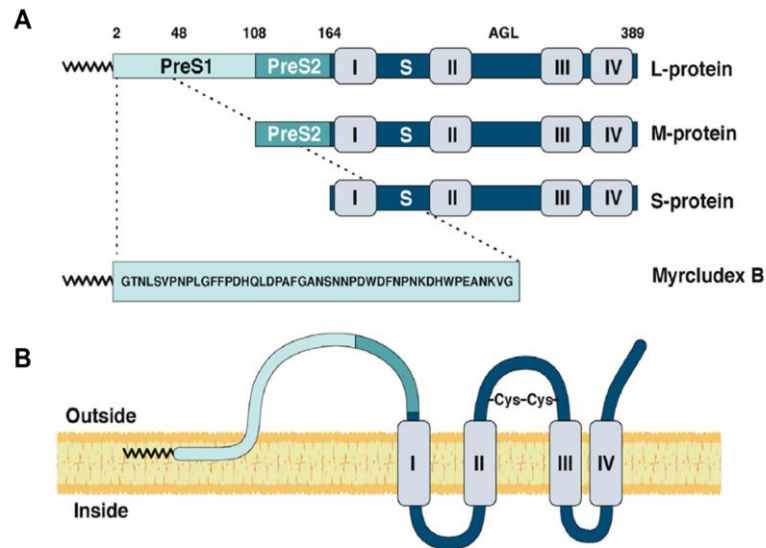


Figure 7. Domain structure of HBV surface proteins

(A) HBV surface protein L, M, and S-HBsAg share the S domain with 4 transmembrane domains (I-IV). The disulfide-linked cysteine moieties, as a part of the antigenic loop (known as AGL) is important for virus infectivity. The M-HBsAg has, in addition to domain S, the preS2 domain. The L-HBsAg contains an additional 107 amino acids (preS1) where interacts with the HBV receptor, NTCP. The myristoylated 47 amino acids of the L-HBsAg known as Myrcludex B, inhibits HBV entry by interruption of receptor binding. **(B)** Transmembrane topology of L-HBsAg in infectious HBV particle. The preS domains are exposed on the external face of the virion; cartoon from reference (48).

2.5.2. HBV core or capsid protein, HBcAg

The 21 kD HBV capsid protein core, or HBcAg, is translated from pgRNA transcript. Core dimerizes and dimers associate to form the viral capsid. The core protein is highly conserved among all HBV genotypes (62). Core protein dimers form the basic structural unit of the HBV capsid and ultimately provide the icosahedron symmetry of the capsid (39). Two types of capsids (icosahedral symmetry T=3, 30 nm in diameter; and T=4, 34 nm in diameter) have been observed by cryo-electron microscopy (63). The core protein is composed of two separate domains. The N-

terminal domain (NTD) is essential to form the capsid shell (64), while the C-terminal domain (CTD), that can be phosphorylated is required for viral RNA packaging and DNA synthesis (65-67).

HBeAg is an indicator of active viral replication in HBV-infected patients, like HBeAg, but in contrast to HBeAg it is not secreted. It has been suggested that core binds to HBV cccDNA in the nucleus and reduces the spacing of nucleosomes on cccDNA-histones complexes which regulate HBV transcription (68, 69). However, it is still controversial thus further investigation is required.

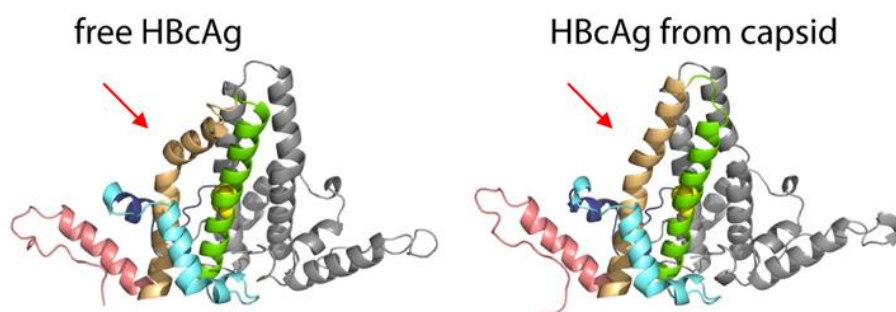


Figure 8. HBV core protein dimers depend on their activity

The structure of HBcAg has been resolved in 1999 (70). HBcAg dimers differ structurally from monomers. The intradimer helical bundle (Red narrow) is distorted in free HBcAg, resulting in an impossibility to form an icosahedra capsid; cartoon from reference (71).

2.5.3. HBV e antigen, HBeAg

HBeAg (15kD) is a glycoprotein encoded by the precore/core genes. The precore/core protein is cleaved in the endoplasmic reticulum at its N-terminus at a signal peptidase recognition motif and at its C-terminus by a peptidase before secretion in the extracellular medium or the blood stream (72). Interestingly, HBeAg is not associated with virions and is secreted independently from HBV infected cells (73). From a diagnostic perspective, the presence of HBeAg in the serum is an important indicator of active HBV replication. It has been reported that HBeAg suppresses immune responses induced by HBV core proteins (74, 75). However, the

exact role of HBeAg is still unclear.

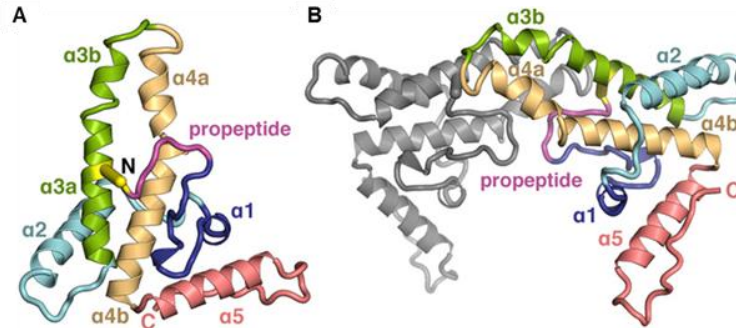


Figure 9. The crystal structure of HBeAg

Ribbon diagram of the HBeAg monomer **(A)** and dimer **(B)**. **(A)** The blue to red color from N- to C-terminus, with the propeptide (magenta) shown, forming an intramolecular disulfide bond (yellow). **(B)** Front subunit is colored gray and each color in structure represents according to the diagram. Hairpins of the a3b and a4a helices from each subunit form the dimer interface, supported by the propeptides intercalated between subunits; cartoon from reference (76).

2.5.4. HBV polymerase

Approximately, 80% of the viral genome encodes the viral polymerase (also referred to as Pol). Pol (94 kD) consists of functional domains and one variable spacer region. There is a terminal protein (TP) domain at the amino end, a spacer domain, the reverse polymerase/transcriptase (RT) domain and an RNase H domain.



Figure 10. The four domains of the HBV polymerase (genotype D)

The domain of HBV polymerase are shown. Numbering of TP domain and spacer domain is according to genotype D, and follows the standardized numbering for RT and RNase H domains; cartoon from reference (77, 78).

The TP domain at the N-terminus of the HBV polymerase is responsible for initiation of genome replication, including binding to the pgRNA, and RNA packaging (57, 79, 80). The spacer domain separates the TP domain from the RT domain. The spacer domain brings flexibility to the protein and supports numerous mutations (81). Various studies have shown that most amino acids within the spacer region can be mutated without altering polymerase domain functions (82, 83). The Pol/RT domain encodes an RNA-dependent DNA-polymerase activity and a DNA-dependent DNA-polymerase. The reverse transcription activity is important for genome replication, as it catalyzes the synthesis of the DNA genome minus-strand using pgRNA as a template. Subsequently, the DNA dependent DNA polymerase activity is important for the synthesis of the DNA plus-strand, by using the DNA minus-strand as template. The polymerase is the target for currently approved anti-HBV drugs (84). Several teams have developed a model of the HBV RT domain by comparison with the human immunodeficiency virus (HIV) RT (83, 85). This model is used for uncovering potential recognition sites for NAs. The RNase H domain degrades the pgRNA templates during synthesis of the minus-stranded genomic DNA. It has also been shown that this domain is responsible for pgRNA packaging (86).

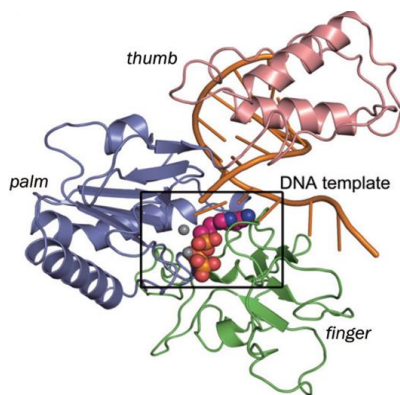


Figure 11. The 3D structural model of HBV polymerase

The finger, palm, and thumb subdomains in HBV polymerase are represented in green, blue and salmon ribbons. DNA template-primer duplex for replication is shown in orange cartoon mode. The insert indicates the catalytic subdomains; cartoon from reference (87).

2.5.5. HBV X protein, HBx

HBx protein (17kD) is encoded by the smallest HBV ORF. The X ORF is exclusive to orthohepadnavirus genus. Various studies have shown that HBx has a multifunctional role during HBV replication, especially for initiation of viral transcription from cccDNA (88-90). HBx can interfere with host signal transduction, transcriptional activation, DNA repair, and inhibition of protein degradation proliferation signaling (89, 91-93). It was also reported that Wnt/ β -catenin,

p53, and AKT (which have been implicated in hepatocellular carcinoma (HCC) are affected by HBx proteins by promoting cell cycle progression (91, 94, 95).

2.6. The viral replication cycle

The molecular details of *hepadnavirus* replication were initially demonstrated using DHBV and later extended to HBV, similarities between HBV and DHBV are striking (96, 97).

HBV has developed unique mechanisms to actively replicate in the infected cells without cytotoxicity. Unlike other viruses, HBV genome replicates via reverse transcription of pgRNA inside the virion (52, 97).

The replicative HBV cycle is a sophisticated process that is regulated by both host and viral factors. Although the mechanisms of HBV replication have been investigated in depth, certain aspects of the cycle are still poorly understood and the HBV replication cycle has yet to be fully elucidated. The different steps of HBV replication are briefly illustrated in **Figure 12**.

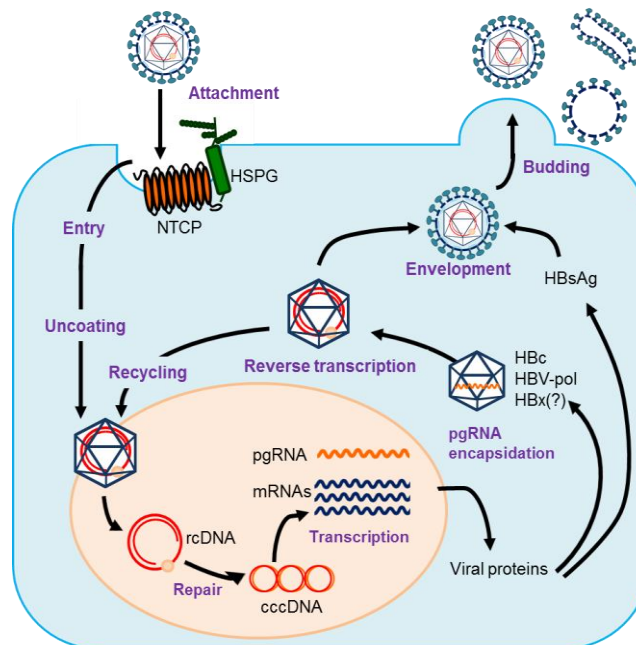


Figure 12. HBV replication cycle

HBV enters hepatocytes by attachment to HSPGs then binding to NTCP. Following fusion, the nucleocapsid

is transferred to the host nucleus, allowing the viral genome (rcDNA) to enter into host nucleus. The rcDNA is repaired by host enzymes to form cccDNA. The viral mRNAs and pgRNA are transcribed from the cccDNA by the host RNA polymerase II, once capped and polyadenylated they are exported into the cytoplasm where they are translated in viral proteins. pgRNA is packaged by core protein with the viral polymerase, and the viral genome is reverse transcribed to produce progeny rcDNA. The mature nucleocapsid is enveloped and released from HBV infected cells or transported back to the nucleus for recycling. *Abbreviations used in this figure: HSPGs, surface heparan sulfate proteoglycans; NTCP, sodium/taurocholate cotransporting polypeptide; rcDNA, relaxed circular DNA; cccDNA, covalently closed circular DNA; pgRNA, pregenomic RNA.*

2.6.1. HBV attachment and entry

HBV exclusively infects hepatocytes. This tissue specificity suggests that liver-specific HBV receptors and/or co-factors are mainly expressed at the surface of hepatocytes (98). From the virus point-of-view, 75 amino acid residues in the N-terminal region of the preS1 domain of the HBV large envelope protein are crucial for binding to the viral receptor(s) (1, 49). Indeed, although the preS1 domain mediates viral attachment to ubiquitous cell surface heparan sulfate proteoglycans (HSPGs) including glypican 5 (GPC5) (99, 100) specific receptors on the hepatocyte surface are also required. Recently, NTCP, a bile acid transporter mainly expressed at the basolateral membrane of human hepatocytes (101), has been identified as an HBV receptor allowing virus entry by interaction of the N-terminal preS1 domain of the L protein (98). Interestingly, NTCP overexpression in human hepatoma cell lines such as Huh7 or HepG2 cells (which lack the expression of the receptor and cannot be infected by HBV *in vitro*) renders them susceptible to HBV infection and provides unique cell culture models to study HBV entry (98, 102).

After receptor binding, the virion envelope fuses with either the plasma or endosomal membranes. A recent study has suggested that clathrin-mediated endocytosis is likely required for HBV entry steps (103). Caveolin-1 mediated endocytosis has been proposed as an alternative mechanism for HBV entry (104). This process may be induced by low pH and/or proteolytic cleavage of envelope protein (105). The nucleocapsid is then transported via microtubules to the nuclear pore complexes (NPCs) at the nucleus membrane (106). Upon reaching the NPCs, the C-terminus of the HBV core protein interacts directly with nucleoporin 153, an essential component of the basket of NPCs (107). However, the detailed mechanisms of capsid transport

and genome release into the nucleus after endocytosis are still poorly understood.

2.6.2. cccDNA formation in the nucleus

Following nuclear entry, HBV rcDNA is converted to a plasmid-like cccDNA (52). This process is probably carried out by host cell DNA repair machinery and is independent of viral polymerase activity (108). Moreover, cccDNA is complexed with both histone and non-histone proteins, including transcription factors, coactivators, chromatin-modifying enzymes and viral proteins such as HBc and HBx (68). Interestingly, cccDNA is rapidly transcriptionally silent in absence of HBx suggesting a key role of this viral protein in promoting HBV replication (88). Therefore, the transcriptional activity of cccDNA, which behaves like a nucleosome bound minichromosome is highly modulated by epigenetic modifications, such as methylation, acetylation, ubiquitination and SUMOylation (109). It seems that cccDNA can be eliminated following cell division (108). However, chronic HBV infection persists in the absence of productive replication of the virus (52). Thus, the elimination of cccDNA remains a therapeutic challenge.

2.6.3. Transcription of viral RNA

In the nucleus, the cccDNA serves as template for transcription by the cellular RNA-polymerase II of viral mRNA transcripts and the pgRNA (110). The 5' capped and 3' polyadenylated viral mRNA transcripts are transported to the cytoplasm and translated by ribosomes to form viral proteins (i.e., core, surface antigens and HBx).

The pgRNA also transfers to the cytoplasm via nuclear pore export. The pgRNA has a two crucial functions: (i) it is a bicistronic mRNA acting as the template for precore/core and the viral polymerase translation and (ii) it is the template for viral rcDNA synthesis.

The ϵ stem-loop structure is essential both for the binding of pgRNA to the viral polymerase and for pgRNA packaging into capsid particles (111). However, how the pgRNA/viral polymerase complex is recognized by the assembled core protein dimers is not well understood.

2.6.4. HBV pgRNA packaging and encapsidation

A unique property of HBV is that reverse transcription occurs inside the immature capsid.

Within the capsid, the viral DNA polymerase binds to the 5' end of the pgRNA to initiate nucleocapsid assembly and reverse-transcription of the pgRNA into the minus-strand of the viral genome. The ϵ stem-loop structure, approximately 60 nucleotides, is located at both 5' and 3' ends of the pgRNA. Only the ϵ stem-loop structure at the 5' end of pgRNA promotes the packaging of viral pgRNA with the polymerase into the capsid (112, 113). The ϵ stem-loop induces the structural changes to initiate reverse transcription (52).

For reverse transcription initiation, the ϵ stem-loop element recruits a 3' terminal OH group of tyrosine residue from the TP domain of the viral polymerase (57, 114, 115) and forms a covalent tyrosyl-5'-DNA-phosphodiester linkage. This allows then to add the first 3-4 nucleotides using bulge regions within ϵ element that serve as template for elongation (97). Subsequently, reverse transcription of the pgRNA occurs and synthesis of minus-strand viral DNA from 5' to 3' direction provides a unit length minus-strand DNA copy of the pgRNA carrying a small terminal redundancy ('r'). Simultaneously, most of pgRNA is degraded by activation of RNase H of the TP domain of the polymerase (53). Completion of minus-strand DNA synthesis results in a genome-length single minus-strand DNA. However, a 15-18 length of nucleotides at the 5' capped pgRNA including DR1 sequences remain. This RNA sequence functions as a RNA primer for synthesis of plus-strand genomic DNA. In this template switch, the plus-strand primer moves from DR1 to DR2 and initiates plus-strand DNA synthesis from DR2. As 'r' at the other end has the identical sequence, exchange of the two ends allows plus-strand DNA synthesis to proceed. Finally partially dsDNA with over length minus-strand carrying covalently linked polymerase, and an incomplete plus-strand is synthesized, constituting the rcDNA (**Figure 13**).

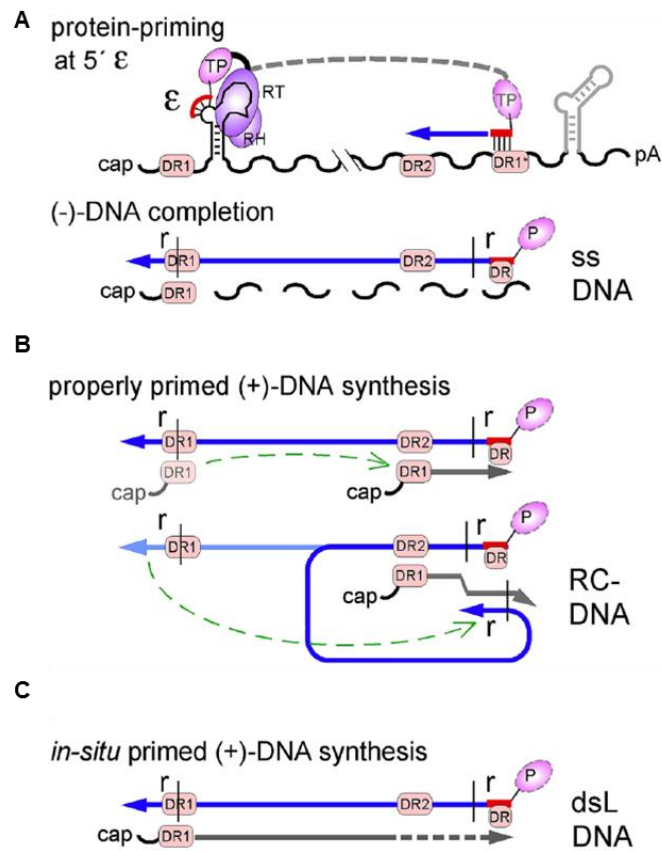


Figure 13. Model of HBV reverse transcription

(A) The viral polymerase TP domain initiates minus-strand DNA synthesis at the bulge of the ϵ element at the 5' end of pgRNA. The first 3-4 nucleotides are synthesized with the ϵ sequence used as the template (protein-priming at 5' ϵ). Following the minus-strand DNA synthesis, RNase H activity of polymerase degrades the pgRNA template ((-) DNA completion). **(B)** Non degraded pgRNA primer including DR1 sequence translocate to DR2 and initiates the plus-strand DNA synthesis until the 5' end of the minus-strand DNA, where it runs out of template. **(C)** Rarely, an *in-situ* priming process occurs, the plus-strand DNA synthesis is initiated from the DR1 sequence on the minus-strand template, resulting in the dsL DNA form of genome; cartoon from reference (108). *Abbreviations used in this figure: TP, terminal domain; RT, reverse polymerase/transcriptase domain; pA, polyadenylated RNA; cap, capped RNA; ss, single-stranded; pgRNA, pregenomic RNA; DR, direct repeat; dsL DNA, double-strand linear DNA.*

When rcDNA is formed, nucleocapsids are matured and enter the endoplasmic reticulum where they acquire their envelope. Alternatively, rcDNA is recycled to the nucleus to form new

cccDNA molecules (111, 116, 117), which may explain how the cccDNA level can be maintained in the absence of reinfection (118). It has been shown that DHBV not HBV rcDNA efficiently converts into cccDNA by cross-species transfection assays (119). Thus, the knowledge on rcDNA recycling is verified by experiments performed in the DHBV model.

Rarely, *in-situ* elongation of RNA primer provides double-strand linear DNA molecules (dsl DNA) (47, 48). Interestingly, dsl DNA is frequently detected in HBV related HCC patients (49), suggesting that it can be integrated into host chromosome.

2.6.5. Production of viral particles

HBV has three envelope proteins known as L-HBsAg, M-HBsAg, and S-HBsAg. They are all synthesized from the same ORF of the viral genome, by using different start codons. Thus, M-HBsAg has S gene and additional amino acid known as preS2. L-HBsAg consists of S gene with preS1 and and preS2 additional amino acids, respectively. Nascent envelope proteins are quickly oligomerized in the ER. Finally, the maturing nucleocapsids containing rcDNA are enveloped at the post-endoplasmic reticulum-pre-Golgi membrane (120, 121) and infectious progeny virions are secreted. Of note, an important proportion of oligomerized envelope proteins formed at this stage are not associated with nucleocapsids and enter the Golgi apparatus to be secreted by the infected cell. These empty particles are the spherical and filamentous empty particles observed in patient sera and cell culture as we described above (**Figure 5**).

3. Host response to viral infection

The innate immune system is the first line of host defense against infections. It is usually initiated by the recognition of pathogen-associated molecular patterns (PAMPs) (122), which are pathogens conserved structures recognized by the host pattern recognition receptors (PRRs) to initiate antiviral responses and restrict virus spreading. These receptors are located at the cell surface, in the cytosol or in endosomal compartments. Upon PAMP engagement, PRRs trigger downstream signaling cascades ultimately inducing the expression of a variety of proinflammatory cytokines, chemokines, and interferons (IFN). These molecules coordinate the early stage of response to infection and at the same time represent an important link to the adaptive immune

response, which provides long-term anti-viral protection by mounting an HBV-specific T and B lymphocyte response (123, 124). In particular, the type I IFN family has diverse effects on the immune system during pathogen infection, by directly or indirectly inducing supplementary mediators. In humans, the type I IFN family is a multi-gene cytokine family that encodes 14 partially homologous IFN α subtypes and a single species of IFN β , IFN κ , IFN ω , and IFN ϵ , while there is only one type II IFN known as IFN γ .(125). The IFN α and IFN β (referred to as IFN α/β) are broadly expressed. Their ability to induce antiviral effects in both virally-infected and their bystander cells has been well documented (126).

After initial exposure to a specific antigen, adaptive immunity, an antigen-specific immune system, produces memory cells, which persist in the body and are able to mount a rapid response to a second infection. It has been shown and is widely accepted that adaptive immunity is needed for efficient clearance of HBV infection (127). However, it is still controversial whether HBV induces innate immune responses in the early stages of infection. This stage is more difficult to analyze in humans, due to the lack of patients identified in the early stage of HBV infection. However, in acutely HBV-infected chimpanzees, HBV infection did not induce any innate antiviral responses in hepatocytes and in the liver (12). Recently, the development of cell culture models provided insights into the temporal and spatial immunological changes during HBV infection. It also highlighted the importance of innate immune responses during HBV infection (128).

3.1. Pattern recognition receptors

Upon PAMPs recognition, PRRs initiate production of IFN α/β by activating several intracellular signaling pathways. PAMPs are derived from pathogens and thus distinguishable from “self” (129, 130).

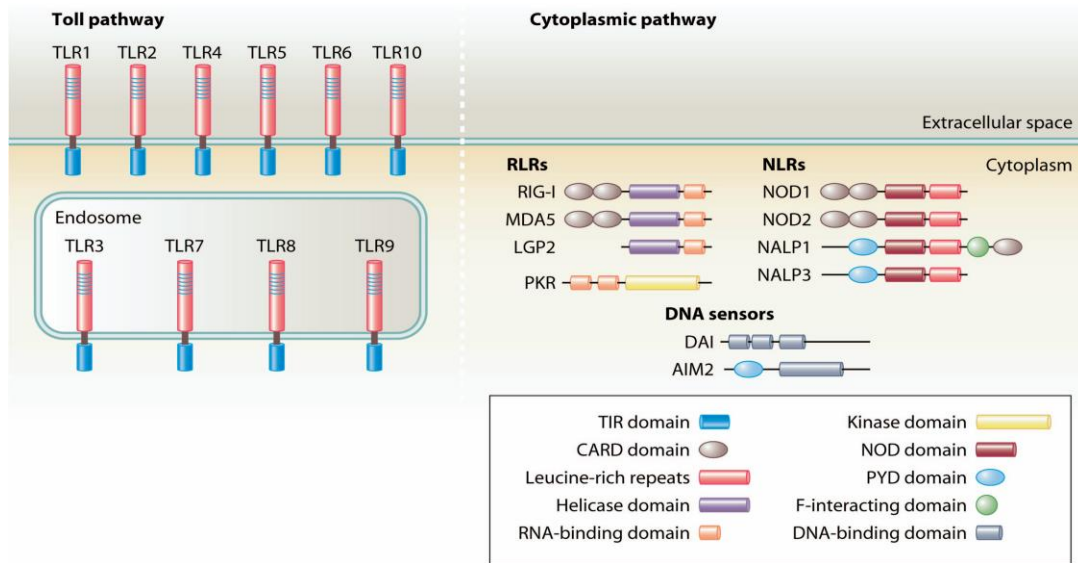


Figure 14. Cellular PRRs

TLRs are localized at the cell surface or at the endosomal membrane. PAMPs are recognized via the LRR domain (pink) and activate signaling cascades through the TRIF domain (blue). RLRs and NLRs activate TLR-independent pathways that have functional roles in the cytoplasm. The cartoon is taken from reference (131). *Abbreviations used in this figure: TLRs, Toll-like receptors; PAMP, pattern associated molecular pattern; LRR, leucine-rich repeat; TRIF, TIR-domain-containing adapter-inducing interferon- β ; RLR, retinoic acid-inducible gene I RIG-I-like receptors; NLR, nucleotide-binding oligomerization domain-like receptors; TIR, Toll/interleukin-1 receptor; CARD, caspase recruitment domain; NOD, Nucleosome binding oligomerization; PYD, pyrin domain.*

Generally, the PRRs can be categorized into two major classes depending on their subcellular localization. The extracellular PAMPs are typically found in the plasma or endosomal membranes. These, include several Toll-like receptors (TLRs), RIG-I-like receptor (RLR), Nod-like receptor (NLR), and C-type lectin receptors (CLRs) (132). In most cases, these membrane-bound PRRs are predominantly expressed in immune cells. In contrast, intracellular PRRs are found in the cytoplasm or nucleus of most mammalian cells. The different families of PRRs are shown in **Figure 14**. In this study, we will focus on the PRRs that recognize foreign nucleic acids in the cytosol to trigger immune signaling cascades.

Nucleic acids generated during pathogen infection are effective PAMPs. Several PRRs leading to the production of pro-inflammatory cytokines including IFNs can detect viral nucleic

acids (133).

3.2. Nucleic acid sensing by TLRs

Nucleic acids generated during pathogen infection are effective PAMPs. In general, TLRs are integral glycoproteins with extracellular or luminal ligand-binding domains containing leucine-rich repeat (LRR) motifs and a cytoplasmic signaling Toll/interleukin-1 (IL-1) receptor homology (TIR) domain (134). Upon the recognition of PAMPs by TLRs, they subsequently undergo oligomerization then induce intracellular signaling cascades. Despite sharing common structures and functional features, individual TLRs have unique characteristics, including the subcellular localization. TLRs 1, 2, 4, 5, and 6 are localized at the cell surface, while TLRs 3, 7, 8, 9, and likely 11, 12, and 13 are localized within intracellular compartments (135-138).

Notably, four TLRs (TLR3, TLR7, TLR8 and TLR9) are localized in endosomal membranes and recognize different types of foreign nucleic acid. For instance, TLR3 recognizes dsRNA species, such as polyinosine-polycytidylic acid (poly (I:C), a synthetic analog of dsRNA) as well as dsRNA derived from protozoa, fungi, replication or transcription intermediates (126). TLR7 and TLR8 are both sensors for single-stranded (ss) RNA and are structurally related. TLR9 recognizes unmethylated CpG motif in dsDNA.

Following the recognition of viral components by endosomal TLRs, adaptor proteins are recruited, such as TIR-domain-containing adapter-inducing interferon- β (TRIF) or myeloid differentiation primary response protein 88 (MyD88), which then activate signaling cascades via interferon regulatory factors (IRFs) and nuclear factor kappa B (NF- κ B). This leads to the induction of type I IFNs, proinflammatory cytokines and chemokines. These molecules not only contribute to control viral replication but also activate adaptive immunity.

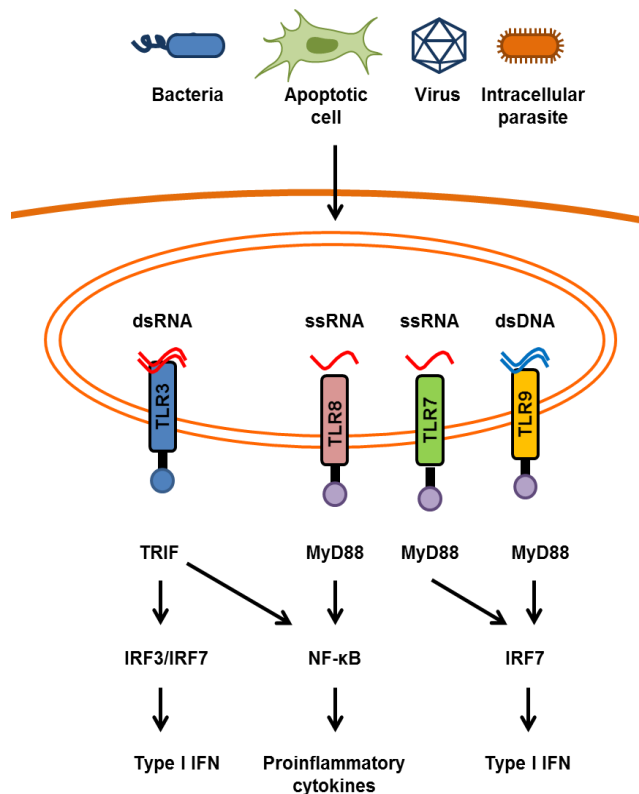


Figure 15. Endosomal Toll-like receptors specialized for RNA and DNA binding

Endosomal TLRs including TLR3, TLR7/8, and TLR9 detect nucleic acids derived from pathogens. Activation of these receptors leads to the recruitment of adaptor protein TRIF or MyD88, which induce signaling cascades via IRF3 and NF- κ B and lead to the up-regulation of type I IFN and inflammatory cytokines; The cartoon is taken from reference (139). *Abbreviations used in this figure: ds, double-stranded; ss, single-stranded; TLR, Toll-like receptor; TRIF, TIR-domain-containing adapter-inducing interferon- β ; MyD88, myeloid differentiation primary response protein 88; IRF, interferon regulatory factors; NF- κ B, nuclear factor kappa B*

Most viruses have evolved effective mechanisms to avoid recognition by host sensors, or to inhibit the activation of PRRs and/or their downstream signaling cascades. HBV infection, especially in early stage, modulates neither innate antiviral responses nor intrahepatic innate immune responses in HBV infected chimpanzee experiments (12). It has been reported that the TLR signaling pathway is blocked by HBV viral proteins (140). For instance, HBsAg suppresses TLRs signaling pathway via induction of IL-10 expression (141) and interferes with the JNK and MAP kinase pathway (142, 143). HBV polymerase suppresses activation of TLR3 and TLR4

mediated NF- κ B signaling pathway in hepatoma cells (144). Moreover, down-regulation of TLR3 (145), TLR4 (146), TLR7 (147), and TLR9 (148) has been reported in immune cells from CHB patients in HBV immune escape phase. However, there is no evidence that explains how HBV DNA or RNA templates function as PAMPs that trigger antiviral responses via TLRs.

Table 3. Innate immune signaling pathways suggested to be interfered by HBV viral proteins; from reference (140)

Nucleic acid sensor related cellular targets	HBV viral proteins	Reference
TLR2-pathway	HBsAg, HBeAg	(142)
TLR3-pathway	Polymerase	(149)
TLR4-pathway	HBsAg	(75)
TLR9-pathway	HBsAg	(150)

Abbreviations used in this table: TLR, Toll-like receptor; HBs, HBV surface antigen; HBe, HBV envelop antigen.

However, it has been reported that TLR-independent sensing can successfully be accomplished by retinoic acid-inducible gene I (RIG-I)-like receptors (RLRs) (151) and nucleotide-binding oligomerization domain (NOD)-like receptors (NLRs) (152). These will be discussed in the following section.

3.3. Cytosolic RNA sensing

Several cytosolic RNA sensing pathways including RLRs and NLRs, are activated by detection of dsRNA by TRL3 or ssRNA by TRL7 and TLR8. RLRs have been identified as crucial cytosolic RNA sensors broadly expressed by immune and non-immune cells *in vivo* (153). There are three RLR members: RIG-I, melanoma differentiation-associated protein 5 (MDA5, also known as IFIM1) and laboratory of genetics and physiology 2 (LGP2, also known as DHX58) which are expressed in most cell types (154).

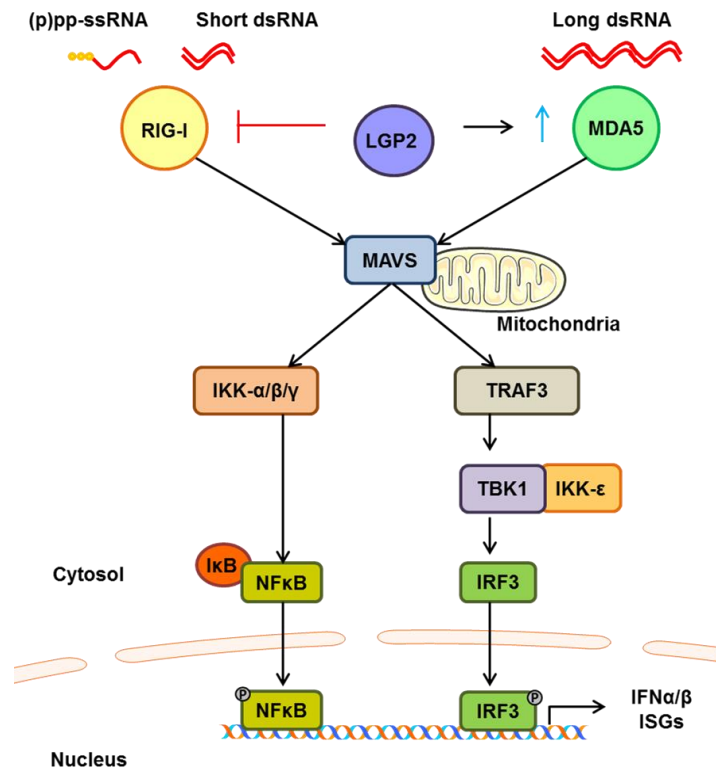


Figure 16. Intracellular RNA sensing by RLRs

RIG-I and MDA5 play an important role in RNA sensing through recognition of different types of RNAs. RIG-I detects short dsRNA or 5'ppp RNA, whereas MDA5 detects long dsRNA. LGP2 may function as a modulator of RIG-I and MDA5 signaling. Activation of RIG-I and MDA5 trigger the polymerization of MAVS in the mitochondria, which activates downstream signaling cascades, resulting in the induction of antiviral responses. *Abbreviations used in this figure: RIG-I, Retinoic acid-inducible gene I; MDA5, Melanoma differentiation-associated protein 5; MAVS, Mitochondrial antiviral-signaling protein.*

RIG-I and MDA5 participate in type I IFN production via adaptor molecules cascades. RLR members have an essential role as sensor proteins. RIG-I and MDA5 both recognize viral RNA, but they have different ligand specificity. RIG-I recognize both poly(I:C) and 5'-triphosphate RNA from negative-strand RNA viruses such as rhabdoviruses, and influenza (154). Moreover, transcription intermediates produced during DNA viruses infections, including Epstein-Barr virus (EBV) (155), Kaposi sarcoma-associated virus herpesvirus (KSHV) (156), herpes simplex virus (HPV) (157), adenovirus (158) and HBV (159), can also be detected by RIG-I (154). MDA5 has been shown to sense RNA species arising during picornavirus, dengue virus, and West Nile virus

infection. Interestingly, poly (I:C) can be detected by both RIG-I and MDA5. It has been suggested that the length of dsRNA is an important factor for recognition by these sensors. Indeed, the long length of poly (I:C) is recognized by MDA5 (160), whereas small self-RNA produced by the antiviral endoribonuclease RNase L could activate RIG-I signaling (161). By contrast, LGP2 negatively regulates RIG-I signaling while promoting the binding of RNA to MDA 5 (149, 154).

NLRs are a family of cytosolic proteins with diverse immune functions (152). Generally, NLRs act as adaptor molecules rather than as receptors. Recently, NOD2, known as a sensor of bacterial envelopes, was also implicated in the production of type I IFNs in response to viral infection through the sensing of ssRNA produced during infection by a respiratory syncytial virus (RSV) and a paramyxovirus (162).

As for other intracellular RNA sensors, Protein kinase R (PKR) senses viral dsRNA, while oligo-adenylate synthase (OAS) activates RNase L to degrade viral and cellular RNAs to block viral propagation and to induce apoptosis respectively (163).

The HBV viral genome could potentially be detected by cytosolic nucleic acid sensors, when viral nucleocapsid are destabilized and disassembled (164). It has been suggested that HBV polymerase interferes with RIG-I and MAVS-mediated antiviral activity (149, 165). Although it has been reported that MDA5 suppresses HBV replication, CHB patient in immune escape phase present an alteration of MDA5 expression but not RIG-I (166, 167). Indeed, 5' ε stem-loop element of HBV pgRNA that is crucial for viral replication is sensed by RIG-I, resulting in activation of innate immunity in human hepatocytes. In addition the authors showed that RIG-I counteracts the interaction of HBV polymerase with pgRNA (159).

However, there is no definitive evidence from *in vivo* models demonstrating that RNA sensors are associated with detection of HBV RNA in human hepatocytes.

3.4. Cytosolic DNA sensing

DNA is regarded as an excellent stimulator of immune responses, even though it is the host genetic material. The presence of aberrant DNA in the cytosol, such as pathogenic DNAs during infection, the leak of self-DNA from the nucleus, mitochondria or lysosome, is considered as a danger signal in the cells. These conditions allow the induction of immune responses, including production of type I and type III IFNs (154, 168, 169). After type I IFNs are produced,

IFN α / β binds to the receptors comprised of the IFN receptors (IFNAR) 1 and IFNAR2 subunits. This binding activates downstream signaling through the Janus kinase/signal transducers and activators of transcription (JAK/STAT) pathway, leading to the activation of transcription of interferon stimulated genes (ISGs) (124).

Several cytosolic dsDNA sensors able to induce type I IFN production (170) have been identified and characterized, including absent in melanoma 2 (AIM2, pyrin and HIN (PYHIN) domain-containing protein family), DNA-dependent activator of IRFs (DAI), DExD/H box helicase protein 41 (DDX41), IFN-inducible protein 16 (IFI16), and cyclic GMP-AMP (cGAMP) synthase (cGAS) (153, 171).

DAI was shown to trigger type I IFN expression upon dsDNA binding and TBK1-IRF3 interaction. Several researches have reported that DAI induces type I IFN response in HBV infected cells (172, 173). DDX41 is a DNA sensor that depends on Stimulator of Interferon Genes (STING) to induce type I IFNs (174). AIM2 is part of the inflammasome and plays a role in defense against viral and bacterial DNA (175). AIM2 was identified as a cytosolic DNA sensor capable of inducing inflammatory responses. It has been reported that AIM2 increased inflammation in renal glomeruli of HBV infected patients in the HBV immune tolerant phase (176). Another PYHIN protein IFI16 was suggested to act as a DNA sensor able to induce type I IFN production in a STING-dependent manner. It was shown that the stability of IFI16 in HSV-infected human fibroblasts was promoted by cGAS (177). cGAS, was recently identified as a cytosolic DNA sensor that induces type I IFN responses in a STING-dependent manner (178). The detailed information and functional role of cGAS will be described in following parts.

The detection of HBV DNA by cellular sensors within infected cells is still poorly understood. *In vivo* data strongly suggest that HBV behave like a “stealth” virus not able to trigger any innate immune response (12, 179). Only a couple a studies suggests that HBV-derived dsDNA fragments (180) and viral nucleocapsid destabilization and disassembly (164) could induce innate immune responses.

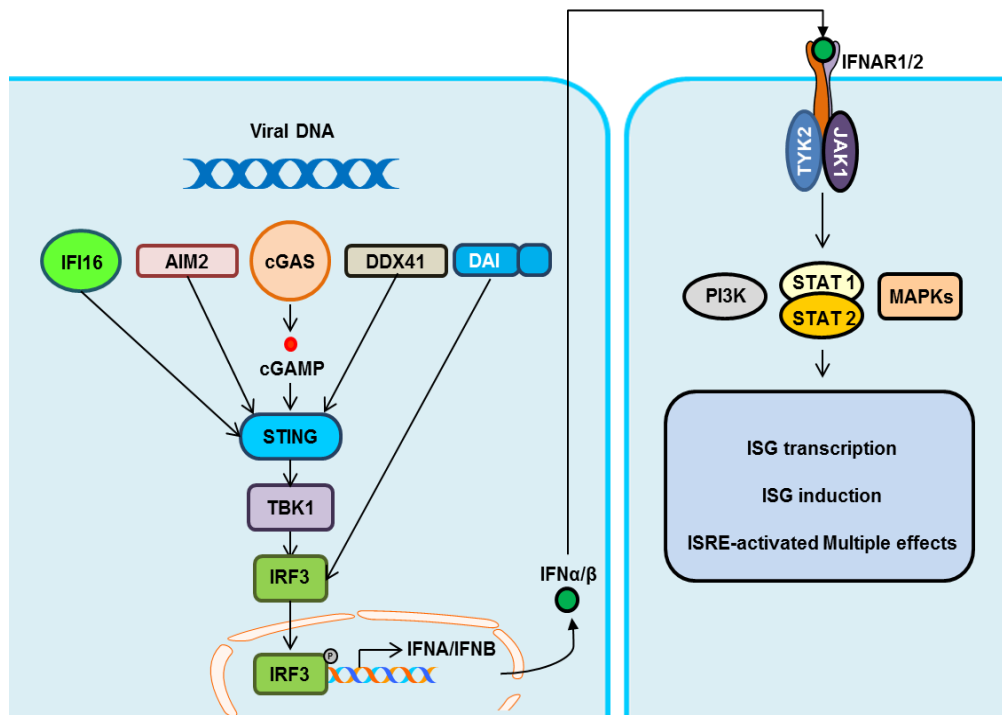


Figure 17. Pathways of type I interferon induction by intracellular DNA sensors and receptor signaling

Double-stranded DNA (dsDNA) binding to cytosolic sensors triggers expression of the genes encoding type I IFNs, which is mediated by several signaling pathways that all point on the STING/TBK1/IRF3/IRF7 cascade. After binding of type I IFNs to the IFNAR1/2, signaling cascades are activated, including JAK/STAT, MAPKs, and PI3K pathways, thereby leading to expression of ISGs and the establishment of an antiviral state. *Abbreviations used in this figure: dsDNA, double-stranded DNA; AIM2, absent in melanoma 2; DAI, DNA-dependent activator of IRFs; DDX41, DExD/H box helicase protein; IFI16, IFN-inducible protein 16; cGAS, cyclic GMP-AMP (cGAMP) synthase; IFN, interferon; IFNAR1/2, IFN receptors 1/2; JAK/STAT, Janus kinase/signal transducers and activators of transcription, MAPKs, Mitogen-activated protein kinase; PI3K, Phosphoinositide 3-kinase; ISRE, Interferon-sensitive response element.*

3.5. Identification and characterization of the cGAS-STING pathway

cGAS has been recently identified as a cytosolic DNA sensor. Activated cGAS produces the second messenger cGAMP, which directly binds to and activates STING to strongly trigger type I IFN production (178, 181).

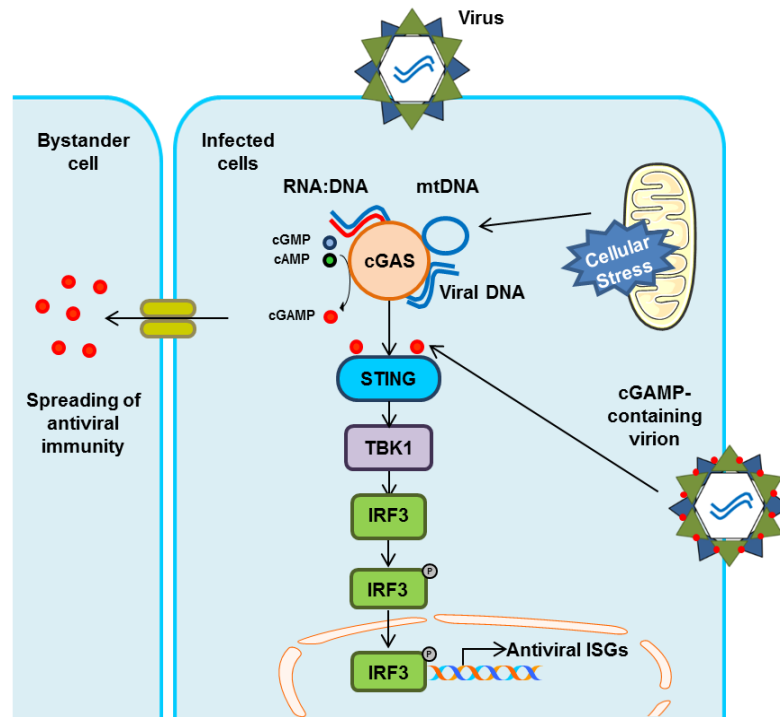


Figure 18. cGAS-STING pathway for sensing of cytosolic DNA

Cytosolic DNA arising during microbial infection binds to cGAS, which then synthesizes 2'3'-cGAMP to bind to and activate the adaptor STING. STING activation triggers signaling through TBK1 cascades. Phosphorylated TBK1 recruits IRF3 for phosphorylation, and phosphorylated IRF3 forms dimers, which then transfer to the nucleus to activate the expression of type I IFNs. *Abbreviations used in this figure: mtDNA; mitochondrial DNA.*

3.5.1. 2'3'-cyclic GMP-AMP synthase, cGAS

cGAS is the 2'3'-cyclic GMP-AMP synthase, that was identified by biochemical fractionation and quantitative mass spectrometry approaches (178). The product synthesized by cGAS, 2'3'-cGAMP (cGAMP), was discovered just before the function of cGAS (181). Human cGAS is composed of an unstructured and poorly conserved N terminus (1-160 amino acid) and a highly conserved C-terminus (161-330 amino acid) (182). The cGAS protein contains a nucleotidyltransferase (NTase) domain and a DNA binding domain (Mab21) (6). The Zinc-ribbon domain within Mab21 domain interacts with the major groove of the DNA (183, 184). Human cGAS presents structural similarities with human OAS1 which is activated by dsRNA sensing (185).

cGAS binds to dsDNA to form a 2:2 complex (186, 187), then undergoes conformational changes allowing the synthesis of 2'3'-cGAMP (referred as cGAMP) (178, 186).

Binding of dsDNA to cGAS is sequence-independent, since cGAS is thought to bind to the sugar-phosphate backbone of the DNA (188). Short dsDNA efficiently binds and activate cGAS *in vitro*. However, in cells, dsDNA of at least 15 base pairs in length is required for activation of the cGAS-mediated pathway. cGAS can bind to ssDNA and synthesizes cGAMP, although the binding affinity to ssDNA is much lower than for dsDNA binding (184). Recent reports showed that stem-loop structure of ssDNA derived from retroviral (HIV-1) replication intermediates and RNA:DNA hybrids can activate cGAS to produce cGAMP (189, 190).

The function of cGAS is regulated by various mechanisms and factors. It was reported that direct interaction between Beclin-I autophagy protein and cGAS not only inhibits cGAMP production to decrease IFN production upon either dsDNA transfection or HSV-1 infection, but also enhances degradation of pathogenic DNA in the cytosol to prevent excessive cGAS activation (191). The AKT kinase was also reported to act as a negative regulator of cGAS enzymatic activity by phosphorylation, resulting in the reduction of cGAMP and IFN β production and increase in HSV1 replication (192).

More recently, tubulin tyrosine ligase-like enzyme (TTL) 6 (polyglutamylation) or TTL4 (monoglutamylation) were identified, and it was shown that glutamylation of cGAS by these proteins interferes with its synthase activity and DNA-binding ability. Moreover, deglutamylation by cytosolic carboxypeptidase (CCP) 6 (polyglutamylation) and CCP5 (monoglutamylation) lead to the activation of cGAS (193).

3.5.2. 2'3'-cGAMP

The 2'3'-cGAMP produced by cGAS functions as a second messenger. It directly binds to STING to induce conformational changes in STING allowing the subsequent activation of TBK1, ultimately leading to induction of type I IFNs (178, 181).

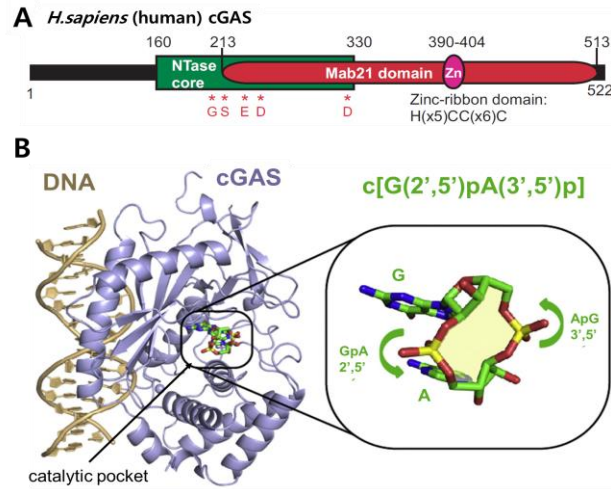


Figure 19. The crystal structure of human cGAS

(A) Functional domains in human cGAS proteins. Five red stars indicate key catalytic residues (G212, S213, E225, D227 and D319). Mab21 domain contains the zinc-ribbon domain bearing critical amino acids for DNA binding. **(B)** Binding of dsDNA to cGAS induces conformational changes that lead to formation of a catalytic pocket where cGAMP is synthesized. The model is shown as ribbon representation with annotated domains and secondary structure according to references (182, 194).

cGAMP has two phosphodiester bonds, one between the 2'-OH of GMP and 5'-phosphate of AMP, and the other between the 3'-OH of AMP and 5'-phosphate of GMP (185). These 2'-5' and 3'-5' linkages are catalyzed by cGAS to form 2'3'-cGAMP. So far, the mechanisms regulating the intracellular cGAMP level are not known, especially as no intracellular cGAMP phosphodiesterase has been identified so far.

cGAMP can spread between cells via gap junctions (195), which allows infected cells to activate the interferon pathway in non-infected neighboring cells to resist to virus infection. Interestingly, it was reported that cGAMP can be incorporated into viral particles and thus is delivered to cells during infection (196, 197). These findings highlight mechanisms allowing quick responses to virus infection.

3.5.3. Role of the cGAS-STING pathway in pathogen infection

Most pathogens have evolved mechanisms to evade immune responses in their host.

Since the discovery of the cGAS-STING pathway, the ability of cGAS to sense dsDNA or RNA:DNA intermediates and induce immune responses has been investigated for many different pathogens (198).

Indeed, many DNA virus infections activate the cGAS-STING pathway after sensing of their viral DNA, including HSV-1 (199, 200), murine gamma-herpesvirus 68 (MHV68) (201), KSHV (202), vaccinia virus (VV) (201), adenovirus(203), human papillomaviruses (HPV) (204), and human cytomegalovirus (HCMV) (205) and even HIV after genome reverse transcription (190).

Moreover, cellular damage or cell death signaling caused by pathogen infection may induce antiviral responses through the cGAS-STING pathway. For example, HSV-1, VSV and dengue infections can induce cellular stress and trigger mitochondrial DNA (mtDNA) release into the cytosol, resulting in cGAS-STING-dependent type I interferon production (206, 207).

Table 4. Viruses and intracellular DNA sensors; from reference (208)

Virus	Sensor	Experiment model	Response	Reference
HSV-1	cGAS	Mice	Type I IFN	(187, 200)
MHV68	cGAS	Mice	Type I IFN	(201)
AdV	cGAS	Murine macrophages Endothelial cell lines	Type I IFN	(203)
HIV-1	cGAS	Human macrophages	Type I IFN response	(209, 210)
HCMV	cGAS	Human macrophages	Type I IFN response	(205)
VV	cGAS	Mice	Type I IFN	(201)
HSV-1	IFI16	Human macrophages Human fibroblast	Type I IFN, IL-1 β	(177, 211, 212)
HCMV	IFI16	Human macrophages Human fibroblast	Type I IFN	(211, 213)
KSHV	IFI16	Human dermal microvascular endothelial cells	IL-1 β	(214)
EBV	IFI16	Human B cell lines	IL-1 β	(215)
HIV-1	IFI16	Human macrophages and human T cells	Type I IFN Pyroptosis	(210)
MCMV	AIM2	Mice	IL-18	(175)
VV	AIM2	Murine macrophages	IL-1 β	(216)

Abbreviations in this table: AdV, adenovirus; cGAS, cyclic GMP–AMP synthase; EBV, Epstein-Barr virus; HCMV, human cytomegalovirus; HSV, herpes simplex virus-1; IL, interleukin; IFN, interferon; KSHV, Kaposi's sarcoma-associated herpesvirus; MCMV, murine CMV; MHV68, murine gammaherpesvirus 68; VV, vaccinia virus. .

As well, RNA virus infection induce antiviral responses through the cGAS-STING pathway due to formation of RNA:DNA replication intermediates. For instance, lentivirus replication generates different forms of replication intermediators such as RNA:DNA hybrids, ssDNA, and dsDNA (217). Both stem-loop structures in ssDNA and unpaired Y-form dsDNA derived from HIV-1 replication activate the type I IFN production via sensing by cGAS (190).

Many viruses encode antagonists that enable the evasion of innate immunity by inactivating cGAS or the cGAS-STING pathway (208, 218). For example, the KSHV protein ORF52 was shown to inhibit cGAS enzyme activity through direct binding to cGAS (219). The cytoplasmic form of KSHV nuclear antigen LANA also inhibits cGAS activity (220). Moreover, HSV-1 regulatory protein ICP27 targets STING and TBK1 to prevent the phosphorylation of IRF3 by TBK1 (221). DNA tumor viruses such as HPV18 and human adenovirus 5 (hAd5) inhibit the cGAS-STING pathway using their viral oncoproteins E7 and E1A, respectively (222). In the case of HBV, the DNA polymerase disrupts K63-linked ubiquitination of STING to block its signaling (223).

One effective way for viruses to evade the cGAS-STING pathway is by “hiding” their viral DNA. cGAS is a key sensor for retroviruses, including HIV-1 and HIV-2 (209, 224). After HIV infection of macrophages, reverse transcription occurs inside the viral capsid to convert viral RNA into cDNA. The encapsidated viral DNA is thus shielded from cytosolic DNA sensors until it is transported to the nucleus, where it can be integrated into the host genome. However, as soon as HIV-1 replication intermediates are present in the cytoplasm, they are highly and specifically recognized by cGAS and trigger the induction of interferon via cGAS (190).

Cytosolic sensing of HBV pgRNA has been indicated to inhibit HBV replication, but does not display a decrease of viral load (149). It was suggested that HBV probably evades the sensing of pgRNA by readily package the pgRNA into capsid to prevent recognition by cellular sensors (225).

Recently, it is has been show that the cGAS-STING pathway inhibits HBV replication and

viral assembly in cell culture models (180, 226), even though endogenous expression of cGAS and STING is lower in hepatocyte-derived cell lines, particularly the commonly used Huh7 and HepG2 cells than in immune cells (227). These findings suggest that the cGAS-STING pathway may not be crucial for sensing HBV infection in hepatocytes. A recent report described that type I IFN production is not induced by foreign DNA or HBV infection due to lack of STING expression in human and murine hepatocytes (227). It suggests that hepatic non-parenchymal cells such as Kupffer cells, liver sinusoidal endothelial cells and other cell types may contribute to regulation of innate immune responses to HBV infection, rather than hepatocytes themselves.

4. HBV experimental models

Due to the lack of a suitable *in vitro* HBV experimental model, it was difficult to deeply study the HBV life cycle for many years. In recent years, the development of new experimental models has allowed advances in the understanding of the HBV replication cycle and HBV virus-host interactions, the important steps are resumed **Figure 20** (128).

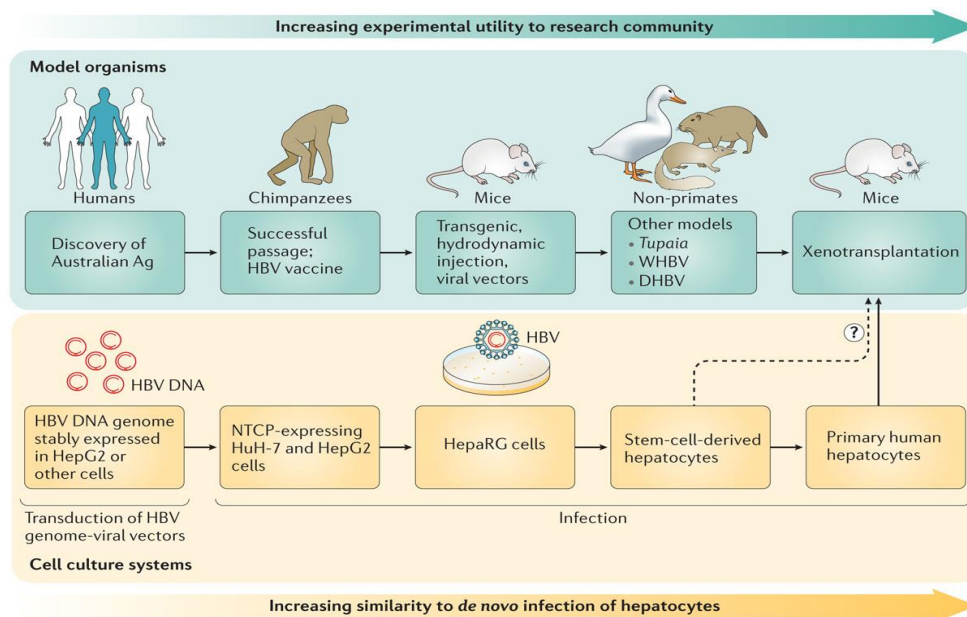


Figure 20. Development of HBV experimental models

The organism models for studying HBV have shifted to non-primates models. Several HBV mouse models

have been developed within the last decades. Cell based systems initially used hepatoma-derived cell lines engineered to express the HBV DNA genome. These models have transitioned to infectious systems since NTCP was identified as an entry receptor, providing the first cell culture models to allow the study of early steps in infection. Stem-cell-derived hepatocyte-like cells and primary hepatocytes also support HBV infection. Cartoon from reference (128). *Abbreviations in this figure: WHBV, woodchuck hepatitis B virus; DHBV, duck hepatitis B virus; NTCP, sodium/taurocholate cotransporting peptide.*

4.1. Primate models for the study of HBV infection

The initial experiments in animal models allowed the understanding of virus-host interactions in HBV infection. The early studies in HBV research were performed in chimpanzees, other animal models such as woodchuck hepatitis virus and duck hepatitis virus (hepadnaviruses closely related to HBV) have been also successfully developed (79, 228, 229).

The most relevant model for HBV vaccine development is the chimpanzee. Because of their high genetic similarity with humans and natural susceptibility for infection with hepatitis viruses, chimpanzees have proven to be the most useful model for studying viral hepatitis, especially immune responses to infection. However, the limited supply, ethical implications and high cost of this animal have precluded their use today. Moreover, there are distinct differences in spectrum of liver disease compared to humans (230, 231).

4.2. Mouse models for the study of HBV infection






Meanwhile, other small animal models have been developed: Either full-length HBV-replicating or individual HBV protein-expressing transgenic mouse models allowed to study immune responses to HBV infection and to evaluate antiviral treatment strategies *in vivo* (232, 233). As an example, hydrodynamic injection of HBV genome into mice allowed the establishment of a model leading to demonstrate the role of the innate immune system during HBV replication (234). Using the adenoviral gene delivery system, the HBV genome could be targeted to mice liver. This method was used to study chronic HBV infection, adaptive immune responses and for anti-HBV drug testing (235, 236). Nonetheless, as different host factors are expressed on human hepatocytes compared with murine hepatocytes, investigating viral entry and the initiation of infection remains impossible in transgenic mice (237). Accordingly, whereas cccDNA formation is efficiently observed in the transgenic mice liver, allowing the study of cccDNA biology (238), the

integration of the HBV genome into the genome of these mice, however, limits the utility of the model for identifying therapeutic cures.

Humanized chimeric mice provide an attractive strategy to study HBV infection (239). These immunodeficient mice engrafted with human hepatocytes can be infected by HBV purified from patient serum. Thus, it allows the different HBV genotypes as well as mutants to be studied. First, isolated primary human hepatocytes (PHH) are injected into the mouse liver to repopulate the mouse liver tissue. Replacement of the murine hepatocytes with human hepatocytes can also induce liver injury, thereby creating a growth advantage for engrafted human hepatocytes. Transplanted human hepatocytes maintain functional innate immunity. Accordingly, this model is ideal for studying the interactions of HBV with innate antiviral responses in human hepatocytes (240). This approach first used severe combined immunodeficiency (SCID) mice carrying a urokinase plasminogen activator transgene that is activated by a liver-specific albumin promoter (Alb-uPA) (241). Since then, additional humanized mouse models have been developed. Genetically engineered mice with human homologs of two HCV entry receptors allowed successful HCV infection and replication as well (242) and studies are underway to pursue a similar approach for HBV infection.

While murine cells expressing human NTCP are susceptible to HDV infection, they do not support HBV infection, suggesting that essential host factors for HBV infection may not be expressed (243). However, a recent paper described one mouse liver cell line that was susceptible to HBV infection following over-expression of human NTCP (244). A summary of the *in vivo* models used to study HBV infection is presented in **Table 5**.

Table 5. Characterization of HBV infection in primary hepatocytes from different species expressing human NTCP; from reference (245)

Primary hepatocytes transcomplemented with hNTCP					
Myrcludex-B binding	+++	+++	+++	+++	+++
HBV infection HBs positive cells	+++	++	-	-	-
HBc positive cells	+++	++	-	-	-
HBe secretion	+++	++	-	-	-

HBV RNA detection	+++	++	-	-	-
HBV cccDNA detection	+++	++	-	-	-
HBV genome secretion	++	++	-	-	-

Abbreviations used in this table: cccDNA, covalently closed circular DNA; HBs, hepatitis B surface antigen; HBc, hepatitis B core antigen; HBe, hepatitis B e antigen; +++, strong; ++, moderate; +/-, weak; - negative.

4.3. Cell-based experimental model

For many decades, the absence of HBV infectious cell culture models hampered the progress in the understanding HBV life cycle. More recently, *in vitro* cell culture systems supporting complete HBV life cycle have been established when the first bona fide HBV entry receptor NTCP, a bile acid transporter was identified in 2012 (98). This finding opened new avenues for the establishment of cell culture models suitable for uncover of new virus-host interactions and the biology of the HBV life cycle.

4.3.1. Hepatoma-derived cell lines

As for most infection models, hepatic tumor-derived cell lines have been useful and powerful tools to study partly HBV-host interactions.

The Huh7 cell line was isolated from a well-differentiated human HCC tumor (111, 246). This cell line has been used to study certain complex aspects of the HBV life cycle, especially epigenetic modifications of the episomal HBV DNA, as these cells enable the establishment of cccDNA following transfection of viral linear genomes (69).

In contrast to the Huh7 cell line, the HepG2 cell line (derived from a patient with well-differentiated hepatoblastoma) is polarized (247). It has proven to be very useful for studying HBV, although the difference between these cells are unexplored. The HBV genome can be stably expressed in HepG2 cells, and these cells support both HBV replication and cccDNA formation. HepAD38 and HepG-H1.3 cell lines, derived from HepG2 cells, are also suitable for studying certain steps of the HBV life cycle, especially late steps of HBV replication and clearance of cccDNA by host defense pathways (248). The HepaRG cell line (an hepatic progenitor cell line that retains many characteristics of primary human hepatocytes (249)) can be used for the study

of HBV infection too (250, 251). HepaRG cells can be differentiated into either biliary or hepatocyte-like cells and can be indefinitely divided (250). DMSO treatment is needed for differentiation into hepatocyte-like cells. This cell line was demonstrated to be a useful model for HBV infection studies. However, despite polyethylene glycerol (PEG) treatments leading to increased binding affinity between the HBV virion and entry receptor(s), the overall infection rate remains low with minimal cell-to-cell spread of the virus (100).

Although hepatoma-derived cells are valuable research tools, they cannot exactly mimic the physiological environment of natural HBV infection. PHH are considered the ideal *in vitro* experimental system for studying HBV because they are the natural target cells for HBV infection in the liver. These cells are typically obtained from patients undergoing liver resection for a hepatic tumor. Although PHH do not divide, these cells express NTCP and readily support virus infection once in culture (60, 252). In addition, PHHs have an intact host defense system that combats the infection and limits viral replication (253). To extend the viability and maintain the differentiation of PHHs in culture, several approaches have been attempted. Micropatterning approach and 3D organoids systems support the extension of cell viability (254, 255). To provide more physiological culture conditions, micropattern systems mimic a tissue-like micro-environment by culturing hepatocytes with other epithelial cells. Although the micropattern system has several benefits compared to single cell line-based studies, an organization of hepatocytes into 3D organoids also offers additional advantages in that hepatocytes interact with major nonparenchymal hepatic cells.

4.3.2. NTCP-overexpressing cell lines

Lack of endogenous NTCP expression in Huh7 and HepG2 cells explains their inability to mediate viral entry and thus efficient infection. Since NTCP has been identified as an HBV entry receptor, many studies have taken advantage of NTCP overexpressing cells lines for studying the entire HBV life cycle (98, 99, 102, 256). Recently, glypican 5 (GPC5) was identified as a novel attachment factor for HBV entry using an NTCP-overexpressing Huh7 cell line (99). This study also suggested that additional factors may be required to achieve optimal HBV viral infection.

NTCP-overexpressing hepatoma cells have been shown to be useful for screening anti-HBV drugs including entry inhibitors (256). Several small molecules targeting viral entry, such as Myrcludex B (48, 102, 257-261), cyclosporine A (256), irbesartan (262, 263) and vanitaracin (264), have been reported to have antiviral activity in HBV-infected NTCP-overexpressing cells by

interfering with HBV-NTCP interactions or inhibition of NTCP function. This cell model allowed the discovery of additional viral entry factors as well as entry inhibitors through different screening approaches (256, 257, 265). Collectively, an increasing number of studies exploit NTCP-overexpressing cell lines for understanding virus-host interactions. However, a low level of *de novo* virus production from HBV infected cells are an important limitation of the model.

Table 6. Summary of current cell culture models for study HBV; from reference (128)

Cell biology	HuH-7 cell	HepG2 cell	HepaRG cell	Primary human hepatocytes
Functional innate immunity	Minimal	Moderate	Fully functional	Fully functional
Length of propagation	Indefinite	Indefinite	Indefinite	<1 month
Polarized	No	Yes	Yes	Yes
Immortalized	Yes	Yes	Yes	No
Transformed	Yes	Yes	No	No
Availability	High	High	Medium	Low
Lot variability*	Minimal	Minimal	Moderate	High
Supports HBV infection	No, requires NTCP	No, requires NTCP	Yes, requires differentiation	Yes
Supports HCV infection	Yes	No, requires CD81 and miR-122	Yes, requires differentiation	Yes

* *Low variability is available to change by variation in experimental results between different laboratories.*

II. AIM OF THE THESIS

To date, the recognition of HBV nucleic acids by PRRs remains elusive, although recent studies suggest a putative detection of the pgRNA or other HBV RNAs by either MDA5 (166) or RIG-I (159). Interestingly, HBV only weakly activates innate immune responses *in vivo* (12, 266), which suggests that HBV may be behaving as a “stealth” virus, avoiding detection of its viral DNA and RNA by the innate immune system (127). On the other hand, several studies have suggested that HBV proteins actively inhibit innate immune responses, explaining the absence of strong activation of interferon (IFN) pathways after infection (154). Consequently, the interaction of HBV and the innate immune system of hepatocytes, and especially the sensing of HBV DNA, is still only partially understood.

Detection of foreign nucleic acids by host sensors can trigger early antiviral innate immune responses (198). A recent series of studies identified cGAS (encoded by *MB21D1*) as a new DNA/RNA sensor that exhibits antiviral activity against a broad range of DNA and RNA viruses (178, 201). Binding of dsDNA to cGAS synthesizes the second messenger cGAMP to activate STING to trigger expression of type I interferon-stimulated genes through TBK1 phosphorylation (181, 226). In the context of HBV infection, a couple of recent studies highlighted the antiviral activity of the cGAS-STING pathway against HBV infection (180, 267), although some observations suggested a lack of STING expression in hepatocytes (227), which would explain the weak activation of innate immunity by HBV (266, 268). Consequently, it is still unclear how HBV infection can be detected by cGAS, and the comprehensive function of cGAS during HBV infection remains elusive. The understanding of these interactions will help to have a better comprehension of the nature of HBV regarding the innate immune sensors and may open perspectives for the development of new immune-based antiviral strategies for the treatment of this major chronic infection.

In this work, I aimed to understand the interaction between cGAS and HBV infection through different approaches. (i) First, I aimed to study cGAS expression in different cell culture systems and primary human hepatocytes to determine whether type I IFNs responses can be induced by cGAS in hepatocytes. (ii) Second, I aimed to characterize the cGAS antiviral function in the context of HBV infection using loss- and gain-of-function strategies. (iii) Third, I aimed to

investigate HBV DNA sensing by cGAS. In particular, I aimed to determine whether the HBV genome is actively sensed by cGAS during HBV infection, or whether HBV DNA is protected by its nucleocapsid as it has been suggested (269). To do so, I designed a set a genes as a marker for cGAS activity including cGAS-related genes described by Schoggins *et al* (201), as well as crucial genes of the cGAS-STING pathway and innate immune response in general. I studied the modulation of gene expression depending on HBV infection or HBV genome transfection in presence or absence of cGAS expression in the common cell culture systems that we are using. (iv) Finally, I aimed to analyze the effect of HBV infection on cGAS expression and activity. I took advantage of the gene set that I designed to analyze the effect of HBV on the expression of cGAS-related genes, in *in vitro* cell culture models as well as HBV-infected chimeric mice, to understand whether HBV could actively evade cGAS-mediated antiviral activity.

III. MATERIALS AND METHODS

1. Human-derived materials

Human material including liver tissue from patients undergoing surgical resections was obtained with informed consent from all patients. PHHs were isolated from liver tissue from patients undergoing liver resection for liver metastasis at the Strasbourg University Hospitals with informed consent. The respective protocols approved by the University of Strasbourg Hospitals, France (CPP 10-17). Surgical resections were performed by Prof. Patrick Pessaux, (Pole Hepato-digestif, Strasbourg University Hospitals) and isolation and preparation of human-derived materials was thankfully managed by Dr. L. Mailly and S. Durand (Inserm, U1110, Strasbourg, France).

2. Maintenance of cell lines and human hepatocytes

The sources for HEK 293T (270), HepG2 (270), and HepG2-NTCP (99) cells have been described. Briefly, HEK 293T cells were maintained with Dulbecco's Modified Eagle Medium (DMEM, GIBCO®) supplemented with 10% FBS. HepG2 and HepG2-NTCP cells were cultured in Dulbecco's Modified Eagle Medium (DMEM, GIBCO®) supplemented with 10% FBS, 1% non-essential amino acids (GIBCO®), and 10 µg/mL gentamycin (GIBCO®). PHHs were maintained and cultured as described (270). The HepAD38 cell line (serotype ayw, genotype D) has been reported in (271) and was kindly provided by Dr. Eberhard Hildt, Paul-Ehrlich-Institut, Langen, Germany. It is an HBV-inducible cell line that harbors an integrated tetracycline-responsive 1.2-fold HBV genome. All cells were incubated at 37°C with 5% CO₂.

3. Reagents and plasmids

DMSO, PEG 8000, poly (I:C) and CT-DNA (Calf thymus DNA used as a dsDNA control) were obtained from Sigma-Aldrich. The preS1-peptide (derived from the HBV envelope protein) and control scrambled peptide were synthesized by Bachem (Switzerland). The ECL reagent and Hyperfilms for Western blots were purchased from GE Healthcare. HBV pgRNA encoding plasmids expressing either wild-type or assembly- defective mutants were a generous gift from

Prof. Jianming Hu (Microbiology and Immunology, University Drive Hershey PA, PA, USA) (272). pReceiver-Lv151 plasmid was obtained from GeneCopoeia™. The lentiCas9-Blast, lentiCRISPR-EGFP sgRNA 1, and lentiGuide-Puro plasmids were gifts from Feng Zhang, Broad Institute of Harvard and MIT, Cambridge, USA (Addgene # 52962, # 51760 and #52963, respectively).

4. Small interfering RNAs for functional studies

Pools of ON-TARGET plus (Dharmacon) small interfering RNA (siRNA) targeting *MB21D1* (cGAS), *TMEM173* (STING), *TBK1*, and *IFI16* expression were reverse-transfected into HepG2-NTCP cells using Lipofectamine RNAi-MAX (Invitrogen) as described (270) and according to manufacturer's instructions. Cells were harvested two days after transfection and target gene expression was monitored using qRT-PCR.

5. Lentivirus production

Lentivirus particles were produced in HEK 293T cells by cotransfection of plasmids expressing the HIV gap-pol, the vesicular stomatitis virus glycoprotein (VSV-G) and either the human *MB21D1* (NM_138441.2) full ORF encoding plasmid or the empty control plasmid (Tebu-bio), or the *MB21D1*-targeting sgRNA encoding lentiGuide-Puro plasmids or the Cas9 expressing plasmid (lentiCas9-Blast) in the ratio of 10:3:10. At 3 days post transfection, supernatants were collected and then pooled and clarified using a 0.45µm filter. The collected supernatants were kept at -80 C° until use.

6. Establishment of HepG2-NTCP-cGAS overexpressing cells

For the establishment of HepG2-NTCP cells overexpressing cGAS protein, first, an antibiotic kill curve test was performed to determine the optimal concentration needed to kill around 90% of cells over the course of one week. To do that, HepG2-NTCP cells (1×10^6 cell/well) were plated on 6-well plates then cultured with medium containing neomycin (G418) in serial concentration. 200 µg/mL of G418 was chosen for selection of transduced cells. After that, HepG2-NTCP cells were plated and transduced with lentiviruses encoding either the human *MB21D1* full ORF or EGFP ORF in pReceiver-Lv151 vector (GeneCopoeia™). After 3 days,

transduced cells were cultured with 200 µg/mL of neomycin (G418). Selected cGAS-over-expressing- and control HepG2-NTCP cells were then cultured in the presence of at 200 µg/mL G418.

7. sgRNA design for CRISPR/Cas9

The Clustered Regularly Interspaced Short Palindromic Repeats (CRISPR) Type II system is a bacterial immune system that has been modified for genome engineering (273). Due to its simplicity and higher efficiency than previous methods, it has become one of the most popular approaches for genome editing. The ease of generating single-guide RNAs (sgRNAs) makes CRISPR one of the most scalable genome editing technologies.

The specificity of the Cas9 nuclease is determined by the 20 nt guide sequence within the sgRNA. For our purpose, *MB21D1* targeting sgRNA were designed using an online CRISPR Design (Broad Institute: [http:// tools.genome-engineering.org](http://tools.genome-engineering.org)) that selects suitable target sites and also offers prediction of off-target for each sgRNA. Using this program, we obtained lists of guide sequences and prediction of their off-targets effect by scores. sgRNA sequences proposed were entered into the NCBI primer BLAST software and compared with the each sgRNA database provided by Broad institute <http://crispr.genome-engineering.org/>. Finally we selected three sgRNA targeting the first exon of *MB21D1* (Table 7).

Table 7. Selected sgRNA targeting *MB21D1*

Name	guide sequence	Complementary strand	Position in the intron 1-exon	Target site
Guide 2	cgcacccctccgtacgagaa	ttctcgtacggagggatgcg	604	605-606
Guide 3	cggcccccattctcgtacgg	No	595	612-613
Guide 4	ggccgcccgtccgcgcaact	No	361	378-379

8. Validation of sgRNA by the Surveyor assay

Surveyor assay (IDT) was used to validate the capacity of the selected guides to target *MB21D1*. HepG2-NTCP cells (2×10^4 cell/well) were transfected with each sgRNA encoding

plasmid (1 µg). At 3 days after transfection, genomic DNA was extracted using the QuickExtract DNA Extraction Solution (Epicentre) following manufacturer's instruction. Briefly, transfected cells were washed with DPBS then incubated with 200 µL of QuickExtract solution for 10 min. Extracts were then incubated at 65°C for 6 minutes, 98° for 2 minutes then store the extracts at -20°C until use. Each sgRNA target site for *MB21D1* was amplified using PCR (**Table 8**). For amplification of *MB21D1* from genomic DNA, we designed 3 primer sets. Primer specificity was validated by sequencing of the amplified PCR product. After amplification, PCR product was run 1 % of agarose gel for 1 hour with 100V. Expected size of PCR product was purified using QiaQuick Spin Column (Qiagen) following the manufacturer's instruction. About 300-400ng of PCR products were used for re-annealing process to form heteroduplexes. Briefly, reannealing was performed using following conditions; 95°C for 10min, 95°C to 85°C ramping at - 2°C/s, 85°C to 25°C at - 0.25°C/s, and 25°C hold for 1 minute. After re-annealing, PCR products were treated with SURVEYOR nuclease and SURVEYOR enhancer S (Transgenomics) for 1 hour, and analyzed on 2.5% agarose gels. Only mismatched reannealed PCR fragments are susceptible to nuclease action. Gels were stained with EtBr (Ethidium bromide) and imaged with a GelDoc gel imaging system.

Table 8. PCR primer list for Surveyor assay

sgRNA	Name	Primer sequence	Length of PCR product (bp)	Expected DNA fragment size (bp)
Guide #2	P4_f	ccaaaaaggcccctcagc	452	224
	P4_r	tagctcccgggttcagca		176
Guide #3	P4_f	ccaaaaaggcccctcagc	400	186
	P4_r	tagctcccgggttcagca		214
Guide #4	P2_f	gccagtagtgcttggttcc	452	304
	P2_r	agaaccagccctggaagag		148

9. Generation of *MB21D1* knock-out cells using CRISPR/Cas9

We initially designed to generate cGAS KO cell line using co-expressing plasmid system. For that, px330 and px458 (GFP encoding) plasmids coding ampicillin resistance, a U6 promoter containing two expression cassettes controlling hSpCas9 and the sg RNA (274). sgRNA oligos

were inserted at *BbsI* restriction sites in these plasmids. Since each sgRNA was inserted into plasmid, they were each used to transform competent bacteria and plated on 100 µg/mL of ampicillin containing LB agar plate. Selected colonies were grown in ampicillin containing LB medium and then plasmid was extracted by min-prep (Qiagen). Each sgRNA insertion was confirmed by sequencing. pX330-U6-Chimeric_BB-CBh-hSpCas9 (px330) and pSpCas9(BB)-2A-GFP (PX458) plasmid were a gift from Feng Zhang (Addgene plasmid # 42230, # 48138).

Due to low transfection efficacy and difficulties of selection of transfected cells, we next used a lentiviral system to establish cGAS KO cell line. We first generated Cas9-expressing HepG2-NTCP cells by transducing HepG2-NTCP cells with the lentiCas9-Blast plasmid (275). Transduced cells were selected with 6 µg/mL Blasticidin S for 10 days. HepG2-NTCP-Cas9 cells were then seeded in six-well plates at 50% confluency 24h prior to transduction with the sgcGAS-encoding lentiviruses expressing sgRNA targeting *MB21D1* and we maintained transduced cell with puromycin. After 3 days, cGAS expression was assessed by Western blot. Finally, 4 cGAS KO clones were selected by limited dilution cloning. The cell lines cGAS KO#1 and cGAS KO#2 were used in our experiments.

10. Analysis of gene expression using qRT-PCR

Total RNA was extracted using ReliaPrep™ RNA Miniprep Systems (Promega) and reverse transcribed into cDNA using Maxima First Strand cDNA Synthesis Kit (Thermo Scientific) according to the manufacturer's instructions. Gene expression was then quantified by qPCR using a CFX96 thermocycler (Bio-Rad). Primers and TaqMan® probes for *MB21D1* (cGAS), *TMEM173* (STING), *TBK1*, *IFI16*, *IFNB1*, and *GAPDH* mRNA detection were obtained from ThermoFisher (TaqMan® Gene expression Assay, Applied Biosystems). All values were normalized to *GAPDH* expression.

11. Protein expression

The expression of cGAS, HBcAg, and β-actin proteins was assessed by Western blot. Cells were lysed in Glo lysis buffer (Promega) and protein concentration was determined using the Bradford assay (Bio-Rad) following the manufacturer's instructions. Normalized cell lysates (20 micrograms of protein) were run on a 10-12% SDS-polyacrylamide gel (SDS-PAGE) and

transferred to polyvinylidene difluoride (PVDF) membrane using the Trans-Blot® Turbo™ Transfer System (Bio-Rad). Membranes were then saturated with 5% milk PBS containing 0.1% Tween 20. Polyclonal rabbit anti-cGAS antibody (Dilution rate; 1:1000, HPA031700, Sigma), monoclonal rabbit anti-TBK1/NAK antibody (Dilution rate; 1:1000, (D1B4), Cell Signaling Technology), polyclonal rabbit anti-HBcAg antibody (Dilution rate; 1:500, B0586, Dako), and a monoclonal anti-β-actin antibody (Dilution rate; 1:1000, mAbcam8226, Abcam) were used for protein detection as described (99). Quantification of protein expression was performed using ImageJ software.

12. HBV purification and infection

The purification of infectious recombinant HBV particles from HepAD38 cells supernatants as well as HBV infection of HepG2-NTCP cells has been previously described (99, 271). Briefly, supernatant from HepAD 38 cells were collected and filtered on 0.45 micro pore filter. Next, recombinant HBV virions (strain ayw, genotype D) from HepAD38 cells supernatants were concentrated 100-fold using 8% PEG by centrifugation (5000g for 45 minutes at 4°C). The virions were resuspended in Opti-MEM solution. Virions were kept at 4°C overnight then stored at -80°C until use. For infection, HepG2-NTCP cells were plated one day prior to incubation with HBV virion from stock in the presence of 4% PEG with or without pretreatment for 1 hour with the preS1-peptide. 16 hours after HBV infection, cells were washed twice with PBS and then cultured in 2% DMSO primary hepatocyte maintenance medium (PMM). The cell culture medium was changed every two or three days for 10 days. HBV infection was assessed by quantification of pgRNA using qRT-PCR with the following primers and probe as described (99, 276): Forward primer: 5'-GGTCCCCTAGAAGAAGAACTCCCT-3'; reverse primer: 5'-CATTGAGATTCCCGAGATTGAGAT-3'; TaqMan® probe: 5'-[6FAM]-TCTCAATCGCCGCGTGCAGA-[TAMRA]-3'. HBV infection was normalized to *GAPDH* mRNA (Applied Biosystems) expression. The expression of HBcAg in infected cells was detected by Western blot using a polyclonal rabbit anti-HBcAg antibody (B0586, Dako) as described above. HBeAg in lysates from transfected cells was quantified using ELISAs N0019 (Diasorin) following manufacturer's instructions.

13. Extraction of HBV rcDNA from HBV infectious particles

For rcDNA extraction, 4 ml of HBV virions purified from supernatant of HepAD38 were prepared. HBV rcDNA was extracted using QiaAMP DNA MiniKit protocol (Qiagen) following manufacturer's instructions. Briefly, proteinase K was mixed with recombinant HBV virions and lysis buffer was added (v/v). The mix was incubated at 56°C for 10 min and then DNA was extracted using spin column centrifugation. In parallel, PEG-precipitated cell supernatants from naive HepG2-NTCP cells were used as non-virion controls. The presence of HBV DNA was confirmed by PCR and quantified by qPCR using the following primers and probe (99) : forward primer 5'-CACCTCGCCTAATCATC-3', reverse primer 5'-GGAAAGAAGTCAGAAGGCA-3'; TaqMan probe 5'-[6FAM]-TGGAGGCTTCAACAGTAGGACATGAAC-[TAMRA]-3'. Copy number of HBV DNA was determined by comparison to the standard curve created from known HBV genome copies. 1 µg of rcDNA or dsDNA (CT-DNA) were transfected in HepG2-NTCP cells using either Lipofectamine 2000 (Invitrogen) or CalPhos Mammalian Transfection Kit (Clontech) according to the manufacturer's instructions. Cells transfected with HepG2-NTCP control supernatants were used as a control. Three days after transfection, total RNA was extracted and purified as described above.

14. HBV cccDNA detection by Southern blot

Southern blot analysis of HBV cccDNA was performed using digoxigenin (DIG)-labelled (Roche) specific probes by our collaborator Dr. J. Lucifora, CRCL, Lyon, France. 30 µg of total DNA from HBV-infected cells was extracted using the previously described method (277). Equal amounts of total DNA were separated by 1.2 % of agarose gels for 24 h and then transferred to a Nylon membrane (Roche). Specific DIG-labelled probes for the detection of HBV and mitochondrial DNAs (mtDNA) were synthesized using the PCR DIG Probe Synthesis Kit (Roche), primers are detailed **Table 9**. After probe hybridization on the membrane (DIG-easy Buffer, Roche), HBV and mtDNA were detected using DIG Luminescent Detection Kit (Roche) according to the manufacturer's instructions.

Table 9. The list of probes to detect HBV cccDNA and mitochondrial DNA; from reference (278)

Target	Name	Sequence
HBV	HBV-F1	TAGCGCCTCATTTTGTGGGT

	HBV-R1	CTTCCTGTCTGGCGATTGGT
	HBV-F2	TAGGACCCCTGCTCGTGTTA
	HBV-R2	CCGTCCGAAGGTTTGGTACA
	HBV-F3	ATGTGGTATTGGGGGCCAAG
	HBV-R3	GGTTGCGTCAGCAAACACTT
	HBV-F4	TGGAACCTTTTCGGCTCCTC
	HBV-R4	GGGAGTCCGCGTAAAGAGAG
	HBV-F6	TACTGCACTCAGGCAAGCAA
	HBV-R6	TGCGAATCCACACTCCGAAA
	HBV-F8	AGACGAAGGTCTCAATCGCC
	HBV-R8	ACCCACAAAATGAGGCGCTA
Mitochondrial DNA	Fw_huND1	CCCTACTTCTAACCTCCCTGTTCTTAT
	Rw_huND1	CATAGGAGGTGTATGAGTTGGTCGTA
	Fw_huND5	ATTTTATTTCTCCAACATACTCGGATT
	Rw_huND5	GGGCAGGTTTTGGCTCGTA
	Fw_huATP6	CATTTACACCAACCACCCAATATC
	Rw-huATP6	CGAAAGCCTATAATCACTGTGCC

15. Transcriptomic analysis using nCounter NanoString

nCounter NanoString technology enables detection of a specific set of nucleic acid sequences at high through-put. The pairs of target gene specific probes with biotin encoding and color-coded tags provide a detection signal, called the “barcode”. Different combinations of barcode colors provide a detection signal corresponding to the genes of interest.

Transcriptomic analyses using nCounter NanoString were performed according to the manufacturer’s instructions. Specific probes for a set of 39 cGAS-related genes (see **Table10**) were chosen according to previous published data (201) and were obtained from the manufacturer. HepG2-NTCP cells, HepG2-NTCP-Cas9 cells and HepG2-NTCP-KO cGAS#2 cells were infected with HBV for two days. Alternatively, HepG2-NTCP cells were transfected with poly (I:C) (100ng) for two days, and HepG2-NTCP-Cas9 cells and HepG2-NTCP-KO cGAS#2 were transfected with rcDNA (1µg) or dsDNA (CT-DNA, 1µg) for three days. Total RNA was then extracted and analyzed using the nCounter Digital Analyzer system (NanoString). cGAS-related

genes were considered as an artificial gene set and the modulation of this gene set depending on the experimental conditions was determined using GSEA (Gene Set Enrichment Analysis) (279). False Discovery Rate (FDR) < 0.05 was considered statistically significant. Data analysis was thankfully performed by Dr. H. El-Saghire (Inserm, U1110, Strasbourg, France).

Table 10. Specific probes for a set of cGAS-related genes

Gene	Accession Number	Target Sequence	Note
ATP5B	NM_001686.3	GAAATTCGGTACATGGTATCGATCGTACGCTCCCTA TGCCAA GGGTGGCAAAA TTGGGCTTTTGGTGGTGGTGGACTGGCAAGACTG	HG
BAG6	NM_001198698.1	CAITGATCAACGGGGCTAGAAAGATATGCGGGAGAGTTTTCCITGGTGCAGITTCACCCAGGTGTGGACATCATCGGCACA AACCTGGAA ITTCTCCA	HG
NDUFA2	NM_001185012.1	ATGGCTAGGGCTTAA GGGTCCGGGTTGGTCA GCGGAGCACTGGCCGAA GACCTGTGAA ITGGGACCTTCCGATA ITAACAA GGTGGCGGCGCGC	HG
ARL9	NM_208919.1	CAGATA TCCATGAA GCTTTGGCA ITTACTGAA GTGGGAAATGACGGAAGATGTTCT ITGTTGGAA CCTACCTGATGAAATGGCTCA GAGATA CCCCTC	Schoggins
CASP1	NM_001223.3	TGGAGACATCCCACTGGGCTGTTTTT TGGAAAGTCA ITGAAACA TATGCAAGAA TATGCCCTGTCTCTGTA ITGGAGAAATTTTCCCAAG	Schoggins
CXCL16	NM_001100812.1	CCATGGGTTCCAGGAA ITGATGACTGTCTGATCTCAAGAA ITGTGGACA TGCITACTCGGGATGTGGCCACCAGAA AGCATTTCTCTACCAGCC	Schoggins
CXCL8	NM_000584.2	ACAGCAGACACAA GCTTATAGGCAAGCCACGGAAGAAACCGGAA GAAACCACTCACTGTGTGTTAAACA TGACTCCAA GCTGGCCGTGGCT	Schoggins
HERC5	NM_016323.2	TGGGCTGCTTTACTTTCCGTTGGTAAACATGGGCAAC ITTGGTCA TAAITCAA CACAGAA TGAAGTAA GACCCTGTTGGTGGCTGAGCCTTTGTTGGG	Schoggins
HERC6	NM_001165136.1	TCCATCA CCA GATTTA TACTTGA GTCA GCGAA GTCCGCTGGTTAAAGATGCTCTGCGTCAA ITTAA GTCAA GCTGAA GCTATGACTTCTGCAAAGTA	Schoggins
HLA-B	NM_005514.6	CCCTGAGATGGGAGCCGCTTCCCA GTCCACCGTCCCA TGTGGGCA ITTGTCTGGCTGGCTGCTCTAGCA ITTGGTCA TCGGAGCTGTGGTCCG	Schoggins
HLA-H	NR_001434.3	GAGGGGAGGGCCGGAGTATGGGACCGAACA CACAGATCTGCAA GGGCCAA GCA CCGA CTGAA CCGA GAA CCGTGGGATCGGGCTCCGCTACTACA	Schoggins
IFI35	NM_005533.3	TGCCCTCTGCTTTCGGGCTCTGCTCTGATCA CCTTTGATACCCCAAGTGGCTGAGCA GGTGCTGCAACAAA GGA GCA CACGATCAACA TGGAGGAGT	Schoggins
IFI44	NM_006417.4	GATGAAA GAAA GATAAAA GGGGTCA ITTGA GCTCA GGAAGAGCTTACTGTCTGCCCTTGA GAACCTTATGAA CCA TATGGA TCCCTGGTTCAACAAA TACGAA	Schoggins
IFIH1	NM_022168.2	GCITGGAGAA ACCCTCTCCCTCTCTGAGAAA GAAA GATGTC GAATGGTA ITCCACA GACGAA ITTCCGCTATCTCA TCTCTGTGCTCA GGGCCAGG	Schoggins
IFI3	NM_001031683.2	CGCCTTAAGGGATGCCCTTCA GCGCA TAGGAGATA ITTCTGTGCA GCA TGTGAGCTGAGGATGTTAGGAA ATTTGGGCA GGGCGAGGTCA GCT	Schoggins
IGS20	NM_002201.5	AGCCCGCAGGGCTGCCCTGGCTGTGTGACGATGAA GCGCCCA TCCAGCCGCTTCCGCA GGGACTAGAGGCTTCCGCA ITTITGGGACAGCAACTA	Schoggins
LRRC17	NM_001031692.1	CAGCACAACCA GATCAAAGTCTTGAGCGGAGGAGTGTCA ITTACACACCTCTCTTGA GCTACCTCGCTTTATGACAA CCCCCTGGCACTACTTTGTG	Schoggins
MX1	NM_002462.2	GCCTTTAATCA GGCATCACTGCTCTCA TCGAAAGGAGGAAACTGTAGGGGAGGAA CACATCGGGCTGTTTACAGACTCCGACACGATCCACAAAT	Schoggins
OAS2	NM_016817.2	TGAAAA CAA ITTTCGAGATCCAGAA GTCCCTTATGGGTTCA CCA TCCAGGTTTCA CAAAATATCA GAAATCTCTTCGAGGCTGGCGCCCTCAA	Schoggins
OASL	NM_198213.1	GGGCTTCTGAGCTTTCCACA GCTTCCAGAGGCA GCGCAAGATGTTCTGAGGCTGTA TATGAAAA CCA ITGTGGCAAA GCCA GGA CCTG	Schoggins
PLC62	NM_002681.2	GCITGAAAA TCTTACACAGGAA GCGATGAA TCCGTCACCGCCACCA TATCGAGATGGCTGAGAAA GCGATA TATCTGTGGATCAA ACCAGAA G	Schoggins
PSMB8	NM_004159.4	ACTCACAGACACGCTATCTGSGAGCCTGTCAA TATGTACCA CATGAA GGAAGATGTTGGTGAAGTA GAAA GTACAGATGTCAGTCCCTGCTGC	Schoggins
PSMB9	NM_002800.4	TCAGGTATATGAAA CCC TGGGAGAA TCGTCACTCGACAGCC ITTGGCCATTTGGGCTCCGCA CACC ITTATCTATGTTATGTGGA TGCA GCA TAT	Schoggins
RARRS3	NM_004585.3	CTGACCCCTGTCGCCCTG TCA GGGGTTCTCTAGATCCTTCTCTGTTCCCTCTCCGCTGGCAAAA GTA TGA TCTAA ITGAAA CAA GACTGAA GGT	Schoggins
SLC15A3	NM_016582.1	GCCGCTTTCAACTGGTTTTA CTGGACATCAA CCTGGGTGCTGTGCTGTGCTGTGGTGGGTTTTA TCA GCGAACA TCA GCTTCTGCTGGG	Schoggins
TNFRSF1B	NM_001066.2	CCAGCTGAA GGGAGCACTGGGACTTCGCTCTTCA GTTGA CTGA ITTGGGTGACAGCC ITGGGCTACTATA TAA TGA GTGTGAACTGTGTC	Schoggins
UBA7	NM_003335.2	GCGGGAGGATGGTCCCTGGAGA ITGGAGACACAACA ITTCTCTCGTACTTCCGCTGGGCTATCACTGAA GTCAA GACCCAA GACTGTGAGA	Schoggins
UBE2L6	NM_004223.3	TGTTTTAAAA CCACTTGGCATCCTGTITAGA ITGCCAGTTCCTGGGACCA GGCCTCAGACTGTGAA GTATATATCC TCCA GCA ITCA GTCAGTCCAGGGGAGCC	Schoggins
ZC3HAV1	NM_020119.3	CTCCTCTTCA CATCTGTA GAAA CATGGCATA TAGGGCTAGAA GCAAGATAGAGATCGGTGTTTCA GGGCA GCCAA GAA ITTCTTGGGCTGTCTCA GC	Schoggins
ZMYND15	NM_032285.1	CCTGAGAGCGGCCGACAA CTGCA TGTCTGGTACTGCA ATGCCCTTCACTTCCACCTTGGTTTCAA AGCTGTCAA GGA GCGGGCCCGCCCGCGCC	Schoggins
PMALIP1	NM_021127.2	CTAGTTTTTCCGGA GATA CCGCTGGCTACTGTGAA GGGAGTAGCTGTGTA ITAGACTGGGCGGCTGGGAGAAA CAGTTCAGTGA TTTGTTT	Schoggins
GBP4	NM_052941.4	TTCTACAA GATATGCCATGGGCTTTTCA CAGGGACACAGGCTTTTAAACAACC GGGCTTCTCA CCGCTATGCTCTTTTATA CAA GCTGTGCTCC	Schoggins
TMEM173	NM_198282.1	CTGGCATGTGCTATA ITACA TCGGATATCTCGCGTGA TCTCGCAGGCTCCAGGCTCCAGGCTCCCA GGGCCGGA ITCGAA CTTACAATCA GCA TTAACAACCTGCTACGGG	STING
IFIH6	NM_005531.1	ACGACTGAA CAAATCAAA CTGTGAGGAA GGA TAAACTGAAACTCA CCA GCTTTGAA ITGGCACCCGAAA GTGGGAA TACCGGGGAGTTGAGATCTGTA	
IFNB1	NM_002176.2	ACA GACTTACA GGTTACCTCCGAAA CTGAA GATCTCTCA GCTCTGTGCCCTCTGGGACTGCA AATTTGCTCAA GCA TTTCTTCAA CCA GCA GATGCTTTTA	
IRF3	NM_001571.5	TCA TGGCCCA GGA CCGCTGGACCA GCGCTGCTGTGATGGTAAAGGTTTGGCCAC GGGCTTCA GGGCTTGGTATGAA ITTCCGCGGGTGA GGGGGT	
IRF7	NM_001572.3	CAGACGCTGA GGGTGTCTCCCTGGATGAGGACCGCTTGCCTTGCCTGCTCCAGCCCTTCA CCGCTTCA GCGCCAA CAGCTCTATGACGACATCGAGTCTTCCATATGA	
STAT1	NM_139266.1	ACAGTGGTTAGAAA GCAA GACTGGGAGCAGCTGCCCA TGA TGTTTCA ITTGCCACCA TCCGTTTTTCA TGACCTCTGCA CCGTGTCA CAAT	
TBK1	NM_013254.2	ACCA GCTTCA GGGATACAGACAGATATCTCCAGGTGGA TCACTGGCAGCGGATGGGCACTCAA GGGCACTCAA TCCGAAA GACAGAAATGTAG	

HG, Housekeeping genes; Schoggins, cGAS-related gene list described by Schoggins et al., Nature 2014 (201)

16. HBV infection of human liver chimeric mice

These experiments were carried out in our animal facility at the UMR_S1110. Production of chimeric mice, HBV infection and harvesting of mouse livers was thankfully performed by Dr. L. Maily (Inserm, U1110, Strasbourg, France). Isolated PHH were transplanted into 3 weeks-old uPA/SCID-bg mice by intrasplenic injection as described (280). Transplantation of PHH into mice liver was assessed 4 weeks later by quantification of human serum albumin by ELISA (ref. E80-129, Bethyl Laboratories). Humanized uPA-SCID mice were then infected with HBV and sacrificed 16 weeks after virus inoculation. HBV viral load in the mouse serum was determined by qPCR (Laboratoire Schuh-groupement Bio67) before sacrifice. Analysis of cGAS expression and the cGAS-related genes (cGAS signature) in the livers of HBV infected mice was performed by myself as described above. All mice were kept in a pathogen-free housing facility. The respective protocols were approved by the Ethics Committee of the University of Strasbourg Hospitals (number AL/02/19/08/12 and AL/01/18/08/1202014120416254981 and 02014120511054408).

17. Statistical Analysis

Each *in vitro* experiment (except digital multiplexed gene profiling experiments) was performed at least three times in an independent manner. Statistical comparisons of the samples were performed using a Mann-Whitney U test. For *in vivo* experiments, a two-tailed unpaired Student's t-test was performed to compare gene expression in non-infected and HBV-infected mice. $p < 0.05$ (*), $p < 0.01$ (**), and $p < 0.001$ (***) were considered significant. Significant p values are indicated by asterisks. Each digital multiplexed gene profiling experiment was performed using three biological replicates per condition and the induction or repression of the gene set was analyzed using GSEA. FDR < 0.05 was considered statistically significant.

IV. RESULTS

Several studies recently reported the antiviral function of cGAS against HBV using transfection systems (198). They described that cGAS displays anti-HBV activity targeting viral replication and assembly (267), and that transfection of dsDNA fragments derived from HBV was detected by cGAS, resulting in the induction of innate immune response (180). However, it still remains largely unexplored whether the cGAS-STING pathway exerts an antiviral action against HBV infection, and if detection of HBV DNA by the host cellular sensors occurs in the infected cell. My PhD work aimed to study the functional role of cGAS in the HBV life cycle and unravel the mechanisms of viral evasion using loss- and gain-of-function experiments combined with cGAS effector gene expression profiling in an infectious cell culture model and HBV-infected humanized chimeric mice.

1. cGAS expression in different cell types

The HepG2 cell line is commonly used as a cellular model for HBV replication studies. However, the lack of HBV receptors at their surface hampered infection studies. Recently, NTCP was identified as the first receptor for HBV entry (98). Indeed, Yan *et al.*, demonstrated that NTCP overexpressing HepG2 cells became susceptible to HBV infection, as demonstrated by detection of HBV pgRNA and HBsAg at 10 days post-inoculation (dpi). In this study, we used HepG2-NTCP cells established in our laboratory that are highly permissive to HBV infection (99).

Several studies reported that the basal level of cGAS expression is very low in the hepatic cell lines that are suitable for HBV infection studies (180, 267). Thus, prior to functional characterization of cGAS, we first investigated whether cGAS protein is expressed in different cell types by Western blot. As we show in **Figure 21**, cGAS protein expression was clearly detected by Western blot in HepG2 and HepG2-NTCP hepatoma-derived cell lines, as well as in PHH from two different donors. Expression of cGAS in PHH was at similar levels as observed in HepG2-NTCP cells. We also validated the specificity of cGAS detection using siRNA (sicGAS) specifically targeting the expression of *MB21D1*. HEK 293T cell lysates were used as a negative control (178).

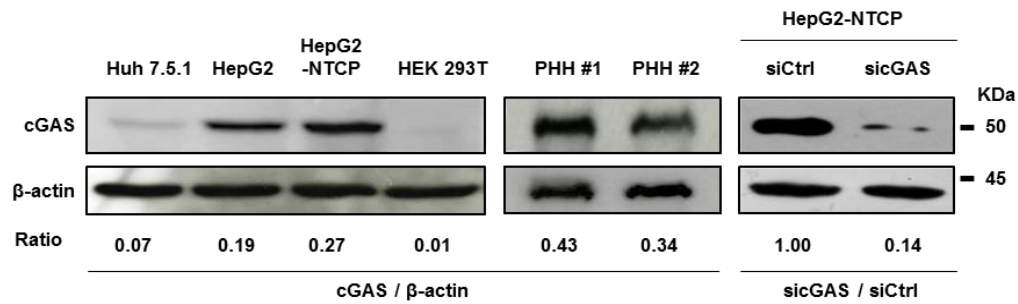


Figure 21. HepG2, HepG2-NTCP cells, and PHH express cGAS

Detection of endogenous cGAS protein expression in different cell types by Western blot. Cell lysates from Huh7.5.1, HepG2, HepG2-NTCP, and HEK 293T were used, as well as lysates from PHH isolated from two different donors (PHH #1 and PHH #2). HepG2-NTCP cells were reverse transfected with a siRNA targeting *MB21D1* (sicGAS) or a non-targeting siRNA control (siCtrl) two days before cGAS detection. Protein expression was normalized to β -actin and was quantified using the ImageJ software. (Yim, Verrier *et al.*, 2017, submitted to Gut).

2. Validation of the HepG2-NTCP cells as a model to study innate immune responses

Aiming to perform functional perturbation studies, we next characterized the innate immune responses in the HepG2-NTCP cell line established in our laboratory, cell line that is robustly permissive to HBV infection (99). We confirmed the ability of HepG2-NTCP cells to induce *IFNB1* expression following stimulation by poly (I:C) (100 ng/1X10⁵ cells in 24-well plate), a well-known innate immune inducer, or increasing concentrations (from 0.5 to 4 micrograms/ 1X10⁵ cells) of CT-DNA (dsDNA), a known cGAS activator following transfection (222, 281). As presented **Figure 22**, we observed a three log increase in the level of *IFNB1* expression 3 days following poly (I:C) transfection. Similarly, transfection of 2 μ g CT-DNA lead to around 5 fold increase in *IFNB1* expression.

Moreover, cGAS protein expression was induced by both poly (I:C) (around 5 times) (**Figure 22A**) and CT-DNA (2.44 times, 4 μ g transfection) stimulation (**Figure 22B**), further confirming the ability of our cell culture model to establish an efficient IFN response leading to the upregulation of ISGs. *IFNB1* induction was decreased when cells were transfected with 4 μ g of CT-DNA, whereas cGAS protein expression already increased (**Figure 22B**), suggesting a negative feedback regulation of IFN responses by cGAS expression (282).

The poly (I:C) and CT-DNA experiments demonstrate that robust innate immune responses are obtained in these cells and that the HepG2-NTCP cell line is suitable for functional studies.

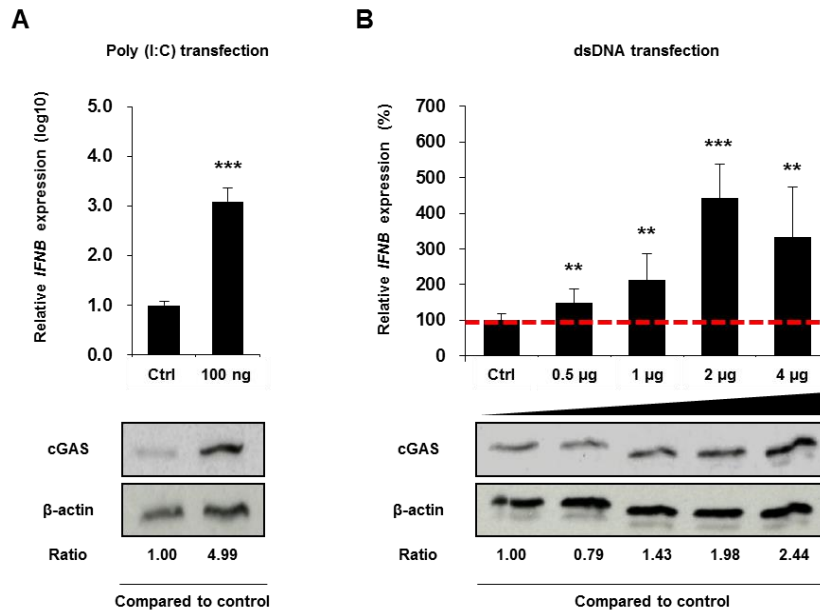


Figure 22. HepG2-NTCP cells express cGAS and induce *IFNB1* expression

The poly (I:C) and CT-DNA (dsDNA) transfection induce *IFNB1* expression in HepG2-NTCP cells. HepG2-NTCP cells were transfected with 100 ng of poly (I:C) (A) or CT-DNA (B) at the indicated concentrations. *IFNB1* mRNA expression was quantified by qRT-PCR, and cGAS protein expression was assessed by Western blot 72 hours after transfection. Gene expression was normalized to *GAPDH* mRNA expression. Data are expressed as means \pm SD from three independent experiments performed in triplicate. *IFNB1* expression was compared to Ctrl (set at 1(A) and set at 100 (B)). β -actin was detected as a Western blot loading control. Protein expression normalized to β -actin was quantified using the ImageJ software. $p < 0.01$ (**), and $p < 0.001$ (***) were considered significant. (Yim, Verrier *et al.*, 2017, submitted to Gut).

3. Decrease in cGAS-, STING-, and TBK1 expression leads to an increase in HBV infection

Previous work performed at UMR S1110 had aimed to evaluate the antiviral activity of the cGAS-STING pathway in HBV infection. Thus, expression of *MB21D1* (encoding the cGAS protein), *TMEM173* (encoding the STING protein), *TBK1* and *IFI16* (encoding the gamma-

interferon-inducible protein 16) were silenced using specific siRNA in HepG2-NTCP cells 2 days prior to infection with HBV. HepG2-NTCP cells (2×10^4 cell/well in 96-well plate) were infected with HBV. Sixteen hours after infection, cells were cultured with 2% DMSO containing medium. HBV pgRNA level was assessed at 10 dpi by qRT-PCR. As shown in **Figure 23**, silencing of *MB21D1*, *TMEM173* and *TBK1* expression induced a two-fold increase in HBV infection at 10 dpi. In contrast, silencing of *IFI16* had no effect on HBV infection.

Since IFI16 is a cytoplasmic DNA sensor able to activate STING independently of the cGAS-STING pathway (198), these data suggest that HBV infection in HepG2-NTCP cells might be hampered by a cGAS-specific antiviral activity.

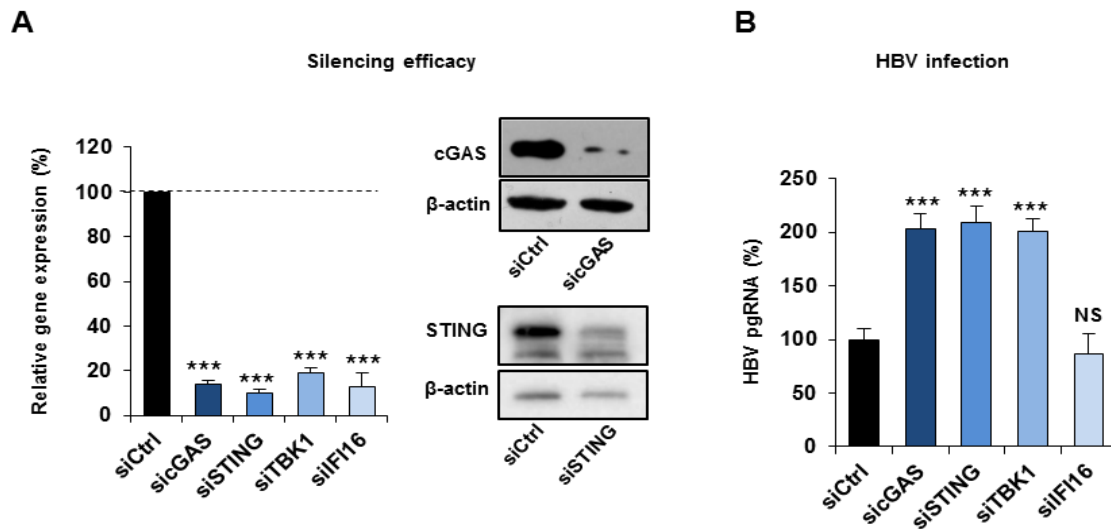


Figure 23. The silencing of cGAS-related gene expression increases HBV infection

siRNA targeting *MB21D1* (siGAS), *TMEM173* (siSTING), *TBK1* (siTBK1), *IFI16* (siIFI16) or a non-targeting siRNA (siCtrl) were reverse transfected into HepG2-NTCP cells 2 days prior to HBV infection. Silencing efficacy was assessed by qRT-PCR and silencing of cGAS and STING protein was assessed by Western blot 2 days after siRNA transfection (**A**). Gene expression was normalized to *GAPDH* mRNA. Results are expressed as means \pm SD % gene expression relative to siCtrl (set at 100%) from four independent experiments performed in technical duplicates. β -actin was detected as a Western blot loading control. (**B**) HBV infection was assessed by quantification of HBV pgRNA by qRT-PCR at 10 dpi. Gene expression was normalized to *GAPDH* mRNA expression. Non-significant results are indicated as NS. Results are expressed as means \pm SD % of HBV pgRNA expression relative to siCtrl (set at 100%) from four independent experiments performed in technical duplicate. $p < 0.001$ (***) were considered significant. (Yim,

4. Validation of sgRNA using Surveyor assay

In order to confirm the cGAS-mediated antiviral activity, we generated *MB21D1* (cGAS) KO cell lines using the CRISPR/Cas9 approach. For that, we designed *MB21D1* targeting sgRNA using an online CRISPR Design tool. First, we designed three sgRNA targeting different sites within the first exon of *MB21D1*. Each sgRNA was cloned into plasmids co-expressing Cas9 (px330 and px458, co-expressing plasmid). Insertion of the sgRNA was confirmed by sequencing. To validate their gene knock-out efficiency, each sgRNA encoding plasmid was transfected into HepG2-NTCP cells (1×10^5 cell/well in 24-well plate), and then genomic DNA was extracted 48 hours after transfection. To validate the capacity of the sgRNA target properly the first exon of *MB21D1*, we performed a Surveyor nuclease assay. Surveyor nuclease recognizes mismatches in dsDNA and cleaves single base mismatch or small insertions or deletions (indels). As shown in **Figure 24**, expected DNA fragments were obtained using guide #3 (Red stars). We obtained unexpected DNA fragments for guide #4 (approximately 340 bp instead of 304 bp, Blue stars) transfection compared with control. This may be explained by the fact that guide #4 targets another sequence within the first exon of *MB21D1*. According to these results, we used guide #3 encoding plasmids for the generation of cGAS KO cells.

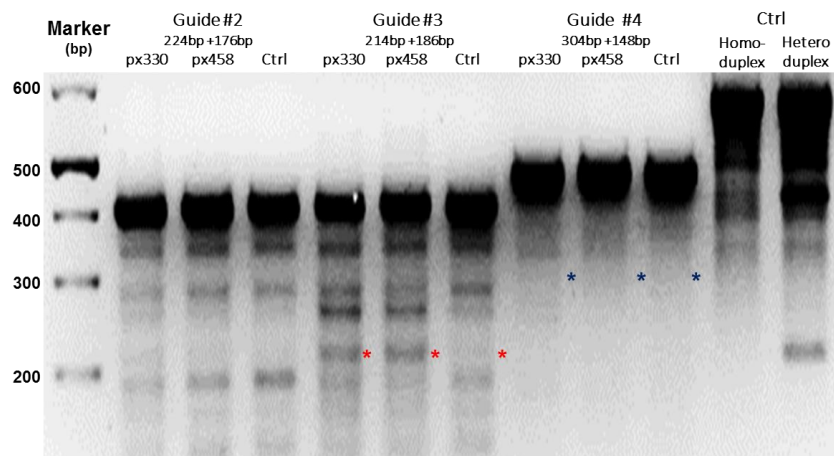


Figure 24. Representative gel image showing a typical Surveyor nuclease assay

Digestion products were analyzed by gel electrophoresis on a 2.5% agarose gel. 400 bp PCR product was

amplified from genomic DNA extracted from empty plasmid (Ctrl), guide #2, and guide #3 transfected cells. 452 bp amplicon was produced from genomic DNA extracted from guide #4. It represents the unmodified genomic target. Around 214 bp of DNA fragment indicates the presence of indel (Guide 3, red star). Unexpected dsDNA fragments (around 340 bp) were observed in (guide #4) transfected cells. Homo/Hetero duplex, provided by the manufacturer, were used as a Surveyor assay control.

5. Selection of cGAS KO cells generated by co-expressing plasmid system

HepG2-NTCP cells were transfected with guide #3 encoding plasmids (1×10^5 cell/well in 24-well plate). Due to low transfection efficiency (around 30%) and impossibility to apply specific antibiotic selection (the cell line and the plasmids had the same antibiotic resistance), transfected cells were immediately selected from the whole population by limited dilution cloning and were cultured independently. Approximately 2-3 weeks later, cGAS expression was tested by Western blot. In total, 30 colonies were grown and around 10 individual clones were tested for cGAS expression. Unfortunately, cGAS protein was detected in all tested clones, and genomic modification was not observed after sequencing (Figure 25). In order to overcome these difficulties, we decided to apply an alternative strategy by using lentiviral expressing systems to generate cGAS KO cells.

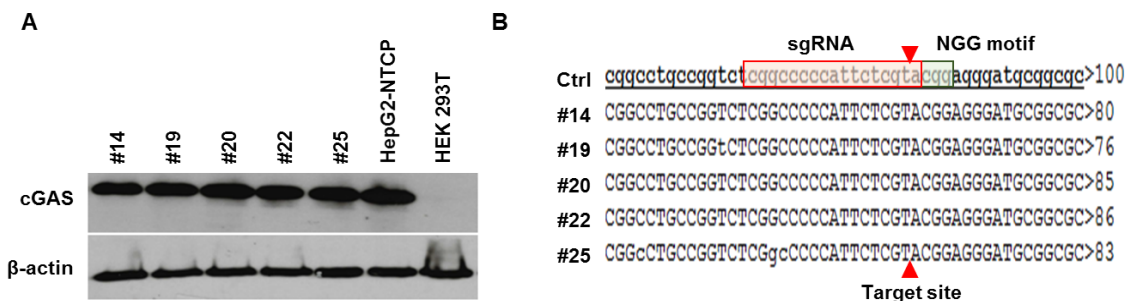


Figure 25. Validation of cGAS KO cells generated by co-expressing plasmid system

cGAS targeting sgRNA (guide #3) encoding co-expressing plasmid (px330) were transfected into HepG2-NTCP cells. Transfected cells were selected by limited dilution cloning. About 2-3 weeks after incubation, cGAS expression in each single colony was validated by Western blot (A). HEK 293T lysates were used as a negative control. β -actin was detected as a Western blot loading control. (B) cGAS KO was validated by sequencing. sgRNA and NGG motif of guide #3 position is indicated by color boxes and sgRNA target

site is pointed the by red narrow.

6. Establishment of cGAS KO cell lines using the lentivirus transduction

To improve transduction of sgRNAs, I next used lentivirus transduction system to generate cGAS KO cells. Prior to generate sgRNA encoding lentiviruses, we established stable Cas9 expressing HepG2-NTCP cells. To do that, we performed antibiotic kill curve tests to determine the antibiotic concentration useful for selection. First, HepG2-NTCP cells (1×10^6 cell/well) were seeded on 6-well plate then cultured with medium containing Blasticidin S in serial concentration. Six $\mu\text{g}/\text{mL}$ of Blasticidin S was chosen as the concentration useful for optimal selection of the transduced cells. After that, I transduced HepG2-NTCP cells with lentiviruses encoding Cas9 and further cultured the cells for 10 days with 6 $\mu\text{g}/\text{mL}$ Blasticidin S containing culture medium. To select high level of Cas9 expressing HepG2-NTCP cells, cells were highly diluted and then cultured again for 2 weeks. Finally, 4 different highly Cas9 expressing cells were selected (#1, #7, #8, and #22). Meanwhile, cGAS sgRNA (we used the same sgRNA as for the co-expression system) was inserted into a lentiGuide-Puro plasmid. *MB21D1* (cGAS) targeting sgRNA encoding lentiviruses were produced and transduced in the 4 different clonal HepG2-NTCP-Cas9 cells. Sixteen hours after transduction, medium was replaced. cGAS expression was validated by Western blot 3 days after transduction. As shown in **Figure 26**, cGAS expression decreased in both guide #3 encoding lentivirus transduced HepG2-NTCP-Cas 9 #8 (refer to as #8-3) and guide #4 encoding lentivirus transduced HepG2-NTCP-Cas 9 #22 (refer to as #22-4). These cells are referred as pool cGAS KO cell lines.

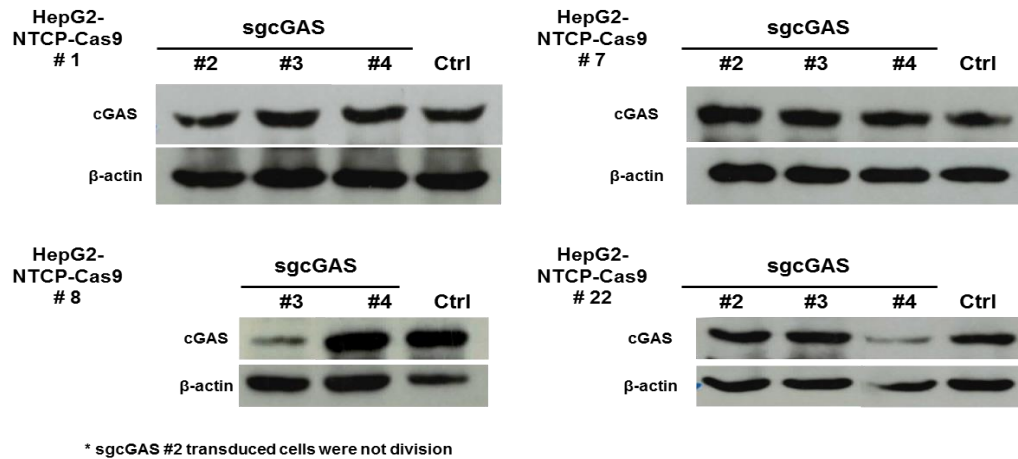


Figure 26. Validation of pool cGAS KO cell lines

cGAS gene targeting sgRNA encoding lentiviruses were transduced in single clonal HepG2-NTCP-Cas9 cells. Medium was change 16 hours after transduction. Transduced cells were harvested 2 days after further incubation. Twenty μg of total cell lysates were used for Western blot. β -actin was detected as a Western blot loading control. HepG2-NTCP-Cas9 cells were used as a control (Ctrl).

Since a low level of cGAS was still expressed in pool cGAS KO cells, cGAS KO cells #8-3 were seeded at limiting dilution and further cultured to select clonal cGAS KO cells. Approximately 2-3 weeks after, 9 clonal cGAS KO cells were selected and tested by Western blot for cGAS expression. Finally, we selected two single clones of cGAS KO cells #1 (referred to as cGAS KO#1) and #3 (referred to cGAS KO#2) for further investigation (**Figure 27**).

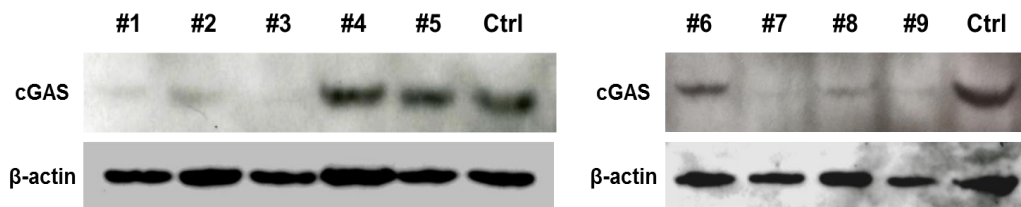


Figure 27. Validation of clonal cGAS KO cell lines

Pool cGAS KO cells were plated at limiting dilution. After 3 weeks, 9 clonal cGAS KO cells were tested by Western blot for cGAS expression. 20 μg of total cell lysates was used for Western blot. β -actin was detected as a Western blot loading control. HepG2-NTCP-Cas9 cell lysates were used as a control (Ctrl). (Yim, Verrier *et al.*, Gut, Submitted).

7. Confirmation of the role of cGAS in the regulation of HBV infection

As a confirmation of the cGAS role in HBV infection, cGAS KO cell lines (cGAS KO#1 and cGAS KO#2; 2×10^4 cell/well in 96-well plate) were infected with HBV. At 10 dpi, the level of pgRNA was assessed by RT-qPCR in the two selected cGAS KO cell lines and compared to HBV infected HepG2-NTCP-Cas9 cells as a control. As shown in **Figure 28A**, the absence of cGAS led to a significant increase in HBV infection reaching 3 fold in cGAS KO#1 and 5 fold in cGAS KO#2 cells. As a further confirmation of cGAS antiviral function, cGAS overexpressing HepG2-NTCP cells were generated in our laboratory. cGAS overexpressing cells (cGAS OE) and control cells derived from HepG2-NTCP cells (Ctrl ORF) were infected with HBV and again, pgRNA was quantified at 10 dpi. As shown in **Figure 28B**, the overexpression of cGAS led to a significant decrease in HBV infection (around 40%), validating the antiviral effect of the cGAS in our model.

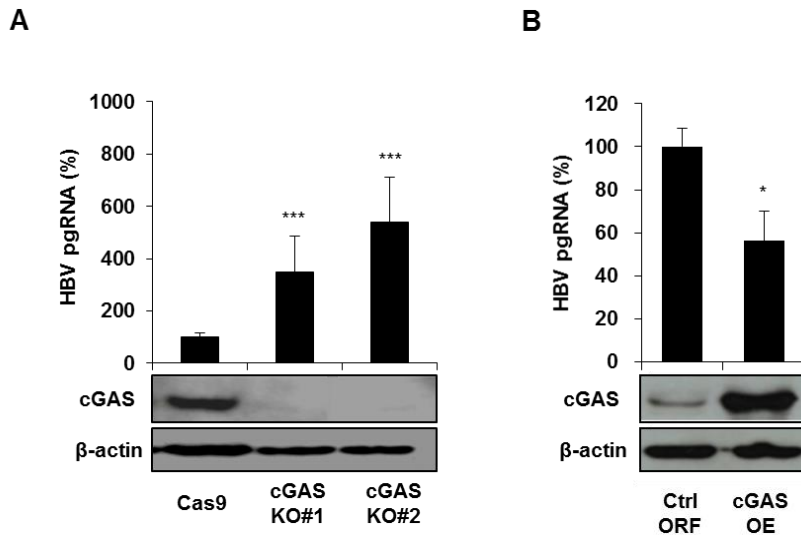


Figure 28. cGAS expression alters HBV infection

(A) Knock-out of the *MB21D1* gene increases HBV infection. *MB21D1* KO HepG2-NTCP cell lines (cGAS KO#1 and cGAS KO#2) were generated using CRISPR/Cas9 technology. The absence of cGAS protein was confirmed by Western blot (lower panel). β-actin was detected as a Western blot loading control. HepG2-NTCP-Cas9 (Cas9) and cGAS KO cell lines (cGAS KO#1 and cGAS KO#2) were infected with HBV and viral infection was assessed by pgRNA quantification by qRT-PCR. Gene expression was normalized

to *GAPDH* mRNA expression. Results are expressed as means \pm SD % HBV pgRNA expression relative to control cell line (Cas9, set at 100%) from three independent experiments performed in triplicate. **(B)** HepG2-NTCP cells were transduced with lentiviruses encoding either a control plasmid (Ctrl ORF) or a plasmid encoding the full-length of *MB21D1* ORF (cGAS OE). cGAS protein expression was assessed by Western blot (lower panel). β -actin was detected as a Western blot loading control. Cells were then infected with HBV and viral infection was assessed at 10 dpi as described above. Gene expression was normalized to *GAPDH* mRNA expression. Results are expressed as means \pm SD % HBV pgRNA expression relative to Ctrl ORF (set at 100%) from three independent experiments performed in triplicate. $p < 0.05$ (*) and $p < 0.001$ (***) were considered significant. (Yim, Verrier *et al.*, 2017, submitted to Gut).

Next, I analyzed the role of cGAS in HBV replication by detection of HBV DNA. For that, I validated the specificity of HBV DNA detection by treatment of HBV preS1-derived peptide, which inhibits HBV infection by binding to NTCP. After pre-incubation of HBV preS1-derived peptide and Ctrl peptide in HepG2-NTCP cells, cells were infected with HBV and level of HBV DNA was detected at 10 dpi. As shown in **Figure 29A**, HBV infection was inhibited by preincubation of preS1-peptide, resulting in low levels of rcDNA and cccDNA compared with Ctrl-peptide treated cells (HBV (+) with Ctrl). After that, the level of cccDNA in cGAS KO cells (cGAS KO#1 and cGAS KO#2) and cGAS overexpressing cells, at 10 dpi was analyzed. Genomic DNA was prepared from these cells and the level of cccDNA was quantified at 10 dpi by Southern blot (performed in collaboration with Dr. J. Lucifora, CRCL, Lyon, France). As shown **Figure 29B**, the level of cccDNA was significantly increased in cGAS KO cells (1.5 fold increase in cGAS KO#1 and 4 fold increase in cGAS KO#2 cells) and decreased in cGAS overexpressing cells (cGAS OE) (around 50 % decreased) as compared with the control.

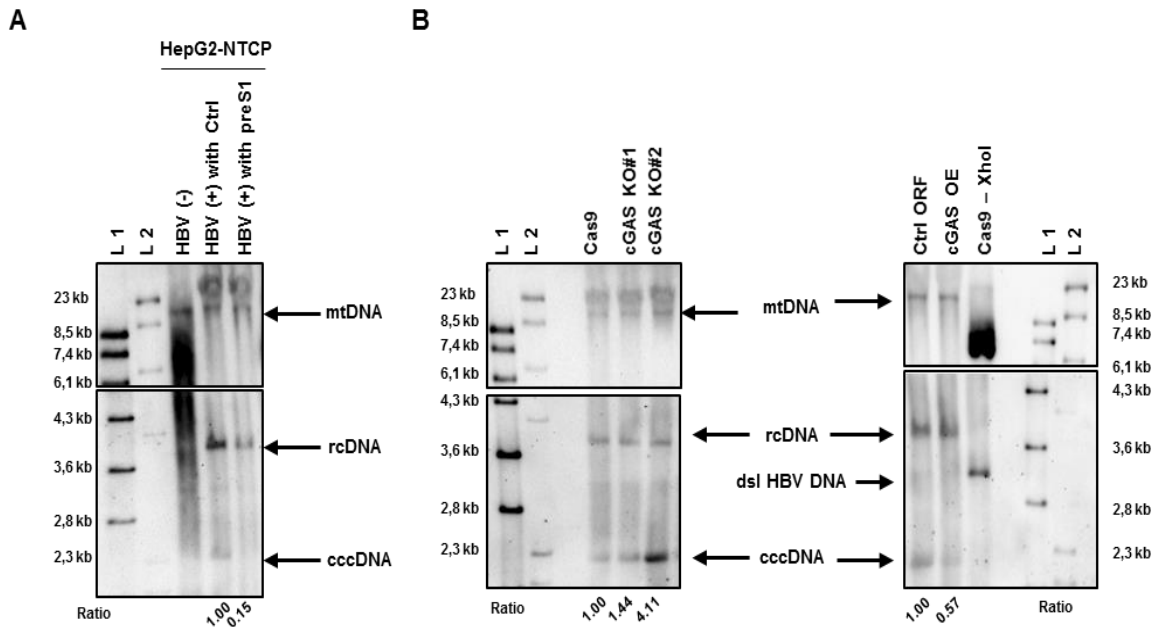


Figure 29. Detection of HBV cccDNA by Southern blot

(A) HepG2-NTCP cells were plated one day prior to incubation with HBV virions with or without pre-treatment for 1h with the control (Ctrl) or HBV preS1-derived peptide (preS1). After that, total DNA was extracted at 10 dpi and HBV DNA were detected by Southern blot. Non-infected HepG2-NTCP cells was used as a negative control (HBV(-)). **(B)** HepG2-NTCP-Cas9-derived cGAS KO cells (cGAS KO#1 and cGAS KO#2), HepG2-NTCP-Cas9 cells (Cas9) and cGAS over expressing cells (cGAS OE) with control cells (Ctrl ORF) were infected for 10 days with HBV. Total DNA from indicated HBV infected cells were extracted and HBV DNA was detected by Southern blot. Two DNA ladders (L1 & L2) were used. *XhoI* digestion of DNA extracted from HBV-infected HepG2-NTCP-Cas9 cells (Cas9-*XhoI*) was used as a control and resulted in a single 3.2 kb band (double stranded linear (dsl) HBV DNA). Mitochondrial DNA (mtDNA) was detected as a loading control. Quantification of cccDNA was compared with mtDNA using image J software (performed in collaboration with Dr. J. Lucifora, CRCL, Lyon, France). (Yim, Verrier *et al.*, 2017, submitted to Gut).

Altogether, our data of loss- and gain-of-function studies demonstrate clearly the antiviral role of cGAS in HBV infection. Most importantly, the level of HBV cccDNA which is key HBV viral nucleic acid responsible for viral persistence is robustly modulated by cGAS expression.

8. HBV infection fails to induce cGAS-related innate immune responses at early time points

To investigate the functional role of cGAS as a DNA sensor, we first analyzed whether HBV infection is sensed by cGAS. To address this question, HepG2-NTCP cells were infected with recombinant HBV and expression of *IFNB1* at day 1, 2 and 3 following HBV infection was quantified. As shown in **Figure 30A**, *IFNB1* expression was not induced at early time points of HBV infection in HepG2-NTCP cells. In contrast, transfection with poly (I:C) led to a 4 log₁₀ increase in *IFNB1* expression at day 1. These results suggest poor or absent HBV detection by cellular sensors in these cells. Since cGAS has been shown to induce the expression of a large set of innate effector genes (such as *OAS2* or *IFI44*, see (201)), the analysis of expression of a single effector gene such as *IFNB1* may not be sufficient to evaluate cGAS sensing. We thus analyzed whether cGAS-stimulated genes were modulated by HBV infection by quantifying the expression of a gene-set called “cGAS signature”. This gene-set encompasses genes modulated by cGAS activity as well as important innate immune genes that have been described by Schoggins *et al* (201) (for details see **Table 10**).

For that, we extracted total RNA from HBV-infected HepG2-NTCP, HepG2-NTCP-Cas9 cells as well as cGAS KO#2 at 2 dpi. Gene expression was measured using nCounting NanoString technology. This powerful technology, derived from the DNA microarray method, allows the simultaneous quantitative analysis of the expression of a selected gene-set using an unique RNA:probe hybridization reaction. Various conditions can thus be analyzed side by side and compared. Nanostring results were analyzed, in our unit, using GSEA (Gene Set Enrichment Analysis), a computational analysis that interprets gene expression based on the statistically significant, association between two biological states. As shown in **Figure 30B**, only weak modulation of the cGAS signature was detected, regardless of the expression of cGAS. Indeed the modulation was similar in HepG2-NTCP, HepG2-NTCP-Cas9 control cells and in cGAS KO#2 cells. In contrast, control experiment performed with HepG2-NTCP cells transfected with 100ng of poly (I:C) presented strong induction of the global cGAS signature (FDR = 0.004). Altogether, these data suggest that HBV is not sensed in HepG2-NTCP cells by either cGAS or other cellular sensors.

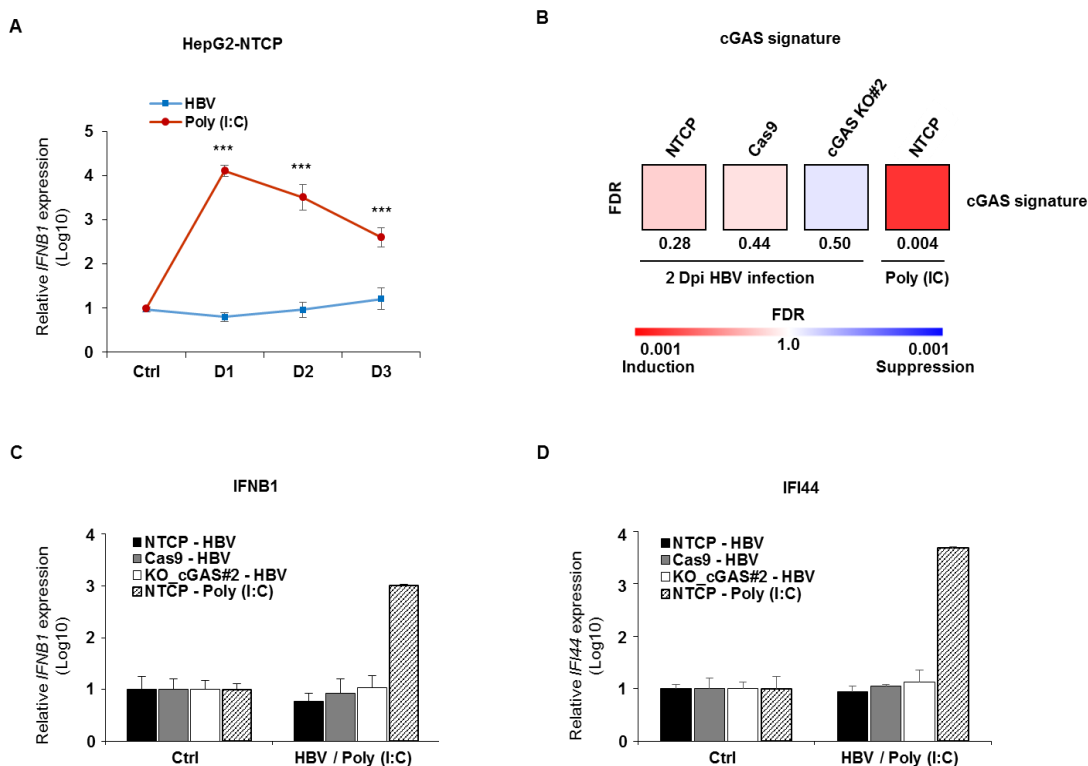


Figure 30. HBV infection is associated with a very weak or absent innate immune response in cell culture

(A) HBV infection does not induce *IFNB1* expression at the early stage of infection. HepG2-NTCP cells were infected with HBV and total RNA was extracted every day for 3 days. *IFNB1* expression was then assessed by qRT-PCR. Poly (I:C) transfection in HepG2-NTCP cells was used as a control. Total RNA extracts from non-infected or non-transfected cells was used as a control (Ctrl). Results are expressed as means \pm SEM of *IFNB1* relative expression (log10) compared to controls (Ctrl, both set at 1) from three independent experiments performed in triplicate (poly (I:C) transfection) or four independent experiments performed at least in duplicate (HBV infection). **(B)** cGAS-related genes are weakly affected by HBV infection. HepG2-NTCP (NTCP), HepG2-NTCP-Cas9 (Cas9) and cGAS KO#2 were infected with HBV. Alternatively, HepG2-NTCP cells were transfected with 100ng of poly (I:C). Two days after infection or transfection, total RNA was extracted. Gene expression of the cGAS signature gene-set was then analyzed using nCounting NanoString. Results were analyzed by GSEA enrichment compared to non-transfected or non-infected controls **(C-D)** *IFNB1* (C) and *IFI44* (D) gene expression are presented to illustrate nCounting Nanostring technology results. NanoString results analyzed by GSEA enrichment were compared to non-transfected or non-infected controls (Set at 1). One experiment performed in triplicate is shown. (Yim, Verrier *et al.*, 2017, submitted to Gut).

9. HBV rcDNA is sensed by cGAS

The HBV genome is encapsidated by the HBV core protein during its intracellular transport to the nucleus after viral entry (105). Moreover, pgRNA resulting from the transcription of the viral cccDNA in the nucleus, is capped and polyadenylated like a regular cellular mRNA before its transfer into the cytoplasm. Once in the cytoplasm, pgRNA is encapsulated in the viral capsid associated with the viral polymerase. Viral reverse transcription by the viral polymerase from the pgRNA form to the genomic rcDNA form occurs inside the virion, allowing HBV rcDNA to be protected from the cellular sensors. Thus, it has been suggested that the HBV genome and its replication intermediates evades recognition by the innate immune sensors responsible for initiating immune responses (283). Having observed failure of *IFNB1* induction at the early stage of infection, we next studied whether naked HBV DNA could be sensed by cGAS. We first purified viral rcDNA from recombinant infectious HBV particles (**Figure 31A**). HepG2-NTCP cells (1×10^5 cell/well) were seeded in 24-well plate one day prior to transfection. One μg of either CT-DNA (dsDNA) or purified HBV rcDNA was transfected into HepG2-NTCP cells using calcium phosphate transfection. HBV virion precipitation control prepared from non-infected HepG2-NTCP cell supernatants was used as control (Ni Ctrl). Medium was changed 16 hours after transfection, total RNA was extracted at 3 days after transfection.

Again, using nCounting Nanostring technology, we investigated the potential modulation of cGAS-related genes in CT-DNA (dsDNA) and HBV rcDNA transfected cells, 3 days post transfection. Nanostring results were analyzed, in our unit, using GSEA enrichment method. As shown in **Figure 31B**, a significant increase (FDR = 0.02) in expression of the cGAS signature gene-set was observed after CT-DNA (dsDNA) and rcDNA transfection in HepG2-NTCP Cas9 cells. This finding suggests that naked HBV genomes are sensed by either cGAS or other cellular sensors. However, since induction of the cGAS-related genes was no longer observed in cGAS KO#2 cells, it appears that a cGAS-specific activation of innate immunity by both CT-DNA (dsDNA) and rcDNA transfection occurs.

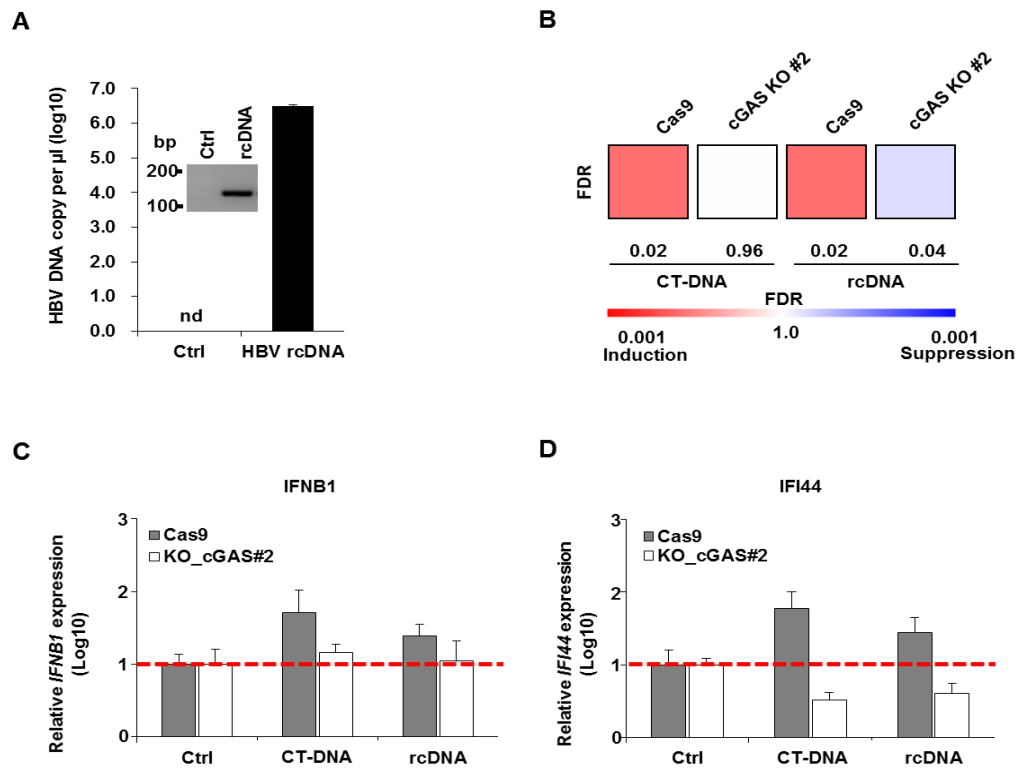


Figure 31. HBV genome exposure induce a cGAS-mediated innate immune response

(A) Preparation of purified HBV rcDNA. HBV rcDNA was purified from HBV virions and analyzed by qPCR before transfection. Expected amplicon size is 148 bp. **(B)** cGAS-related genes are induced by CT-DNA (dsDNA) or HBV rcDNA in a cGAS specific manner. HepG2-NTCP-Cas9 (Cas9) and cGAS KO#2 cells were transfected with 1 μ g of CT-DNA (dsDNA) or 1 μ g of HBV rcDNA. Three days after transfection, total RNA was extracted. Gene expression of the cGAS signature gene-set was then analyzed using nCounting NanoString. Results were analyzed by GSEA enrichment compared to non-transfected or non-infected controls **(C-D)** *IFN1*(C) and *IFI44* (D) gene expression compared to non-transfected control (Ctrl) are presented to illustrate Nanostring results. One experiment performed in triplicate is shown. (Yim, Verrier *et al.*, 2017, submitted to Gut).

In order to confirm the hypothesis that HBV is a virus hidden from cellular sensors recognition in its capsid, we transfected HBV pgRNA encoding plasmids expressing either wild-type or assembly-defective mutants (272). One μ g of HBV pgRNA-encoding plasmids were transfected into HepG2-NTCP cells (1X10⁵ cell/well in 24-well plate). Replication of HBV wild-type (WT) or mutants (L60A, L95A, K96A, and I126A) was confirmed by detection of HBV pgRNA,

HBV core antigen (HBcAg) and HBV e antigen (HBeAg) in the transfected cells 3 days after transfection. Transfection of assembly-defective genomes led to effective HBV replication although at variable rates as attested by the pgRNA (**Figure 32A**). Core (HBcAg) detection suggested that capsids are formed in the transfected cells at similar levels. In contrast, variations in HBeAg levels, quantified by ELISA in the cell lysates, likely show different capacities of assembly-defective mutants to express HBeAg or that HBeAg is variably degraded in the cytoplasm of these cells (**Figure 32B**). We next assessed *IFNB1* expression by qRT-PCR. As shown **Figure 32C**, *IFNB1* expression was not or only minimally induced in mutant transfected cells compared to wild-type. Since it has been established that this assembly-defective capsids are able to support proper reverse transcription by the viral polymerase to synthesis rcDNA (272), only two explanations can be proposed, either these “leaky” capsids do not confer better accessibility of the viral rcDNA to cellular sensors or the higher instability of the capsids leads to rapid nuclease degradation of the neosynthesized HBV rcDNA. Alternatively, *IFNB1* expression is not sufficient to detect sensing and a more sensitive approach as described above is needed to study viral sensing. Further studies are needed to determine whether cGAS can sense HBV DNA in variants with mutant core.

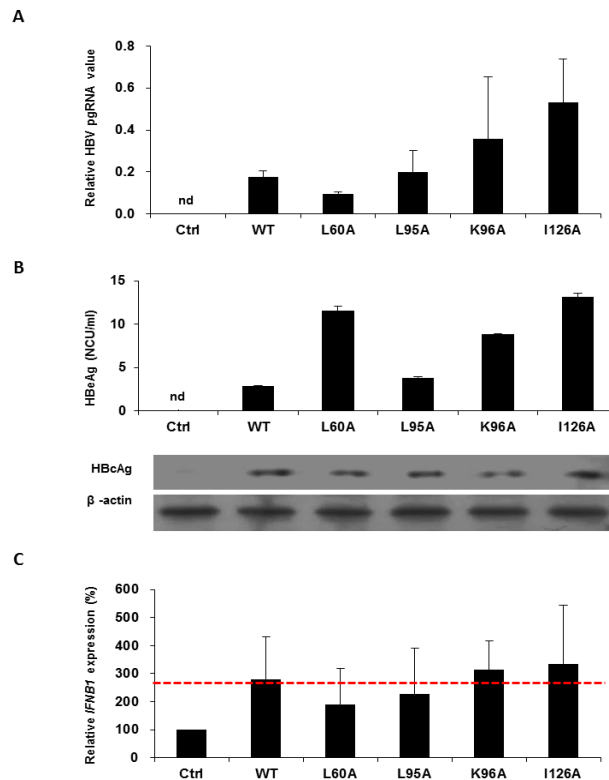


Figure 32. Assembly-defective HBV mutants and *IFNB1* expression

HBV wild type (WT) or assembly-defective mutants encoding plasmids (L60A, L95A, K96A, and I126A) were transfected into HepG2-NTCP cells. **(A-B)** HBV replication was assessed by quantification of pgRNA by qRT-PCR **(A)**, detection of HBeAg from lysates from each plasmid transfected cells by ELISA and HBcAg from lysates of transfected cells by Western at 3 days after transfection. β -actin was detected as a Western blot loading control. No replication (nd) was confirmed in control (Ctrl) **(B)**. **(C)** *IFNB1* expression in each transfected cells was quantified by qRT-PCR. Results are expressed as means \pm SD % *IFNB1* expression relative to empty plasmid transfection in HepG2-NTCP cells (Ctrl, set at 100%) from three independent experiments performed in triplicate. Gene expression was normalized to *GAPDH* mRNA expression.

10. HBV infection down-regulates cGAS-expression in cell culture

As HBV proteins have been shown to inhibit IFN-signaling pathways in experimental model systems (127, 223), we next aimed to determine whether HBV infection was able to interfere with the expression of cGAS and cGAS-related gene expression. To address this question, HepG2-NTCP cells (1×10^5 cells/well in 24-well plate) were infected with HBV. Sixteen

hour after HBV inoculation, cells were washed with DPBS and then cultured in 2% DMSO containing culture medium. cGAS, TBK1 and HBcAg protein expression were detected by Western blot, at 10 dpi. As shown in **Figure 33B**, we observed that 40% of cGAS and 30 % of TBK1 expression was decreased in HBV infected HepG2-NTCP cells (HBV+) compared with HBV non-infected cells (HBV-). Next, we assessed either the mRNA level of *MB21D1* (encodes cGAS) and cGAS-related genes following HBV infection (**Figure 33A**) by qRT-PCR at 2 or 10 dpi. We observed that the *MB21D1* (cGAS), *TMEM173* (encodes STING), and *TBK1* mRNA levels were significantly inhibited in HBV-infected cells (**Figure 33C**). Of note, *TMEM173* (STING) mRNA expression was detected in HBV infected HepG2-NTCP cells (**Figure 33C**). These results indicate that the cGAS-STING pathway is gradually down-regulated during HBV infection in our cell culture model.

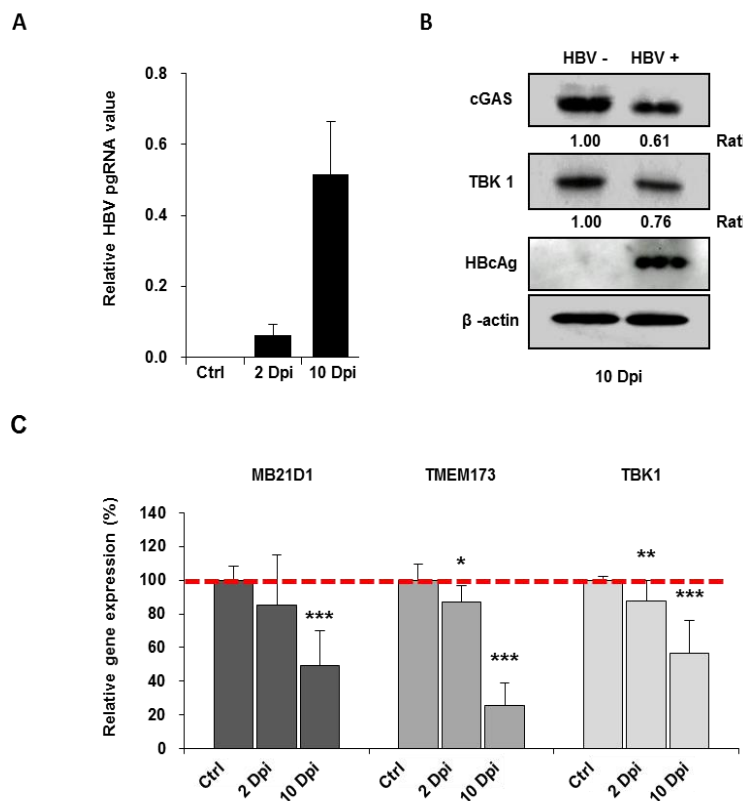


Figure 33. HBV infection reduces cGAS-STING expression in infected HepG2-NTCP cells

(A) HepG2-NTCP cells were infected with HBV for 2 and 10 days. HepG2-NTCP cells were infected with

HBV then total RNA was extracted at 2 and 10 dpi. HBV infection was assessed by detection of HBV pgRNA by RT-qPCR. Three experiments performed in triplicate are shown. **(B)** cGAS, TBK1 protein, and HBcAg expression were detected at 10 dpi by Western blot (One experiment is shown). β -actin was detected as a Western blot loading control. Protein expression normalized β -actin was quantified using the ImageJ software. **(C)** Gene expression of *MB21D1* (cGAS), *TMEM173* (STING), and *TBK1* relative to non-infected control cells was assessed by qRT-PCR at 2 and 10 dpi. Results are expressed as means \pm SD % HBV pgRNA expression relative to non-infected cells (Ctrl, Set at 100%) from three independent experiments performed in triplicate. Gene expression was normalized to *GAPDH* mRNA expression. $p < 0.05$ (*), $p < 0.01$ (**), and $p < 0.001$ (***) were considered significant. (Yim, Verrier *et al.*, 2017, submitted to Gut).

11. HBV infection represses the expression of cGAS-STING pathway related genes *in vivo*

To confirm this observation using an *in vivo* model, we then investigated the expression of human cGAS and cGAS-related genes in HBV-infected humanized uPA/SCID mice by intrasplenic injection as described (280). The liver of these mice was repopulated of PHH as described (280). Transplantation of PHH into mice liver, HBV infection and sacrifice of HBV infected and control mice were performed in our unit UMR_S1110 as described in the Material and Method section.

Sixteen weeks after infection, total RNA was extracted from either HBV infected or non-infected mice livers, and gene expression was assessed by qRT-PCR. As shown in **Figure 34A**, *MB21D1* (cGAS) expression was significantly down-regulated in HBV-infected humanized mice livers compared to control mice livers, confirming our cell culture results. Importantly, *MB21D1* (cGAS) expression levels were not correlated with either albumin levels (attesting the level of PHH liver repopulation) or HBV genotype (**Table 11**). Next we tested *IFNB1* expression is the same samples. *IFNB1* was very low in HBV infected and non-infected mice liver (**Figure 34B**), indicating that HBV infection could not induce innate immunity responses in humanized chimeric mice as suggested previously by others in the Chimp model (230).

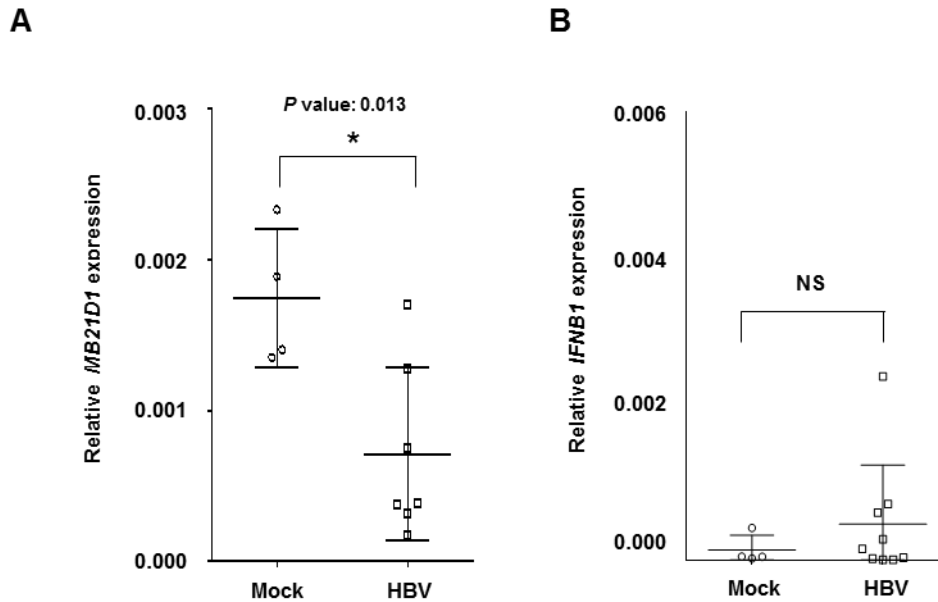


Figure 34. Expression of cGAS-related genes is impaired by HBV infection *in vivo*

Humanized uPA-SCID mice were infected with HBV for 16 weeks. Mice were then sacrificed and the HBV viral load in the serum was quantified (Table 11 below). After total RNA extraction from HBV infected (HBV) and non-infected (Mock) mice liver, human *MB21D1* (cGAS) (**A**) and *IFNβ1* (**B**) expression was assessed in 7 HBV-infected mice and 4 control mice by qRT-PCR. NS means statistically non-significant. Results are expressed as the ratio *MB21D1* mRNA / *GAPDH* mRNA. All individual mice are presented as well as means \pm SD for each group. $p < 0.05$ (*) was considered significant. (Yim, Verrier *et al.*, 2017, submitted to Gut).

We also quantified gene expression of cGAS-related ISGs in the liver of humanized mice by nCounting NanoString technology and analyzed data by GSEA (**Figure 35**). As presented below, the expression of most cGAS-related ISGs was downregulated in HBV-infected humanized mice livers.

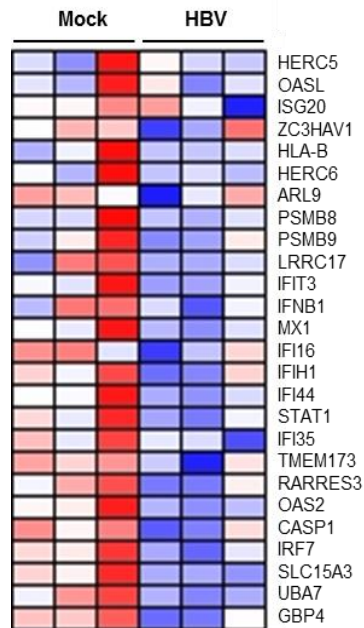


Figure 35. The expression of cGAS-related genes was quantified using the nCounter NanoString Technology and analyzed by GSEA

Livers from mice 6472, 6251, and 6254 (Mock-infected mice, **Table 11**) and 4766, 4771, and 4847 (HBV-infected mice, **Table 11**) were analyzed for expression of a series of cGAS related genes and modulation of expressions were analysed by GSEA. A significant downregulation (FDR = 0.047) of the gene set was observed in HBV-infected mice compared to control mice. Individual Z-scores for the genes significantly modulated between the two groups according to GSEA analysis are presented. Negative Z-score (blue) and positive Z-score (red) correspond to repression and induction of the indicated genes, respectively. (Yim, Verrier *et al.*, 2017, submitted to Gut).

Taken together, our *in vivo* data suggest that HBV infection does not trigger a strong innate immune response and inhibits the expression of *IFNB1*, a major inducer of innate immune responses.

Table 11. cGAS expression in HBV infected human liver chimeric mice

		Mouse	Albumin (μ g/ml)	HBV (IU/ml)	<i>MB21D1</i> m RNA	HBV inoculum (IU)
Ctrl		6410	1280	-	1.40E-03	-
		6472	2720	-	1.40E-03	-
		6251	3240	-	2.30E-03	-
		6254	7870	-	1.90E-03	-
HBV	Gt E	4770	4200	2.9.E+07	1.30E-03	1.25x10 ⁶
		4773	4800	1.5.E+08	1.70E-03	1.25x10 ⁶
		4766	12760	3.6.E+06	3.20E-04	1.25x10 ⁶
		4771	13120	6.2.E+05	3.70E-04	1.25x10 ⁶
	Gt D	4846	2127	5.5.E+05	3.80E-04	5.00x10 ⁵
		4847	10045	1.6.E+08	1.70E-04	1.00x10 ⁵
		4848	1992	6.7.E+06	7.50E-04	1.00x10 ⁷

Levels of human albumin-, HBV viral loads, and *MB21D1* (cGAS) levels in liver tissue from HBV-infected and control humanized mice are shown. *MB21D1* (cGAS) expression is normalized by *GAPDH* expression. The source of HBV (genotype E or D) is indicated. Red mark: mice used for multiplexed gene profiling.

V. DISCUSSION

The interaction between HBV and the innate immune system is a complex process that still remains elusive and controversial (266). While previous reports have studied some aspects of HBV-cGAS association (180, 267), the mechanism of cGAS immune evasion still remains controversial.

In this study, we performed functional studies including loss- and gain-of-function experiments combined with cGAS effector gene expression profiling in an HBV infection-susceptible cell culture model and HBV-infected humanized chimeric mice. Collectively, our data shown that (i) cGAS-STING pathway exhibits robust antiviral activity against HBV infection including reduction of viral cccDNA levels; (ii) naked HBV genomic rcDNA is sensed in a cGAS-dependent manner whereas packaging of the viral genome during infection abolishes host cell recognition of viral nucleic acids; (iii) HBV infection suppresses both cGAS expression and function in cell culture and in humanized liver chimeric mice as shown by down-regulation of cGAS innate immune effector gene expression. (Yim, Verrier *et al.*, 2017, submitted to Gut).

The cGAS-STING pathway is functional in human hepatic cells

We initially examined the basal level of cGAS protein in different cell lines. We detected robust expression of cGAS in our HepG2-NTCP cells as well as in PHH from two different donors (**Figure 21**). We then confirmed that cGAS protein expression was markedly induced by both dsRNA (poly (I:C)) and dsDNA (CT-DNA) stimulation (**Figure 22**), as reported by others in mice liver or bone marrow-derived macrophages (227, 282). This finding demonstrated that cGAS is as an ISGs in our cell lines, like it was already described in other cells lines, i.e. bone marrow-derived macrophages, THP-1 cells, and plasmacytoid dendritic cells (177, 205, 282, 284).

A recent publication reported absence of STING expression in human hepatic cells (227). The authors proposed that absence of STING might explain the weak innate immune response during HBV infection. These observations are not in accordance with the results obtained in the frame of this work. Indeed, we showed that *TMEM173* (encoding STING) was expressed in HepG2-NTCP cells and gradually decreased during the time course of HBV infection from 2 to 10

dpi (**Figure 33**). Moreover, very recently, a new antibody, allowed us to detect STING protein expression in hepatic cells, including PHH. As well, silencing of *TMEM 173* expression significantly increased HBV replication and thus supports that STING is present and active in these cells (**Figure 23**). Finally, rcDNA and dsDNA induced strong *IFNB1* expression in a cGAS-dependent manner (**Figure 31**). Since STING is activated by cGAMP produced by cGAS and thus mediates specifically cGAS activation, functional presence of STING in our cell culture model is definitively proven in our cell culture models. (Yim, Verrier *et al.*, 2017, submitted to Gut).

Collectively, our data demonstrate that the cGAS-STING pathway is expressed and fully functional in the cells used in our study.

cGAS exerts an antiviral activity against HBV infection including reduction of viral cccDNA levels

Using loss- and gain- of function, we demonstrate that cGAS exerts a robust antiviral activity against HBV infection of hepatic cells (**Figure 23, 28**). This finding extends a previous study showing antiviral activity of cGAS against a broad range of RNA and DNA viruses (201) and two other studies showing anti-HBV activity targeting viral replication and assembly (180, 267). The originality of our study was to establish cGAS KO cell lines and cGAS overexpressing cell lines to study function of cGAS as a key player in HBV infection. Using our cGAS KO cell lines, we observed a marked increase in HBV replication (pgRNA levels) and impressive increase in cccDNA in these cells compared to control cells. In parallel, cGAS stable overexpressing cells led to a significant decrease in HBV replication and cccDNA (**Figure 29**). Thus, this work shows conclusive evidence that cGAS exerts antiviral activity against HBV infection including reduction of viral cccDNA. (Yim, Verrier *et al.*, 2017, submitted to Gut).

Despite these interesting findings, it still remains to explain how cGAS exerts antiviral function without viral genome sensing and without induction of innate immune responses. Our next question will be to investigate more deeply the molecular mechanism of cGAS antiviral activity. One line of inquiry will be to investigate the role of the AKT/mTOR signaling pathway in the cGAS antiviral mediated regulation. Indeed, it has been shown that the basal level of the PI3K-Akt pathway regulates HBV replication in HepG2 cells (285). Since AKT can be activated by the HBV HBx oncoprotein (91) a role of AKT phosphorylation in decreasing cGAS activity can be proposed. A recent report supports our hypothesis, it reports that activated AKT by HBx protein

phosphorylates cGAS at Ser 291 or Ser 305, suppressing its enzymatic activity (192). This might in turn inhibit cGAS-STING pathway and thus lead to an increase in viral replication once the cccDNA is formed and viral replication started. Another line of approach would be to study the importance of cGAS SUMOylation in the cGAS antiviral activity. Indeed, SUMOylation and deSUMOylation of RIG-I and MAD5 have been described as crucial for modulation of innate immune responses to viral infection (286). A recent report, published this year shows that SENP7 (sentrin/SUMO-specific protease 7) potentiates cGAS activation by relieving SUMO-mediated inhibition of cytosolic sensing (287). Moreover, modifications catalyzed by tubulin tyrosine ligase-like (TTLL) glutamylases and reversed by members of the cytosolic carboxypeptidase (CCP) family of enzymes have also been recently described as cGAS modulators (193). Investigating this very fast moving field in the context of HBV infection would be of high interest.

HBV capsid protects HBV rcDNA from cellular sensors

The detection of HBV DNA by cellular sensors within HBV infected cells is still poorly understood. *In vitro* and *in vivo* data strongly suggest that HBV behaves like a stealth virus unable to trigger strong innate immune responses (12, 179, 198). Recently, other reports suggested that HBV-derived dsDNA fragments (180) and viral nucleocapsid destabilization and disassembly (164) could induce innate immune responses. In this study, we observed that naked HBV genome (rcDNA) is sensed, resulting in activation of innate immune genes (**Figure 31**) (Yim, Verrier *et al.*, 2017, submitted to Gut). It suggests that HBV genome itself is recognized by the classical sensors, but that (i) HBV DNA recognition by cGAS is impaired due to the encapsidation of the viral genome; (ii) HBV viral proteins might induce alterations of the cGAS-STING pathway thus down-regulating *IFNB1* expression (149, 165, 223). Another possibility is that mitochondrial stress caused by HBV infection (288) leads to the release of mitochondrial DNA (mtDNA) into the cytosol, mtDNA may be sensed by cGAS resulting in induction of antiviral responses, like in HSV infection (206). Interestingly, while HIV replicates its RNA genome to dsDNA in infected macrophage cells, replication intermediates such as the unpaired guanosine in Y-form DNA, and ssDNA, are detected by cGAS, resulting in activation of type I IFN responses (190). However, the capsid of HIV-1 also prevents the sensing of HIV cDNA by cGAS following reverse transcription up to integration, whereas HIV-2 capsid may unmask the cDNA leading to a stronger sensing by cGAS and a lower pathogenicity of the strain (289). Like HIV, the reverse transcription of HBV also

occurs inside the virion. It makes possible to hide replication intermediates from immune sensors. As well, HSV-1 viruses also encapsidate their genomic DNAs inside the virion. However, in macrophages their genomic DNA is detected by DNA sensor, IFI16, following ubiquitination of the capsids and degradation of the capsid by the proteasome (211).

We observed that HBV naked DNA (extracted rcDNA from virion) appears to be properly sensed in hepatic cells by the cGAS-STING pathway and that, in contrast, HBV infection leads to neither induction of *IFNB1* nor of cGAS-related genes, referred as the cGAS signature gene-set in our study (Yim, Verrier *et al.*, 2017, submitted to Gut). To further understand the role of the viral capsid in shielding of the genome, I first tested the capacity of capsid assembly-defective genome to be recognized by the innate immune system. Although 4 different mutant genomes (L60A, L95A, K96A, and I126A) with wild-type were tested, I did not observe a robust *IFNB1* response under my experimental conditions (**Figure 32**) (Yim, Verrier *et al.*, 2017, submitted to Gut). As mentioned above further studies are needed to understand the role of the capsid for viral sensing. Another approach could be the use of capsid inhibitors to investigate whether exposing the encapsidated genome in the cytoplasm will trigger HBV genome sensing by host sensors including cGAS. The heteroaryldihydropyrimidine (HAP) series of compounds, BAY 41-4109 and GLS 4, are well known HBV capsid inhibitors that were tested for their antiviral activity in a uPA-SCID mice infected with HBV or a mouse model of HBV replication engrafted with HepAD38 cells, respectively (290, 291). Thus, we aimed to assess *IFNB1* expression in GLS4 treated HBV-infected cells to investigate the possibility that viral DNA genomes might be sensed once reverse transcription has occurred inside the capsid. Unfortunately, pilot experiments revealed a high cytotoxicity of these molecules in our hepatic cell lines and hampered correct analysis of HBV sensing. However, optimization of our experimental conditions will allow to address unresolved question in the future.

HBV infection suppresses the cGAS-STING pathway *in vivo* and *cell culture* models

Given the antiviral activity of the cGAS-signaling pathway against HBV infection (**Figure 23, 28**), the viral-mediated restriction of *MB21D1* (cGAS) expression plays an important role in HBV immune evasion, as it has been recently reported (180, 267).

It has been recently described that cGAS-depleted mice were more susceptible to RNA virus infection and that cGAS exhibited antiviral activity against a broad range of RNA and DNA

viruses (201). cGAS-depleted cells may thus be more susceptible to viral infections through the downregulation of the basal level of innate antiviral genes (201).

Our data show that HBV can repress the expression of the cGAS and its related genes, such as *MB21D1* (cGAS), *TMEM17* (STING) and *TBK1* (**Figure 33**). More interestingly, we found *MB21D1* and *IFNB1* expression is down-regulated in the liver of HBV-infected mice, confirming the relevance of these findings *in vivo* (**Figure 34**). However, it still remains to be determined whether HBV can target cGAS and cGAS-related factors for an active inhibition of this signaling pathway or whether, down-regulation of *MB21D1* may be the consequence of the global inhibition of the canonical IFN pathways by HBV (292) (Yim, Verrier *et al.*, 2017, submitted to Gut).

Indeed, given its broad antiviral function, cGAS is targeted by many viruses in order to evade immune responses. It has been reported that the KSHV ORF52, an abundant gammaherpesvirus-specific tegument protein, directly binds to cGAS, and hence negatively regulates the cGAS-dependent signaling pathway (219, 293). A recent study elegantly demonstrated an active inhibition of the cGAS pathway by dengue virus through NS2B protein that degraded cGAS in the virus infected cells (294). Moreover, it has been shown that HBV viral proteins interfere with the JAK/STAT signaling pathway, for instance by inhibiting IRF3 activation via the viral polymerase (149, 292). In the same line, most immortalized and tumor cell lines fail to respond to intracellular DNA, whereas primary cells mount a vigorous DNA-activated antiviral response (295). It has been demonstrated that cGAS-STING pathway is inhibited by the constitutive expression of oncoproteins from DNA tumor virus, such as E1A from adenovirus, E7 from HPV, and vIRF1 from gamma-herpes virus oncogenes that transformed these cells (202, 222).

We assume that HBV viral proteins may interfere with cGAS optimal expression in HBV infected cells. We are considering that HBx, known as the HBV oncoprotein, is the most promising one, because it was shown to interfere with numerous cellular processes including: host signal transduction, transcriptional activation, DNA repair, and inhibition of protein degradation, proliferation, signaling, in HBV infected cells (89, 91-93). For this purpose, we plan to follow cGAS expression and functional activity in HBV protein expressing HepaRG cell lines kindly provided by our collaborator (Dr. D. Durantel, CRCL, Lyon, France).

Finally, we analyzed HBV infected humanized mice livers for cGAS expression and confirmed *in vitro* data obtained in cell culture models, i.e. inhibition of the cGAS-STING pathway

gradually with time (**Figure 34**). Moreover, cGAS-related ISGs expression in humanized mice liver was quantified by nCounting nanoString technology and GSEA, indicating down-regulation of cGAS-related ISGs in HBV-infected humanized mice livers (**Figure 35**) (Yim, Verrier *et al.*, 2017, submitted to Gut).

This finding suggests that long-term HBV infection does not trigger a strong innate immune response and is capable of inhibiting the expression of major inducers of innate immune responses. *In vitro* and *in vivo* data corroborate to strongly suggest that HBV behaves like a stealth virus unable to trigger any innate response (12, 179, 296).

Collectively, our results demonstrate that (i) basal level of cGAS is sufficient to induce *IFNB1* expression in our hepatic cell culture model; (ii) cGAS-STING pathway exhibits robust antiviral activity against HBV replication and infection, including viral cccDNA levels modulation; (iii) naked HBV genomic rcDNA is strongly sensed in a cGAS-dependent manner whereas leaktight packaging of the viral genome during infection virtually abolishes host cell recognition of viral nucleic acids; (iv) HBV infection suppresses both cGAS expression and function in cell culture and humanized liver chimeric mice as shown by down-regulation of cGAS innate immune effector genes expression.

Overall, this work led to describing new aspects of the complex interaction between HBV and the DNA sensor cGAS in hepatocytes. These findings improve the understanding of virus-innate immune interactions in the liver, and open perspectives for a comprehensive overview of viral sensing and evasion by this chronic hepatotropic virus.

VI. Résumé en français

Introduction

Le virus de l'hépatite B (HBV) est l'agent étiologique de l'hépatite B responsable d'une pandémie. En effet, en 2015, l'Organisation Mondiale de la Santé (OMS) estimait, que parmi les 2 milliards de personnes qui avaient été en contact avec ce virus dans le monde, 257 millions de personnes vivaient avec une infection chronique par le VHB (<http://www.who.int/mediacentre/news/releases/2017/global-hepatitis-report/en/> (3, 4)). L'hépatite chronique B (CHB) est une affection grave du foie, pouvant conduire à la cirrhose hépatique et au cancer du foie ou hépatocarcinome (HCC) (6, 7). Une étude française récente réalisée entre 1994 et 2009, sur une cohorte de plus de 1000 personnes atteintes de CHB montre que ces personnes présentent un risque accru de mortalité de 70%, avec une incidence augmentée de maladie hépatique, de lymphome non-hodgkinien et de cancer hépatique, respectivement de 10, 16 et 9 fois. L'ensemble de ces données illustre le fait que les conséquences du CHB constituent un problème de santé publique majeure en France et dans le monde.

L'hépatite B se transmet de manière horizontale par voie sanguine et sexuelle. Toutefois, la fréquence de la transmission verticale de la mère à l'enfant, lorsque la mère n'est pas traitée, reste très élevée (entre 40 et 90%) et constitue une des principales causes de transmission de l'hépatite B en Afrique et en Asie du Sud-Est. Sans accès à un traitement, la contamination périnatale résulte dans 95% des cas à une infection chronique chez l'enfant (5).

Depuis plus de vingt ans, des vaccins préventifs, sûrs et efficaces, basés sur l'antigénicité des protéines de surface du virus (HBsAg) ont été établis (8). Suite à la vaccination massive des nouveaux-nés préconisée par l'OMS, l'efficacité des vaccins a été actée par la baisse du nombre de porteurs chroniques et la baisse de l'incidence du cancer du foie dans plusieurs pays (37). L'accès au vaccin dans les pays où l'accès aux soins est encore difficile, freine toutefois l'éradication de cette maladie à l'échelle mondiale.

L'infection est majoritairement asymptomatique. De plus, grâce à une réponse immunitaire adaptative robuste, 95% des personnes contaminées résoudront l'infection dans les six mois suivant l'infection (22). Si après six mois la charge virale persiste, on considère l'infection

chronique établie (2).

Le CHB s'étend sur une période de 60 ans, et se caractérise par 4 phases définies par rapport au taux d'ALT, la quantité de DNA viral sérique et la présence d'antigène et d'anticorps HBe (HBeAg, HBeAc). Une première phase « *Immune tolerant* » (DNA Viral et HBeAg élevés et ALT bas) est suivie de la phase « *immune clearance/HBeAg-positive chronic hepatitis* » caractérisée par l'élévation des ALT. Lors de la phase « *inactive carrier* » on observe une baisse voire la disparition de l'HBeAg et du DNA viral et une séroconversion avec apparition de HBeAc. La phase « *reactivation/HBeAg-negative chronic hepatitis* » apparaît tardivement par une réaugmentation de l'ADN viral et des ALT dans le sérum (14).

Pour les patients atteints de CHB les traitements sont proposés lorsque les taux de réplication virale est élevé et l'inflammation chronique du foie avérée après examen clinique approfondi. Les traitements sont basés sur l'administration d'analogues nucléotidiques (NUC) ou d'interféron (IFN)-alpha (22, 23). Les NUCs consistent en trois groupes structuraux L-nucléosides (lamivudine), les alkyl phosphonates (telbivudine, adefovir and tenofovir), et les D-cyclopentanes (entecavir) (24). Bien que ces traitements aient prouvé leur efficacité, pour la négativisation de la charge virale, l'infection virale peut persister de manière occulte ou à bas bruit, en raison de l'établissement dans le noyau de la cellule infectée d'une forme épisomale du génome du HBV nommé cccDNA (covalently closed circular DNA). Cette forme résiste aux traitements actuellement disponibles et est le support de la phase de réactivation de l'infection (108).

Une des voies de développement de nouvelles thérapies consiste en l'identification de facteurs de l'hôte comme cibles thérapeutiques (260).

Le virus de l'hépatite B appartient à la famille des *Hepadnaviridae* comprenant deux genres les orthohepadnavirus (infectant les mammifères), dont il est le prototype, et les avihepadnavirus (infectant les oiseaux), dont le duck hepatitis virus est le prototype (1, 40). Dans le sérum des patients infectés par le HBV, les particules sphériques infectieuses sont appelées particule de Dane (42, 48, 49). Le VHB est un virus à DNA enveloppé qui présente la particularité de posséder un génome DNA circulaire relaxé (rcDNA) dont le brin moins est complet (3,2 kb) et le brin plus incomplet (50). Le génome associé à la polymérase virale est protégé par une capside icosaédrique formée de dimères de la protéine core. L'enveloppe virale issue du réticulum endoplasmique de la cellule infectée dans laquelle sont enchassées les trois types d'antigènes

de surface (Large (L), Middle (M), et Small (S) HBsAg) partageant la même extrémité N-terminale. Le génome code 4 transcrits comprenant des régions codantes chevauchantes, dont un petit transcrit codant la protéine oncogénique x (HBxAg), deux transcrits codant pour les 3 protéines de surface (HBsAg), un transcrit codant la protéine pré-core/core (HBeAg et HBcAg) et la polymérase virale. Ce transcrit constitue également le RNA pré-génomique (pgRNA) qui sera reverse transcrit en génome viral une fois encapsidé (58).

Très récemment le récepteur NTCP (human sodium/taurocholate cotransporting peptide (hNTCP/*SLC10A1*)), un récepteur impliqué dans le transport des acides biliaires a été identifié comme le premier récepteur spécifique du VHB (48, 49, 60). Cette découverte constitue une avancée majeure dans la compréhension du cycle viral du VHB par la possibilité d'établir des modèles de culture cellulaire permissifs au HBV.

Le cycle viral du HBV peut se résumer en 5 étapes principales. Le virus s'attache à la surface des hépatocytes aux Heparan Sulfate Glycoprotein tel Glypican 5 (99, 100) puis entre dans la cellule grâce à la reconnaissance entre les protéines de surface et le récepteur NTCP (98, 101) par un mécanisme en core peu documenté (103, 104). Une fois dans le cytoplasme, la capsid est libérée et acheminée à la membrane nucléaire (106, 107) L'entrée dans le noyau est associée à la libération du DNA viral qui est complété par la DNA polymérase cellulaire et une fois clos forme un mini-chromosome qui sera la base de la transcription du génome, le circular covalently closed DNA ou cccDNA (52). Les RNAs messagers ainsi que le pgRNA sont polyadénylés et coiffés avant de retourner dans le cytoplasme (110). Rapidement le pgRNA est encapsidé avec la polymérase virale et la reverse transcription peut commencer. La reconnaissance spécifique du pgRNA par la capsid se fait grâce à une structure secondaire située en 5' pgRNA (108, 111). La nucléocapsid est ensuite enveloppée à la membrane du réticulum post-endoplasmic-pre-Golgi dans lequel sont enchassées les protéines d'enveloppe (L- M- et majoritairement S HBsAg) (120, 121). En parallèle, la protéine pré-core/core perd son peptide signal au niveau du réticulum endoplasmique ainsi que la région C-terminale riche en Arg pour libérer le HBeAg qui sera excrétée dans le milieu extracellulaire (72, 73). HBeAg est, avec le pgRNA, un des marqueurs précoces d'une réplication active.

Pendant longtemps, les travaux sur le HBV ont été restreints à l'utilisation de lignées cellulaires exprimant de façon stable le génome du HBV intégré dans le génome cellulaire, ainsi la lignée HepAD38 produit des particules virales sous le contrôle d'un promoteur tétracycline

(248). La limite de ces lignées nets qu'elles ne permettent pas d'étudier le cycle biologique complet du HBV. La découverte du transporteur de sels biliaires, NTCP, comme récepteur spécifique du HBV a ouvert de nouvelles perspectives par l'établissement de lignées hépatocytaires exprimant NTCP et devenant de ce fait permissives au HBV, comme la lignée HepG2-NTCP (99). In vivo, le seul modèle animal a longtemps été le modèle chimpanzé qui a permis l'étude de réponse immunitaire innée et acquise en réponse à cette infection (230). Toutefois, le HBV n'induit pas de chronicité dans ces animaux (22, 230). A présent, des modèles de souris humanisées par la transplantation de PHH sont utilisés pour confirmer ou infirmer les données in vitro (245).

L'infection par le HBV provoque une réponse adaptative forte et efficace chez la grande majorité des adultes infectés (22), ceci est en partie dû à la production massive, en plus des particules infectieuses, de particules subviraux sphériques ou filamenteuses portant le HBsAg à leur surface (50). A l'inverse, des travaux menés dans le modèle chimpanzé ont montré que l'infection par le HBV n'induit pas de réponse immunitaire innée (12, 230). De ce fait, le HBV a été qualifié de virus « furtif » capable d'échapper à la surveillance effectuée par les senseurs cellulaires de l'immunité innée.

La réponse immunitaire innée est la première ligne de défense antivirale. Elle est activée par la reconnaissance de motifs structuraux portés par les pathogènes, les « pathogen-associated molecular patterns » ou PAMPs par des récepteurs cellulaires membranaires, endoplasmiques ou cytosoliques, les « pattern recognition receptors » (PRRs) (122). Parmi les PRRs, les Toll like receptors TLR 3, 7, 8, localisés à la membrane de l'endosome sont impliqués dans la reconnaissance de RNA simple brin (ssRNA) et DNA double brin (dsDNA) de virus, alors que les senseurs cytosoliques « RIG-I like receptors » (RLR) et « Nucleotide oligomerisation receptor » (NLR) sont impliqués dans la reconnaissance de structures secondaire des acides nucléiques. Les PRR une fois activés par les PAMPs, dans le cas des virus généralement l'acide nucléique, induisent une cascade de signalisation qui conduit à la production d'interférons (IFN) de type I (alpha/beta), de cytokines pro- et anti- inflammatoires, de chimiokines. Les IFN de type I permettront d'agir de manière autocrine mais aussi paracrine et ainsi d'alerter les cellules voisines et de leur conférer un arsenal antiviral efficace, en induisant la synthèse massive d'« Interferon induced genes » ou ISGs (129). Les IFN stimuleront également la réponse immunitaire adaptative par l'activation de réponse efficace des lymphocytes B et T (126, 127).

Les dsDNA induisent efficacement la réponse immunitaire innée, qu'ils soient issus de l'ADN tumoral, de l'ADN mitochondrial ou de l'ADN viral, en induisant une réponse IFN de type 1 (170). Parmi les senseurs on notera : « absent in melanoma » (AIM2), « DNA-dependent activator of IRFs » (DAI), « DExD/H box helicase protein 41 » (DDX41), « IFN-inducible protein 16 » (IFI16), and « cyclic GMP-AMP (cGAMP) synthase » (cGAS) (153, 171). Seules quelques études suggèrent que la présence de fragments de dsDNA du HBV (180) dans le cytosol des cellules infectées ou la déstabilisation des capsides (164) pourraient induire une réponse immunitaire.

Récemment, le senseur cellulaire cytosolique GMP-AMP synthase (cGAS) a été décrit comme un senseur efficace de molécules ssDNA et dsDNA ainsi que dans une moindre mesure de ssRNA et d'hybride RNA:DNA (187, 192, 193). cGAS a été décrit pour son action antivirale envers de nombreux virus à DNA (HSV-1 (199, 200), murine gamma-herpesvirus 68 (MHV68) (201), KSHV (202), vaccinia virus (VV) (201), adenovirus(203), human papillomavirus (HPV) (204), and human cytomegalovirus (HCMV) (205)) et à RNA (HIV (190)). L'activation de cGAS entraîne la synthèse d'un messenger secondaire le 2'3'cyclic GMP-AMP (cGAMP) qui active par phosphorylation la voie STING-TBK1 et induit la synthèse d'IFN de type 1 et des ISGs. Une fois synthétisé dans la cellule infectée, cGAMP peut diffuser vers les cellules voisines et induire également une réponse antivirale efficace (195).

Objectif de la thèse

Au moment de mon engagement dans ce travail de thèse, la question de la reconnaissance par les PRR de matériel génétique du HBV n'était pas tranchée. En effet, bien que des travaux récents suggèrent une probable détection d'ARNs HBV par MDA5 (166) ou RIG-I (159), il est globalement admis que le HBV n'active pas ou très peu la réponse immunitaire innée *in vivo*, ce qui est en faveur de l'image de virus « furtif » dont le DNA et/ou le RNA viral est dissimulé au système immunitaire inné (127). Toutefois, certaines études ont suggéré que les protéines du HBV inhibaient la réponse immunitaire innée et expliqueraient l'absence d'activation de la voie IFN suite à l'infection (154). Au vu de ces données les interactions entre le HBV et la réponse immunitaire innée des hépatocytes ne sont encore que partiellement comprises.

Le PRR cGAS a été récemment décrit comme exerçant une action antivirale sur un large spectre de virus à DNA et RNA (178, 201) en activant la voie STING/TBK1 suite à la synthèse

d'un messager secondaire 2'3' cGAMP (181, 226). Dans le contexte du HBV, alors certains auteurs suggèrent que la voie cGAS-STING exerce une activité antivirale sur l'infection HBV (180, 267), une autre étude suggère que l'absence de l'expression de STING dans les hépatocytes (227), pourrait expliquer l'absence d'activation de la réponse IFN dans les cellules infectées (266, 268).

Le but de mes travaux de thèse a donc été de contribuer à la compréhension des interrelations existant entre le HBV et les cellules hépatocytaires, à des stades précoces et tardifs de l'infection HBV, en utilisant différentes approches.

Notre stratégie a été (1) de caractériser le modèle cellulaire d'infection HBV mise au point au laboratoire, d'une part pour l'expression de cGAS et d'autre part pour la capacité de ces cellules à induire une réponse IFN robuste en réponse à des inducteurs dsDNA ou dsRNA; (2) d'utiliser des stratégies de perte- et gain- de fonction pour confirmer l'action antivirale de cGAS au cours de l'infection HBV ; (3) d'étudier la reconnaissance par cGAS de la forme génomique rcDNA du HBV au cours des phases précoces de l'infection, et de confirmer ou d'infirmer que le rcDNA du HBV reste invisible au système cGAS-STING lorsqu'il est encapsidé comme cela a été suggéré par d'autres (269). Pour cela, j'ai choisi un ensemble de gènes constituant des marqueurs de l'activité cGAS incluant les gènes utilisés dans l'étude de Shoggins et *al.* (270), des gènes de la voie cGAS-STING et des gènes importants pour la réponse immunitaire innée; l'expression de l'ensemble de ces gènes a été analysée par une technologie innovante, la « nCounting Nanostring Technology » ; (4) d'analyser l'impact de l'infection par le HBV sur l'expression des gènes de la voie cGAS/SING ainsi que des gènes apparentés à cette voie, ceci, *in vitro* dans notre modèle cellulaire et *in vivo* dans des souris humanisées infectées.

Le but ultime de ces travaux étant de comprendre par quels mécanismes le HBV échappe à la réponse immunitaire innée.

Résultats

1. Validation du modèle cellulaire HepG2-NTCP pour l'étude du rôle de cGAS au cours de l'infection par HBV

Au cours de mes travaux, j'ai utilisé des cellules hépatocytaires de la lignée HepG2 exprimant de manière stable le récepteur NTCP. Ces cellules, établies au laboratoire, sont

fortement permissives à l'infection HBV (99). Dans un premier temps, nous avons validé ce modèle d'infection pour notre étude. Dans un premier temps, nous avons analysé l'expression de cGAS dans ces cellules, ainsi que dans les hépatocytes primaires humains (PHH). Dans un deuxième temps nous avons quantifié une forte induction d'IFN beta 1 après transfection de dsRNA (poly I:C) ou de dsDNA (calf-thymus DNA). Ces résultats confirment que les cellules HepG2-NTCP constituent un bon modèle pour l'étude du rôle de cGAS dans l'infection HBV et que la protéine STING est présente et active dans ces cellules (Yim, Verrier *et al.*, 2017, submitted in Gut).

2. cGAS exerce une activité antivirale sur l'infection HBV

Des stratégies de perte- et gain- de fonction de cGAS, ont été ensuite utilisées afin d'estimer le rôle de cGAS dans l'infection par le HBV. Pour cela, l'expression des protéines cGAS, STING et TBK1 a été inhibée par RNA interférence, puis l'infection HBV a été quantifiée par le dosage du pgRNA viral. Une augmentation significative de l'infection virale a ainsi été observée. Afin de confirmer cette observation j'ai alors établi des cellules cGAS KO en utilisant la technique CRISPR-CAS9. Après plusieurs tentatives avec des systèmes plasmidiques différents, j'ai réussi à sélectionner des cellules cGAS KO n'exprimant plus cGAS. Ces cellules, une fois infectées par HBV, répliquent de 3 à 5 fois plus le HBV que les cellules infectées contrôle, confirmant ainsi les premières expériences utilisant l'inactivation de gènes par RNA interférence. En parallèle, des cellules surexprimant cGAS (cGAS OE) ont été obtenues au laboratoire, l'infection de ces cellules par le HBV est 2 fois moins efficace que dans les cellules contrôle HepG2-NTCP, ce qui est en faveur d'un rôle important de cGAS au cours de l'infection HBV.

Afin de vérifier que la forme génomique nucléaire de HBV ou cccDNA, est également affecté par cGAS, j'ai isolé l'ADN HBV de cellules cGAS KO et de cellules cGAS OE et ces dans on été soumis à la détection du cccDNA par Southern blot (collaboration J Lucifora, CRCL Lyon). Le cccDNA de ces cellules est respectivement inhibé et augmenté en fonction de la présence ou non de cGAS, confirmant au niveau génomique l'importance de l'action antivirale de cGAS au cours de l'infection par HBV (Yim, Verrier *et al.*, 2017, submitted in Gut).

3. L'infection par le HBV n'induit pas de réponse immunitaire innée par la voie cGAS-STING

J'ai ensuite suivi l'induction de la voie INF lors de l'infection HBV. Ceci en quantifiant

l'expression INF beta1 de 1 à 3 jours après infection par le HBV. La transfection de poly (I:C) a été utilisée comme contrôle positif de l'induction. L'infection HBV n'induit pas de réponse interféron dans ces conditions. Afin d'aller plus loin dans cette étude, nous avons ensuite sélectionné un ensemble de 29 gènes soit de la voie cGAS-STING, soit apparentés à cette voie, soit impliqués dans la réponse immunitaire innée en général, l'ensemble de ces gènes a été nommé « signature cGAS ». Nous avons testé l'induction ou la répression de manière simultanée de ces gènes dans des cellules cGAS KO et cellules contrôle HepG2-NTCP suite à l'infection par le HBV en utilisant la « nCounting Nanostring Technology », une technique quantitative innovante dérivée du microarray. L'analyse des données obtenues a été réalisée par un spécialiste du laboratoire en utilisant le « Gene Set Enrichment Analysis, GSEA ». L'analyse des données a montré que HBV n'était pas détecté par les cellules qu'elles soient KO ou non pour cGAS, alors que le contrôle positif constitué de cellules contrôle HepG2-NTCP transfectées par le poly (I:C) induisait fortement l'expression de la signature cGAS validant ainsi l'expérience.

Ces résultats montrent que le HBV est un virus furtif qui n'est pas reconnu par la réponse immunitaire innée (Yim, Verrier *et al.*, 2017, submitted in Gut).

4. Le rcDNA du HBV est détecté par la voie cGAS-STING

Afin de vérifier si cette « invisibilité » du HBV était due uniquement à la protection du génome par dans la nucléocapside ou si la forme relaxée du génome, le rcDNA du fait de sa particularité (DNA circulaire incomplet) n'était pas détectée, j'ai purifié du rcDNA HBV à partir de virions infectieux. Nous avons ensuite réitéré l'analyse de la « signature cGAS » par des expériences de nCounting Nanostring, cette fois après avoir transfecté du rcDNA ou du dsDNA dans des cellules contrôle HepG2-NTCP ou des cellules cGAS KO. Les résultats obtenus, analysés par GSEA, montrent clairement la détection du rcDNA et du dsDNA dans les cellules contrôle HepG2-NTCP, alors qu'aucune induction de la signature cGAS n'est observée dans les cellules cGAS KO.

Ces expériences démontrent que le rcDNA est bien détecté par les senseurs cellulaires dans les cellules contrôle HepG2-NTCP et que cette détection est spécifique de la voie cGAS-STING, l'effet disparaissant lorsque cGAS était invalidé. De plus, ces résultats confirment le fait que l'étanchéité de la capsid assure la protection du génome viral une fois encapsidé (Yim, Verrier *et al.*, 2017, submitted in Gut).

5. L'infection HBV inhibe l'expression des protéines de la voie cGAS-STING dans le modèle cellulaire HepG2-NTCP et dans un modèle de souris humanisés par transplantation de PHH.

J'ai ensuite analysé l'expression des protéines de la voie cGAS-STING au cours de l'infection HBV. L'expression de *M2B21* (cGAS), de *TEM173* (STING) et de *TBK1* a été analysé par qRT-PCR à jour 2 et jour 10 après infection de cellules HepG2-NTCP par le HBV. Une inhibition forte de l'expression de ces trois gènes est observée à 10 jours post-infection. Ceci suggère une inhibition de la voie cGAS-STING au cours de l'infection. Nous avons confirmé ces résultats, par détection d'une inhibition conséquente de la protéine cGAS par western blot à 10 post-infection.

Afin de confirmer cette observation dans un modèle *in vivo*, nous avons quantifié le taux de mRNA *M2B21* (cGAS) dans des foies de souris humanisées infectées par HBV durant 16 semaines. Dans ce cas aussi, l'expression de cGAS est significativement inhibée dans les 9 souris infectées analysées en comparaison aux souris contrôle non infectées. Finalement, l'expression des gènes de la « signature cGAS » a été analysée dans les foies de ces souris et a montré une inhibition globale de l'expression de l'ensemble des gènes testés.

Ces résultats suggèrent que l'infection HBV inhibe la voie cGAS-STING, ce qui pourrait expliquer en partie la capacité du HBV à échapper aussi efficacement à la réponse immune innée (Yim, Verrier *et al.*, 2017, submitted in Gut).

Discussion

Mes travaux de thèse démontrent par des expérience de perte- et gain- de fonction, que le senseur cytosolique cGAS exerce une activité antivirale envers l'infection par le HBV. L'analyse de la réponse IFN beta1 et d'un ensemble de gène de 29 gènes constituant la « signature cGAS » aux temps précoces de l'infection par le HBV, montre que le HBV n'induit pas de réponse IFN de type 1 efficace. Ces résultats confirment que le HBV est un virus « furtif ». L'échappement à la réponse immunitaire innée est dû à la protection très efficace du DNA génomique encapsidé (rcDNA) par la capsid virale. De plus, l'analyse de temps plus long d'infection montre une inhibition globale de l'expression des acteurs de la voie cGAS-STING à la fois en système cellulaire et *in vivo* en souris infectées par le HBV humanisées par transplantation de PHH et

infectés par le HBV.

Mes travaux invalide la thèse d'une absence de STING dans les cellules hépatocytaires expliquant l'échappement du HBV à la réponse immunitaire innée et démontrent la capacité de notre modèle cellulaire à activer la voie cGAS-STING par des acides nucléiques et de mettre en place une réponse INF de type 1 de manière efficace. Cette partie de mes travaux pourra se compléter avec l'utilisation de virus codant des capsides déficientes pour l'assemblage (272) et qui pourraient ainsi libérer ou rendre accessible le rcDNA dans le cytoplasme des cellules infectées. Une autre alternative serait d'utiliser des inhibiteurs de capsides au cours de l'infection (290, 291).

Concernant l'inhibition des acteurs de la voie cGAS-STING au cours de l'infection HBV, une action du virus et en particulier de protéines virales sur l'expression de ces gènes est probable. De tels effets inhibiteurs exercés par des protéines virales sont courantes, permettant aux virus de modifier sur le long terme l'efficacité des voies de signalisation impliquées dans la réponse immunitaire innée. Je souhaite à présent tester le rôle des protéines virales du HBV sur la synthèse des protéines cGAS-STING. Pour cela, j'utiliserais des lignées cellulaires exprimant chacune des protéines du HBV individuellement (Collaboration D. Durantel, CRCL, Lyon, France) et nous analyserons l'expression des protéines de la voie cGAS-STING afin d'identifier quelle protéine de HBV est impliquée dans l'inhibition d'expression de cGAS et des acteurs de la voie cGAS-STING et d'en comprendre le mécanisme moléculaire.

Conclusion

Au cours de mes travaux nous avons démontré (1) que cGAS exerce une activité antivirale envers le HBV; (2) que la nucléocapside protège le DNA génomique viral et l'empêche d'être détecté par la réponse immunitaire innée et que (3) l'infection par HBV diminue l'expression des acteurs de la voie cGAS-STING in vitro et in vivo. Ce dernier point met en lumière un nouveau mécanisme d'échappement du HBV au système immunitaire inné dans les cellules hépatocytaires.

VII. REFERENCES

1. Seeger C, Zoulim F, W. M. Hepadnaviruses. 6 ed. Philadelphia: Wolters Kluwer/Lippincott Williams & Wilkins Health, 2014.
2. WHO. Global hepatitis report. <http://www.who.int/hepatitis/publications>. (accessed April 2017).
3. Trépo C, Chan HLY, Lok A. Hepatitis B virus infection. *The Lancet* 2014;384:2053-2063.
4. Zeisel MB, Lucifora J, Mason WS, Sureau C, Beck J, Levrero M, Kann M, et al. Towards an HBV cure: state-of-the-art and unresolved questions--report of the ANRS workshop on HBV cure. *Gut* 2015;64:1314-1326.
5. Zampino R, Sagnelli C, Boemio A, Sagnelli E, Coppola N. Treatment of chronic HBV infection in developing countries. *Ann Hepatol* 2016;15:816-823.
6. El-Serag HB. Epidemiology of viral hepatitis and hepatocellular carcinoma. *Gastroenterology* 2012;142:1264-1273 e1261.
7. Huang YT, Jen CL, Yang HI, Lee MH, Su J, Lu SN, Iloeje UH, et al. Lifetime risk and sex difference of hepatocellular carcinoma among patients with chronic hepatitis B and C. *J Clin Oncol* 2011;29:3643-3650.
8. Jiang HY, Wang SY, Deng M, Li YC, Ling ZX, Shao L, Ruan B. Immune response to hepatitis B vaccination among people with inflammatory bowel diseases: A systematic review and meta-analysis. *Vaccine* 2017;35:2633-2641.
9. Wu J, Chen ZJ. Innate immune sensing and signaling of cytosolic nucleic acids. *Annu Rev Immunol* 2014;32:461-488.
10. Guidotti LG, Chisari FV. Immunobiology and Pathogenesis of Viral Hepatitis. *Annu. Rev. Pathol. Mech. Dis.* 2006;1:23-61.
11. Park SH, Rehmann B. Immune responses to HCV and other hepatitis viruses. *Immunity* 2014;40:13-24.
12. Wieland SF, Thimme R, Purcell RH, Chisari FV. Genomic analysis of the host response to hepatitis B virus infection. *Proc Natl Acad Sci U S A* 2004;101:6669-6674.
13. Chisari FV, Isogawa M, Wieland SF. Pathogenesis of hepatitis B virus infection. *Pathol Biol (Paris)* 2010;58:258-266.
14. Kwon H, Lok AS. Hepatitis B therapy. *Nat Rev Gastroenterol Hepatol* 2011;8:275-284.
15. Croagh CM, Lubel JS. Natural history of chronic hepatitis B: phases in a complex relationship. *World J Gastroenterol* 2014;20:10395-10404.
16. Ponde RA. Atypical serological profiles in hepatitis B virus infection. *Eur J Clin Microbiol Infect Dis* 2013;32:461-476.
17. Chan HL. Changing scene in hepatitis B serology interpretation. *Hosp Med* 2002;63:16-19.

18. Chevaliez S, Pawlotsky JM. Diagnosis and management of chronic viral hepatitis: antigens, antibodies and viral genomes. *Best Pract Res Clin Gastroenterol* 2008;22:1031-1048.
19. Juszczak J. Clinical course and consequences of hepatitis B infection. *Vaccine* 2002;18:S23-S25.
20. Jung MC, Pape GR. Immunology of hepatitis B infection. *The Lancet Infectious Diseases* 2002;2:43-50.
21. Liang TJ. Hepatitis B: the virus and disease. *Hepatology* 2009;49:S13-21.
22. Rehermann B, Nascimbeni M. Immunology of hepatitis B virus and hepatitis C virus infection. *Nat Rev Immunol* 2005;5:215-229.
23. Haleboua-De Marzio D, Hann HW. Then and now: the progress in hepatitis B treatment over the past 20 years. *World J Gastroenterol* 2014;20:401-413.
24. Gish R, Jia JD, Locarmini S, and Zoulim F. Selection of chronic hepatitis B therapy with high barrier to resistance. *The Lancet infectious diseases*. 2012;12:341-353.
25. Rijckborst V, Janssen HL. The Role of Interferon in Hepatitis B Therapy. *Curr Hepat Rep* 2010;9:231-238.
26. Baltayiannis G, Karayiannis P. Treatment options beyond IFNalpha and NUCs for chronic HBV infection: expectations for tomorrow. *J Viral Hepat* 2014;21:753-761.
27. Nassal M. New insights into HBV replication: new opportunities for improved therapies. *Future Virology* 2009:55-70.
28. Umeda M, Marusawa H, Seno H, Katsurada A, Nabeshima M, Egawa H, Uemoto S, et al. Hepatitis B virus infection in lymphatic tissues in inactive hepatitis B carriers. *J Hepatol* 2005;42:806-812.
29. Jin HJ, Li HT, Sui HX, Xue MQ, Wang YN, Wang JX, Gao FG. Nicotine stimulated bone marrow-derived dendritic cells could augment HBV specific CTL priming by activating PI3K-Akt pathway. *Immunol Lett* 2012;146:40-49.
30. Song J, Li S, Zhou Y, Liu J, Francois S, Lu M, Yang D, et al. Different antiviral effects of IFNalpha subtypes in a mouse model of HBV infection. *Sci Rep* 2017;7:334.
31. Zanetto A, Ferrarese A, Bortoluzzi I, Burra P, Russo FP. New Perspectives on Treatment of Hepatitis B Before and After Liver Transplantation. *Annals of Transplantation* 2016;21:632-643.
32. Brind A, Jiang J, Samuel D, Gigou M, Feray C, Bréchet C, Kremsdorf D. Evidence for selection of hepatitis B mutants after liver transplantation through peripheral blood mononuclear cell infection. *J Hepatol* 1997;26:228-235.
33. Loggi E, Conti F, Cucchetti A, Ercolani G, Pinna AD, Andreone P. Liver grafts from hepatitis B surface antigen-positive donors: A review of the literature. *World J Gastroenterol* 2016;22:8010-8016.
34. Grellier L, Mutimer D, Ahmed M, Brown D, Burroughs AK, Rolles K, McMaster P, et al. Lamivudine prophylaxis against reinfection in liver transplantation for hepatitis B cirrhosis. *The Lancet* 1996;348:1212-1215.
35. Fu XY, Tan DM, Liu CM, Gu B, Hu LH, Peng ZT, Chen B, et al. Early hepatitis B viral DNA clearance

predicts treatment response at week 96. *World J Gastroenterol* 2017;23:2978-2986.

36. Yuen MF, Seto WK, Chow DH, Tsui K, Wong DK, Ngai VW, Wong BC, et al. Long-term lamivudine therapy reduces the risk of long-term complications of chronic hepatitis B infection even in patients without advanced disease. *Antivir Ther* 2006;12:1295-1303.
37. Zanetti AR, Van Damme P, Shouval D. The global impact of vaccination against hepatitis B: a historical overview. *Vaccine* 2008;26:6266-6273.
38. Szmunes W, Stevens CE, Zang EA, Harley EJ, Kellner A. A controlled clinical trial of the efficacy of the hepatitis B vaccine (Heptavax B): a final report. *Hepatology* 1981;1:377-385.
39. Tajiri K, Shimizu Y. Unsolved problems and future perspectives of hepatitis B virus vaccination. *World J Gastroenterol* 2015;21:7074-7083.
40. Fauquet CM, Mayo MA, Maniloff J. *Virus Taxonomy: Eighth Report of the International Committee of Taxonomy of Viruses*. San Diego: CA: Elsevier Academic Press; 2005.
41. Piasecki T, Harkins GW, Chrzastek K, Julian L, Martin DP, Varsani A. Avihepadnavirus diversity in parrots is comparable to that found amongst all other avian species. *Virology* 2013;438:98-105.
42. Piasecki T, Kurenbach B, Chrzastek K, Bednarek K, Kraberger S, Martin DP, Varsani A. Molecular characterisation of an avihepadnavirus isolated from *Psittacula krameri* (ring-necked parrot). *Arch Virol* 2012;157:585-590.
43. Drexler JF, Geipel A, Konig A, Corman VM, van Riel D, Leijten LM, Bremer CM, et al. Bats carry pathogenic hepadnaviruses antigenically related to hepatitis B virus and capable of infecting human hepatocytes. *Proc Natl Acad Sci U S A* 2013;110:16151-16156.
44. Paraskevis D, Magiorkinis G, Magiorkinis E, Ho SY, Belshaw R, Allain JP, Hatzakis A. Dating the origin and dispersal of hepatitis B virus infection in humans and primates. *Hepatology* 2013;57:908-916.
45. Dane DS, Cameron CH, Briggs M. Virus-like particles in serum of patients with Australia-antigen-associated hepatitis. *Lancet* 1970;1:695-698.
46. Robinson WS, Clayton DA, Greenman RL. DNA of a Human Hepatitis B Virus Candidate. *J Virol* 1974;14:384-391.
47. Kaplan. P.M., Greenman RL, Gerin JL, Purcell RH, Robinson WS. DNA polymerase associated with human hepatitis B antigen. *J Virol* 1973;12:995-1005.
48. Urban S, Bartenschlager R, Kubitz R, Zoulim F. Strategies to inhibit entry of HBV and HDV into hepatocytes. *Gastroenterology* 2014;147:48-64.
49. Blanchet M, Sureau C. Infectivity determinants of the hepatitis B virus pre-S domain are confined to the N-terminal 75 amino acid residues. *J Virol* 2007;81:5841-5849.
50. Gilbert RJ, Beales L, Blond D, Simon MN, Lin BY, Chisari FV, Stuart DI, et al. Hepatitis B small surface antigen particles are octahedral. *Proc Natl Acad Sci U S A* 2005;102:14783-14788.
51. Heermann KH, Goldmann U, Schwartz W, Seyffarth T, Baumgarten H, Gerlich WH. Large surface proteins of hepatitis B virus containing the pre-s sequence. *J Virol* 1984;52:396-402.

52. Seeger C, Mason WS. Molecular biology of hepatitis B virus infection. *Virology* 2015;479-480:672-686.
53. Gerlich WH, Robinson WS. Hepatitis B virus contains protein attached to the 5' terminus of its complete DNA strand. *Cell* 1980;21.
54. Summers J, O'Connell A, Millman I. Genome of hepatitis B virus: Restriction enzyme cleavage and structure of DNA extracted from Dane particles *Proc. Nat. Acad. Sci. USA* 1975;72:4597-4601.
55. Delius H, Gough NM, Cameron CH, Murray K. Structure of the hepatitis B virus genome. *J Virol* 1983;47.
56. Haines KM, Loeb DD. The sequence of the RNA primer and the DNA template influence the initiation of plus-strand DNA synthesis in hepatitis B virus. *J Mol Biol* 2007;370:471-480.
57. Bartenschlager R, SCHALLER H. The amino-terminal domain of the hepadnaviral P-gene encodes the terminal protein (genome-linked protein) believed to prime reverse transcription. *The EMBO J* 1988;7:4185-4192.
58. Gish RG, Given BD, Lai CL, Locarnini SA, Lau JY, Lewis DL, Schlupe T. Chronic hepatitis B: *Virology*, natural history, current management and a glimpse at future opportunities. *Antiviral Res* 2015;121:47-58.
59. Doitsh G, Shaul Y. Enhancer I Predominance in Hepatitis B Virus Gene Expression. *Molecular and Cellular Biology* 2004;24:1799-1808.
60. Yan H, Liu Y, Sui J, Li W. NTCP opens the door for hepatitis B virus infection. *Antiviral Res* 2015;121:24-30.
61. McAleer WJ, Buynak EB, Maigetter RZ, Wampler DE, Miller WJ, Milleman MR. Human hepatitis B vaccine from recombinant yeast. *Nature* 1984;307.
62. Chain BM, Myers R. Variability and conservation in hepatitis B virus core protein. *BMC Microbiol* 2005;5:33.
63. Conway JF, Cheng N, Zlotnick A, Wingfield PT, Stahl SJ, Steven AC. Visualization of a 4-helix bundle in the hepatitis B virus capsid by cryo-electron microscopy. *Nature* 1997;3386:91-94.
64. Tan Z, Maguire ML, Loeb DD, Zlotnick A. Genetically altering the thermodynamics and kinetics of hepatitis B virus capsid assembly has profound effects on virus replication in cell culture. *J Virol* 2013;87:3208-3216.
65. Jung J, Hwang SG, Chwae YJ, Park S, Shin HJ, Kim K. Phosphoacceptors threonine 162 and serines 170 and 178 within the carboxyl-terminal RRRS/T motif of the hepatitis B virus core protein make multiple contributions to hepatitis B virus replication. *J Virol* 2014;88:8754-8767.
66. Basagoudanavar SH, Perlman DH, Hu J. Regulation of hepadnavirus reverse transcription by dynamic nucleocapsid phosphorylation. *J Virol* 2007;81:1641-1649.
67. Liu K, Ludgate L, Yuan Z, Hu J, McFadden G. Regulation of Multiple Stages of Hepadnavirus Replication by the Carboxyl-Terminal Domain of Viral Core Protein in trans. *Journal of Virology*

2015;89:2918-2930.

68. Bock CT, Schwinn S, Locarnini S, Fyfe J, Manns MP, Trautwein C, Zentgraf H. Structural organization of the hepatitis B virus minichromosome. *J Mol Biol* 2001;307:183-196.
69. Pollicino T, Belloni L, Raffa G, Pediconi N, Squadrito G, Raimondo G, Levrero M. Hepatitis B virus replication is regulated by the acetylation status of hepatitis B virus cccDNA-bound H3 and H4 histones. *Gastroenterology* 2006;130:823-837.
70. Pumpens P, Grens E. Hepatitis B core particles as a universal display model: a structure-function basis for development. *FEBS Lett* 1999;442:1-6.
71. Zlotnick A, Tan Z, Selzer L. One protein, at least three structures, and many functions. *Structure* 2013;21:6-8.
72. Wu JF, Hsu HY, Ni YH, Chen HL, Wu TC, Chang MH. Suppression of furin by interferon-gamma and the impact on hepatitis B virus antigen biosynthesis in human hepatocytes. *Am J Pathol* 2012;181:19-25.
73. Wang J, Lee AS, Ou JH. Proteolytic conversion of hepatitis B virus e antigen precursor to end product occurs in a postendoplasmic reticulum compartment. *J Virol* 1991;65:5080-5083.
74. Chen MT, Billaud JN, Sallberg M, Guidotti LG, Chisari FV, Jones J, Hughes J, et al. A function of the hepatitis B virus precore protein is to regulate the immune response to the core antigen. *Proc Natl Acad Sci U S A* 2004;101:14913-14918.
75. Chen M, Sallberg M, Hughes J, Jones J, Guidotti LG, Chisari FV, Billaud JN, et al. Immune tolerance split between hepatitis B virus precore and core proteins. *J Virol* 2005;79:3016-3027.
76. DiMattia MA, Watts NR, Stahl SJ, Grimes JM, Steven AC, Stuart DI, Wingfield PT. Antigenic switching of hepatitis B virus by alternative dimerization of the capsid protein. *Structure* 2013;21:133-142.
77. Stuyver LJ, Locarnini SA, Lok A, Richman DD, Carman WF, Dienstag JL, Schinazi RF. Nomenclature for antiviral-resistant human hepatitis B virus mutations in the polymerase region. *Hepatology* 2001;33:751-757.
78. Clark DN, Hu J. Unveiling the roles of HBV polymerase for new antiviral strategies. *Future Virol* 2015;10:283-295.
79. Zoulim F, Saputelli J, Seeger C. Woodchuck hepatitis virus X protein is required for viral infection in vivo. *J Virol* 1994;68:2026-2030.
80. Weber M, Bronsema V, Bartos H, Bosserhoff A, Bartenschlager R, Schaller H. Hepadnavirus P protein utilizes a tyrosine residue in the TP domain to prime reverse transcription. *J Virol* 1994;68:2994-2999.
81. Chen P, Gan Y, Han N, Fang W, Li J, Zhao F, Hu K, et al. Computational evolutionary analysis of the overlapped surface (S) and polymerase (P) region in hepatitis B virus indicates the spacer domain in P is crucial for survival. *PLoS One* 2013;8:e60098.

82. Radziwill G, Tucker W, Schaller H. Mutational analysis of the hepatitis B virus P gene product: domain structure and RNase H activity. *J Virol* 1990;64:613-620.
83. Walsh AW, Langley DR, Colonno RJ, Tenney DJ. Mechanistic characterization and molecular modeling of hepatitis B virus polymerase resistance to entecavir. *PLoS One* 2010;5.
84. Menendez-Arias L, Alvarez M, Pacheco B. Nucleoside/nucleotide analog inhibitors of hepatitis B virus polymerase: mechanism of action and resistance. *Curr Opin Virol* 2014;8:1-9.
85. Xiong Y, Eickbush T. Origin and evolution of retroelements based upon their reverse transcriptase sequences. *The EMBO J* 1990;9:3353-3362.
86. Bartenschlager R, JUNKER-NIEPMANN M, SCHALLER H. The P Gene Product of Hepatitis B Virus Is Required as a Structural Component for Genomic RNA Encapsidation. *Journal of Virology* 1990;64:5324-5332.
87. Li J, Du Y, Liu X, Shen QC, Huang AL, Zheng MY, Luo XM, et al. Binding sensitivity of adefovir to the polymerase from different genotypes of HBV: molecular modeling, docking and dynamics simulation studies. *Acta Pharmacol Sin* 2013;34:319-328.
88. Lucifora J, Arzberger S, Durantel D, Belloni L, Strubin M, Levrero M, Zoulim F, et al. Hepatitis B virus X protein is essential to initiate and maintain virus replication after infection. *J Hepatol* 2011;55:996-1003.
89. Gearhart TL, Bouchard MJ. The hepatitis B virus X protein modulates hepatocyte proliferation pathways to stimulate viral replication. *J Virol* 2010;84:2675-2686.
90. Slagle BL, Bouchard MJ. Hepatitis B Virus X and Regulation of Viral Gene Expression. *Cold Spring Harb Perspect Med* 2016;6.
91. Rawat S, Bouchard MJ. The hepatitis B virus (HBV) HBx protein activates AKT to simultaneously regulate HBV replication and hepatocyte survival. *JVI* 2015;89:999-1012.
92. Gearhart TL, Bouchard MJ. Replication of the hepatitis B virus requires a calcium-dependent HBx-induced G1 phase arrest of hepatocytes. *Virology* 2010;407:14-25.
93. Bouchard MJ, Schneider RJ. The enigmatic X gene of hepatitis B virus. *J Virol* 2004;78:12725-12734.
94. Hsieh A, Kim HS, Lim SO, Yu DY, Jung G. Hepatitis B viral X protein interacts with tumor suppressor adenomatous polyposis coli to activate Wnt/beta-catenin signaling. *Cancer Lett* 2011;300:162-172.
95. Iyer S, Groopman JD. Interaction of mutant hepatitis B X protein with p53 tumor suppressor protein affects both transcription and cell survival. *Mol Carcinog* 2011;50:972-980.
96. Mason WS, Seal G, Summers J. Virus of Pekin ducks with structural and biological relatedness to human hepatitis B virus. *J Virol* 1980;36:829-836.
97. Summers J, Mason W. Replication of the genome of a hepatitis B-like virus by reverse transcription of an RNA intermediate. *Cell* 1982;29:403-415.

98. Yan H, Zhong G, Xu G, He W, Jing Z, Gao Z, Huang Y, et al. Sodium taurocholate cotransporting polypeptide is a functional receptor for human hepatitis B and D virus. *eLIFE* 2012.
99. Verrier ER, Colpitts CC, Bach C, Heydmann L, Weiss A, Renaud M, Durand SD, et al. A Targeted Functional RNA Interference Screen Uncovers Glypican 5 as an Entry Factor for Hepatitis B and D Viruses. *Hepatology* 2016;Vol. 63.
100. Schulze A, Gripon P, Urban S. Hepatitis B virus infection initiates with a large surface protein-dependent binding to heparan sulfate proteoglycans. *Hepatology* 2007;46:1759-1768.
101. Claro da Silva T, Polli JE, Swaan PW. The solute carrier family 10 (SLC10): beyond bile acid transport. *Mol Aspects Med* 2013;34:252-269.
102. Ni Y, Lempp FA, Mehrle S, Nkongolo S, Kaufman C, Falth M, Stindt J, et al. Hepatitis B and D viruses exploit sodium taurocholate co-transporting polypeptide for species-specific entry into hepatocytes. *Gastroenterology* 2014;146:1070-1083.
103. Huang HC, Chen CC, Chang WC, Tao MH, Huang C. Entry of hepatitis B virus into immortalized human primary hepatocytes by clathrin-dependent endocytosis. *J Virol* 2012;86:9443-9453.
104. Macovei A, Radulescu C, Lazar C, Petrescu S, Durantel D, Dwek RA, Zitzmann N, et al. Hepatitis B virus requires intact caveolin-1 function for productive infection in HepaRG cells. *J Virol* 2010;84:243-253.
105. Blondot ML, Bruss V, Kann M. Intracellular transport and egress of hepatitis B virus. *J Hepatol* 2016;64:S49-59.
106. Rabe B, Vlachou A, Pante N, Helenius A, Kann M. Nuclear import of hepatitis B virus capsids and release of the viral genome. *Proc Natl Acad Sci U S A* 2003;100:9849-9854.
107. Schmitz A, Schwarz A, Foss M, Zhou L, Rabe B, Hoellenriegel J, Stoeber M, et al. Nucleoporin 153 arrests the nuclear import of hepatitis B virus capsids in the nuclear basket. *PLoS Pathog* 2010;6:e1000741.
108. Nassal M. HBV cccDNA: viral persistence reservoir and key obstacle for a cure of chronic hepatitis B. *Gut* 2015;64:1972-1984.
109. Levrero M, Pollicino T, Petersen J, Belloni L, Raimondo G, Dandri M. Control of cccDNA function in hepatitis B virus infection. *J Hepatol* 2009;51:581-592.
110. Bock CT, Schranz P, Schröder CH, Zentgraf H. Hepatitis B virus genome is organized into nucleosomes in the nucleus of the infected cell. *Virus Genes* 1994;8:215-229.
111. Bartenschlager R, H. S. Hepadnaviral assembly is initiated by polymerase binding to the encapsidation signal in the viral RNA genome. *The EMBO* 1992;11:3413-3420.
112. Rieger A, Nassal M. Specific Hepatitis B Virus Minus-Strand DNA Synthesis Requires Only the 59 Encapsidation Signal and the 39-Proximal Direct Repeat DR1. *J Virol* 1996:585-589
113. Hirsch RC, Loeb DD, Pollack JR, Ganem D. cis-acting sequences required for encapsidation of duck hepatitis B virus pregenomic RNA. *J Virol* 1991;65:3309-3316.

114. Wang GH, Seeger C. Novel Mechanism for Reverse Transcription in Hepatitis B Viruses. *Journal of Virology* 1993;67: 6507-6512
115. Zoulim F, Seeger C. Reverse transcription in hepatitis B viruses is primed by a tyrosine residue of the polymerase. *J Virol* 1994;68:6-13.
116. Hirsch RC, Lavine JE, Chang LJ, Varmus HE, Ganem D. Polymerase gene products of hepatitis B viruses are required for genomic RNA packaging as well as for reverse transcription. *Nature* 1990;344:552-555.
117. Lentz TB, Loeb DD. Roles of the envelope proteins in the amplification of covalently closed circular DNA and completion of synthesis of the plus-strand DNA in hepatitis B virus. *J Virol* 2011;85:11916-11927.
118. Locarnini S, Mason WS. Cellular and virological mechanisms of HBV drug resistance. *J Hepatol* 2006;44:422-431.
119. Kock J, Rosler C, Zhang JJ, Blum HE, Nassal M, Thoma C. Generation of covalently closed circular DNA of hepatitis B viruses via intracellular recycling is regulated in a virus specific manner. *PLoS Pathog* 2010;6:e1001082.
120. Ou JH, Rutter WJ. Regulation of Secretion of the Hepatitis B Virus Major Surface Antigen by the PreS-1 Protein. *JVI* 1987;61:782-786.
121. Patzer EJ, Nakamura GR, Simonsen CC, Levinson AD, Brands R. Intracellular assembly and packaging of hepatitis B surface antigen particles occur in the endoplasmic reticulum. *J Virol* 1986;58:884-892.
122. Janeway CA. Approaching the asymptote? Evolution and revolution in immunology. *Cold Spring Harb Symp Quant Biol* 1989;54:1:1-13.
123. Watts C, West MA, Zaru R. TLR signalling regulated antigen presentation in dendritic cells. *Curr Opin Immunol* 2010;22:124-130.
124. Ivashkiv LB, Donlin LT. Regulation of type I interferon responses. *Nat Rev Immunol* 2014;14:36-49.
125. Capobianchi MR, Uleri E, Caglioti C, Dolei A. Type I IFN family members: similarity, differences and interaction. *Cytokine Growth Factor Rev* 2015;26:103-111.
126. Gurtler C, Bowie AG. Innate immune detection of microbial nucleic acids. *Trends Microbiol* 2013;21:413-420.
127. Bertoletti A, Ferrari C. Adaptive immunity in HBV infection. *J Hepatol* 2016;64:S71-83.
128. Thomas E, Liang TJ. Experimental models of hepatitis B and C - new insights and progress. *Nat Rev Gastroenterol Hepatol* 2016;13:362-374.
129. Gordon S. Pattern recognition receptors: doubling up for the innate immune response. *Cell* 2002;111: 927-930.
130. Janeway CA, Jr., Medzhitov R. Innate immune recognition. *Annu Rev Immunol* 2002;20:197-216.

131. Mogensen TH. Pathogen recognition and inflammatory signaling in innate immune defenses. *Clin Microbiol Rev* 2009;22:240-273, Table of Contents.
132. Hardison SE, Brown GD. C-type lectin receptors orchestrate antifungal immunity. *Nat Immunol* 2012;13:817-822.
133. Barbalat R, Ewald SE, Mouchess ML, Barton GM. Nucleic acid recognition by the innate immune system. *Annu Rev Immunol* 2011;29:185-214.
134. Opitz B, Puschel A, Schmeck B, Hocke AC, Rosseau S, Hammerschmidt S, Schumann RR, et al. Nucleotide-binding oligomerization domain proteins are innate immune receptors for internalized *Streptococcus pneumoniae*. *J Biol Chem* 2004;279:36426-36432.
135. Kawai T, Akira S. The role of pattern-recognition receptors in innate immunity: update on Toll-like receptors. *Nat Immunol* 2010;11:373-384.
136. Shi Z, Cai Z, Sanchez A, Zhang T, Wen S, Wang J, Yang J, et al. A novel Toll-like receptor that recognizes vesicular stomatitis virus. *J Biol Chem* 2011;286:4517-4524.
137. Pifer R, Benson A, Sturge CR, Yarovinsky F. UNC93B1 is essential for TLR11 activation and IL-12-dependent host resistance to *Toxoplasma gondii*. *J Biol Chem* 2011;286:3307-3314.
138. Andrade WA, Souza Mdo C, Ramos-Martinez E, Nagpal K, Dutra MS, Melo MB, Bartholomeu DC, et al. Combined action of nucleic acid-sensing Toll-like receptors and TLR11/TLR12 heterodimers imparts resistance to *Toxoplasma gondii* in mice. *Cell Host Microbe* 2013;13:42-53.
139. Krieg AM. AIMing 2 defend against intracellular pathogens. *Nat Immunol* 2010;11:367-369.
140. Leong C, Oshiumi H, Suzuki T, Matsumoto M, Seya T. Nucleic Acid Sensors Involved in the Recognition of HBV in the Liver—Specific in vivo Transfection Mouse Models—Pattern Recognition Receptors and Sensors for HBV. *Medical Sciences* 2015;3:16-24.
141. Shi B, Ren G, Hu Y, Wang S, Zhang Z, Yuan Z. HBsAg inhibits IFN-alpha production in plasmacytoid dendritic cells through TNF-alpha and IL-10 induction in monocytes. *PLoS One* 2012;7:e44900.
142. Wang S, Chen Z, Hu C, Qian F, Cheng Y, Wu M, Shi B, et al. Hepatitis B virus surface antigen selectively inhibits TLR2 ligand-induced IL-12 production in monocytes/macrophages by interfering with JNK activation. *J Immunol* 2013;190:5142-5151.
143. Wu J, Meng Z, Jiang M, Pei R, Trippler M, Broering R, Bucchi A, et al. Hepatitis B virus suppresses toll-like receptor-mediated innate immune responses in murine parenchymal and nonparenchymal liver cells. *Hepatology* 2009;49:1132-1140.
144. Liu D, Wu A, Cui L, Hao R, Wang Y, He J, Guo D. Hepatitis B virus polymerase suppresses NF-kappaB signaling by inhibiting the activity of IKKs via interaction with Hsp90beta. *PLoS One* 2014;9:e91658.
145. Karimi-Googheri M, Daneshvar H, Khaleghinia M, Bidaki R, Kazemi Arababadi M. Decreased Expressions of STING but not IRF3 Molecules in Chronic HBV Infected Patients. *Arch Iran Med*

2015;18:351-354.

146. Chen Z, Cheng Y, Xu Y, Liao J, Zhang X, Hu Y, Zhang Q, et al. Expression profiles and function of Toll-like receptors 2 and 4 in peripheral blood mononuclear cells of chronic hepatitis B patients. *Clin Immunol* 2008;128:400-408.
147. Lin KJ, Lin TM, Wang CH, Liu HC, Lin YL, Eng HL. Down-regulation of Toll-like receptor 7 expression in hepatitis-virus-related human hepatocellular carcinoma. *Hum Pathol* 2013;44:534-541.
148. Wu JF, Chen CH, Ni YH, Lin YT, Chen HL, Hsu HY, Chang MH. Toll-like receptor and hepatitis B virus clearance in chronic infected patients: a long-term prospective cohort study in Taiwan. *J Infect Dis* 2012;206:662-668.
149. Yu S, Chen J, Wu M, Chen H, Kato N, Yuan Z. Hepatitis B virus polymerase inhibits RIG-I- and Toll-like receptor 3-mediated beta interferon induction in human hepatocytes through interference with interferon regulatory factor 3 activation and dampening of the interaction between TBK1/IKKepsilon and DDX3. *J Gen Virol* 2010;91:2080-2090.
150. Vincent IE, Zannetti C, Lucifora J, Norder H, Protzer U, Hainaut P, Zoulim F, et al. Hepatitis B virus impairs TLR9 expression and function in plasmacytoid dendritic cells. *PLoS One* 2011;6:e26315.
151. Yoneyama M, Kikuchi M, Natsukawa T, Shinobu N, Imaizumi T, Miyagishi M, Taira K, et al. The RNA helicase RIG-I has an essential function in double-stranded RNA-induced innate antiviral responses. *Nat Immunol* 2004;5:730-737.
152. Kanneganti TD, Lamkanfi M, Nunez G. Intracellular NOD-like receptors in host defense and disease. *Immunity* 2007;27:549-559.
153. Desmet CJ, Ishii KJ. Nucleic acid sensing at the interface between innate and adaptive immunity in vaccination. *Nat Rev Immunol* 2012;12:479-491.
154. Chan YK, Gack MU. Viral evasion of intracellular DNA and RNA sensing. *Nat Rev Microbiol* 2016;14:360-373.
155. Iwakiri D, Takada K. Role of EBERs in the Pathogenesis of EBV Infection. 2010;107:119-136.
156. Brulois K, Jung JU. Interplay between Kaposi's sarcoma-associated herpesvirus and the innate immune system. *Cytokine Growth Factor Rev* 2014;25:597-609.
157. Rasmussen SB, Jensen SB, Nielsen C, Quartin E, Kato H, Chen ZJ, Silverman RH, et al. Herpes simplex virus infection is sensed by both Toll-like receptors and retinoic acid-inducible gene-like receptors, which synergize to induce type I interferon production. *J Gen Virol* 2009;90:74-78.
158. Goubau D, Deddouche S, Reis e Sousa C. Cytosolic sensing of viruses. *Immunity* 2013;38:855-869.
159. Sato S, Li K, Kameyama T, Hayashi T, Ishida Y, Murakami S, Watanabe T, et al. The RNA sensor RIG-I dually functions as an innate sensor and direct antiviral factor for hepatitis B virus. *Immunity* 2015;42:123-132.
160. Kato H, Takeuchi O, Mikamo-Satoh E, Hirai R, Kawai T, Matsushita K, Hiiragi A, et al. Length-

dependent recognition of double-stranded ribonucleic acids by retinoic acid-inducible gene-I and melanoma differentiation-associated gene 5. *J Exp Med* 2008;205:1601-1610.

161. Rehwinkel J, Tan CP, Goubau D, Schulz O, Pichlmair A, Bier K, Robb N, et al. RIG-I detects viral genomic RNA during negative-strand RNA virus infection. *Cell* 2010;140:397-408.

162. Sabbah A, Chang TH, Harnack R, Frohlich V, Tominaga K, Dube PH, Xiang Y, et al. Activation of innate immune antiviral responses by Nod2. *Nat Immunol* 2009;10:1073-1080.

163. Brennan-Laun SE, Ezelle HJ, Li XL, Hassel BA. RNase-L control of cellular mRNAs: roles in biologic functions and mechanisms of substrate targeting. *J Interferon Cytokine Res* 2014;34:275-288.

164. Cui X, Clark DN, Liu K, Xu XD, Guo JT, Hu J. Viral DNA-Dependent Induction of Innate Immune Response to Hepatitis B Virus in Immortalized Mouse Hepatocytes. *J Virol* 2016;90:486-496.

165. Wang H, Ryu WS. Hepatitis B virus polymerase blocks pattern recognition receptor signaling via interaction with DDX3: implications for immune evasion. *PLoS Pathog* 2010;6:e1000986.

166. Lu HL, Liao F. Melanoma differentiation-associated gene 5 senses hepatitis B virus and activates innate immune signaling to suppress virus replication. *J Immunol* 2013;191:3264-3276.

167. Mozer-Lisewska I, Kowala-Piaskowska A, Mania A, Jenek R, Samara H, Kaczmarek E, Sikora J, et al. Expression of pattern recognition receptors in liver biopsy specimens of children chronically infected with HBV and HCV. *Folia Histochem. Cytobiol* 2011;49.

168. Cai X, Chiu YH, Chen ZJ. The cGAS-cGAMP-STING pathway of cytosolic DNA sensing and signaling. *Mol Cell* 2014;54:289-296.

169. Paludan SR, Bowie AG. Immune sensing of DNA. *Immunity* 2013;38:870-880.

170. Keating SE, Baran M, Bowie AG. Cytosolic DNA sensors regulating type I interferon induction. *Trends Immunol* 2011;32:574-581.

171. Unterholzner L. The interferon response to intracellular DNA: why so many receptors? *Immunobiology* 2013;218:1312-1321.

172. Wieland SF, Vega RG, Muller R, Evans CF, Hilbush B, Guidotti LG, Sutcliffe JG, et al. Searching for Interferon-Induced Genes That Inhibit Hepatitis B Virus Replication in Transgenic Mouse Hepatocytes. *Journal of Virology* 2003;77:1227-1236.

173. Chen QY, Liu YH, Li JH, Wang ZK, Liu JX, Yuan ZH. DNA-dependent activator of interferon-regulatory factors inhibits hepatitis B virus replication. *World J Gastroenterol* 2012;18:2850-2858.

174. Zhang Z, Yuan B, Bao M, Lu N, Kim T, Liu Y-J. The helicase DDX41 senses intracellular DNA mediated by the adaptor STING in dendritic cells. *Nat Immunol* 2011;12:959-965.

175. Rathinam VA, Jiang Z, Waggoner SN, Sharma S, Cole LE, Waggoner L, Vanaja SK, et al. The AIM2 inflammasome is essential for host defense against cytosolic bacteria and DNA viruses. *Nat Immunol* 2010;11:395-402.

176. Zhen J, Zhang L, Pan J, Ma S, Yu X, Li X, Chen S, et al. AIM2 mediates inflammation-associated renal damage in hepatitis B virus-associated glomerulonephritis by regulating caspase-1, IL-1beta, and

IL-18. *Mediators Inflamm* 2014;2014:190860.

177. Orzalli MH, Broekema NM, Diner BA, Hancks DC, Elde NC, Cristea IM, Knipe DM. cGAS-mediated stabilization of IFI16 promotes innate signaling during herpes simplex virus infection. *Proc Natl Acad Sci U S A* 2015;112:E1773-1781.

178. Sun L, Wu J, Du F, Chen X, ZJ C. Cyclic GMP-AMP Synthase Is a Cytosolic DNA Sensor That Activates the Type I Interferon Pathway. 2013.

179. Wieland SF, Chisari FV. Stealth and cunning: hepatitis B and hepatitis C viruses. *J Virol* 2005;79:9369-9380.

180. Dansako H, Ueda Y, Okumura N, Satoh S, Sugiyama M, Mizokami M, Ikeda M, et al. The cyclic GMP-AMP synthetase-STING signaling pathway is required for both the innate immune response against HBV and the suppression of HBV assembly. *FEBS J* 2016;283:144-156.

181. Wu J, Sun L, Chen X, Du F, Shi H, Chen C, ZJ C. Cyclic GMP-AMP Is an Endogenous Second Messenger in Innate Immune Signaling by Cytosolic DNA. *Science* 2013;Vol 339.

182. Wu X, Wu FH, Wang X, Wang L, Siedow JN, Zhang W, Pei ZM. Molecular evolutionary and structural analysis of the cytosolic DNA sensor cGAS and STING. *Nucleic Acids Res* 2014;42:8243-8257.

183. Civril F, Deimling T, de Oliveira Mann CC, Ablasser A, Moldt M, Witte G, Hornung V, et al. Structural mechanism of cytosolic DNA sensing by cGAS. *Nature* 2013;498:332-337.

184. Kranzusch PJ, Lee AS, Berger JM, Doudna JA. Structure of human cGAS reveals a conserved family of second-messenger enzymes in innate immunity. *Cell Rep* 2013;3:1362-1368.

185. Gao P, Ascano M, Wu Y, Barchet W, Gaffney BL, Zillinger T, Serganov AA, et al. Cyclic [G(2',5')pA(3',5')p] is the metazoan second messenger produced by DNA-activated cyclic GMP-AMP synthase. *Cell* 2013;153:1094-1107.

186. Zhang X, Wu J, Du F, Xu H, Sun L, Chen Z, Brautigam CA, et al. The cytosolic DNA sensor cGAS forms an oligomeric complex with DNA and undergoes switch-like conformational changes in the activation loop. *Cell Rep* 2014;6:421-430.

187. Li X, Shu C, Yi G, Chaton CT, Shelton CL, Diao J, Zuo X, et al. Cyclic GMP-AMP synthase is activated by double-stranded DNA-induced oligomerization. *Immunity* 2013;39:1019-1031.

188. Yin Q, Fu TM, Li J, Wu H. Structural biology of innate immunity. *Annu Rev Immunol* 2015;33:393-416.

189. Mankan AK, Schmidt T, Chauhan D, Goldeck M, Honing K, Gaidt M, Kubarenko AV, et al. Cytosolic RNA:DNA hybrids activate the cGAS-STING axis. *EMBO J* 2014;33:2937-2946.

190. Herzner AM, Hagmann CA, Goldeck M, Wolter S, Kubler K, Wittmann S, Gramberg T, et al. Sequence-specific activation of the DNA sensor cGAS by Y-form DNA structures as found in primary HIV-1 cDNA. *Nat Immunol* 2015;16:1025-1033.

191. Liang Q, Seo GJ, Choi YJ, Kwak MJ, Ge J, Rodgers MA, Shi M, et al. Crosstalk between the cGAS DNA sensor and Beclin-1 autophagy protein shapes innate antimicrobial immune responses. *Cell Host*

Microbe 2014;15:228-238.

192. Seo GJ, Yang A, Tan B, Kim S, Liang Q, Choi Y, Yuan W, et al. Akt Kinase-Mediated Checkpoint of cGAS DNA Sensing Pathway. *Cell Rep* 2015;13:440-449.
193. Xia P, Ye B, Wang S, Zhu X, Du Y, Xiong Z, Tian Y, et al. Glutamylation of the DNA sensor cGAS regulates its binding and synthase activity in antiviral immunity. *Nat Immunol* 2016;17:369-378.
194. Shu C, Li X, Li P. The mechanism of double-stranded DNA sensing through the cGAS-STING pathway. *Cytokine Growth Factor Rev* 2014;25:641-648.
195. Ablasser A, Schmid-Burgk JL, Hemmerling I, Horvath GL, Schmidt T, Latz E, Hornung V. Cell intrinsic immunity spreads to bystander cells via the intercellular transfer of cGAMP. *Nature* 2013;503:530-534.
196. Bridgeman A, Maelfait J, Davenne T, Partridge T, Peng Y, Mayer A, Dong T, et al. Viruses transfer the antiviral second messenger cGAMP between cells. *Science* 2015;349:1228-1232.
197. Gentili M, Kowal J, Tkach M, Satoh T, Lahaye X, Conrad C, Boyron M, et al. Transmission of innate immune signaling by packaging of cGAMP in viral particles. *Science* 2015;349:1232-1236.
198. Chen Q, Sun L, Chen ZJ. Regulation and function of the cGAS-STING pathway of cytosolic DNA sensing. *Nat Immunol* 2016;17:1142-1149.
199. Li XD, Wu J, Gao D, Wang H, Sun L, Chen ZJ. Pivotal Roles of cGAS-cGAMP Signaling in Antiviral Defense and Immune Adjuvant Effects. *Science* 2013;342.
200. Ishikawa H, Ma Z, Barber GN. STING regulates intracellular DNA-mediated, type I interferon-dependent innate immunity. *Nature* 2009;461:788-792.
201. Schoggins JW, MacDuff DA, Imanaka N, Gainey MD, Shrestha B, Eitson JL, Mar KB, et al. Pan-viral specificity of IFN-induced genes reveals new roles for cGAS in innate immunity. *Nature* 2014;505:691-695.
202. Ma Z, Jacobs SR, West JA, Stopford C, Zhang Z, Davis Z, Barber GN, et al. Modulation of the cGAS-STING DNA sensing pathway by gammaherpesviruses. *Proc Natl Acad Sci U S A* 2015;112:E4306-E4315.
203. Lam E, Stein S, Falck-Pedersen E. Adenovirus detection by the cGAS/STING/TBK1 DNA sensing cascade. *J Virol* 2014;88:974-981.
204. Sunthamala N, Thierry F, Teissier S, Pientong C, Kongyingyoes B, Tangsiriwatthana T, Sangkomkamhang U, et al. E2 proteins of high risk human papillomaviruses down-modulate STING and IFN-kappa transcription in keratinocytes. *PLoS One* 2014;9:e91473.
205. Paijo J, Doring M, Spanier J, Grabski E, Nooruzzaman M, Schmidt T, Witte G, et al. cGAS Senses Human Cytomegalovirus and Induces Type I Interferon Responses in Human Monocyte-Derived Cells. *PLoS Pathog* 2016;12:e1005546.
206. West AP, Khoury-Hanold W, Staron M, Tal MC, Pineda CM, Lang SM, Bestwick M, et al. Mitochondrial DNA stress primes the antiviral innate immune response. *Nature* 2015;520:553-557.

207. Sun B, Sundstrom KB, Chew JJ, Bist P, Gan ES, Tan HC, Goh KC, et al. Dengue virus activates cGAS through the release of mitochondrial DNA. *Sci Rep* 2017;7:3594.
208. Christensen MH, Paludan SR. Viral evasion of DNA-stimulated innate immune responses. *Cell Mol Immunol* 2017;14:4-13.
209. Gao D, Wu J, Wu YT, Du F, Aroh C, Yan N, Sun L, et al. Cyclic GMP-AMP Synthase Is an Innate Immune Sensor of HIV and Other Retroviruses. *Science* 2013;341:903-906.
210. Jakobsen MR, Bak RO, Andersen A, Berg RK, Jensen SB, Tengchuan J, Laustsen A, et al. IFI16 senses DNA forms of the lentiviral replication cycle and controls HIV-1 replication. *Proc Natl Acad Sci U S A.* 2013;110:4571-4580.
211. Horan KA, Hansen K, Jakobsen MR, Holm CK, Soby S, Unterholzner L, Thompson M, et al. Proteasomal degradation of herpes simplex virus capsids in macrophages releases DNA to the cytosol for recognition by DNA sensors. *J Immunol* 2013;190:2311-2319.
212. Johnson KE, Chikoti L, Chandran B. Herpes simplex virus 1 infection induces activation and subsequent inhibition of the IFI16 and NLRP3 inflammasomes. *J Virol* 2013;87:5005-5018.
213. Li T, Chen J, Cristea IM. Human cytomegalovirus tegument protein pUL83 inhibits IFI16-mediated DNA sensing for immune evasion. *Cell Host Microbe* 2013;14:591-599.
214. Kerur N, Veettil MV, Sharma-Walia N, Bottero V, Sadagopan S, Otageri P, Chandran B. IFI16 acts as a nuclear pathogen sensor to induce the inflammasome in response to Kaposi Sarcoma-associated herpesvirus infection. *Cell Host Microbe* 2011;9:363-375.
215. Ansari MA, Singh VV, Dutta S, Veettil MV, Dutta D, Chikoti L, Lu J, et al. Constitutive interferon-inducible protein 16-inflammasome activation during Epstein-Barr virus latency I, II, and III in B and epithelial cells. *J Virol* 2013;87:8606-8623.
216. Hornung V, Ablasser A, Charrel-Dennis M, Bauernfeind F, Horvath G, Caffrey DR, Latz E, et al. AIM2 recognizes cytosolic dsDNA and forms a caspase-1-activating inflammasome with ASC. *Nature* 2009;458:514-518.
217. Abbink TE, Berkhout B. HIV-1 reverse transcription initiation: a potential target for novel antivirals? *Virus Res* 2008;134:4-18.
218. Beachboard DC, Horner SM. Innate immune evasion strategies of DNA and RNA viruses. *Curr Opin Microbiol* 2016;32:113-119.
219. Wu JJ, Li W, Shao Y, Avey D, Fu B, Gillen J, Hand T, et al. Inhibition of cGAS DNA Sensing by a Herpesvirus Virion Protein. *Cell Host Microbe* 2015;18:333-344.
220. Zhang G, Chan B, Samarina N, Abere B, Weidner-Glunde M, Buch A, Pich A, et al. Cytoplasmic isoforms of Kaposi sarcoma herpesvirus LANA recruit and antagonize the innate immune DNA sensor cGAS. *Proc Natl Acad Sci U S A.* 2016;113:1034-1043.
221. Christensen MH, Jensen SB, Miettinen JJ, Luecke S, Prabakaran T, Reinert LS, Mettenleiter T, et al. HSV-1 ICP27 targets the TBK1-activated STING signalsome to inhibit virus-induced type I IFN

expression. *EMBO J* 2016;35:1385-1399.

222. Lau L, Gray EE, Brunette RL, Stetson DB. DNA tumor virus oncogenes antagonize the cGAS-STING DNA-sensing pathway. *Science* 2015;350:568-571.

223. Liu Y, Li J, Chen J, Li Y, Wang W, Du X, Song W, et al. Hepatitis B virus polymerase disrupts K63-linked ubiquitination of STING to block innate cytosolic DNA-sensing pathways. *J Virol* 2015;89:2287-2300.

224. Rasaiyaah J, Tan CP, Fletcher AJ, Price AJ, Blondeau C, Hilditch L, Jacques DA, et al. HIV-1 evades innate immune recognition through specific cofactor recruitment. *Nature* 2013;503:402-405.

225. Protzer U, Maini MK, Knolle PA. Living in the liver: hepatic infections. *Nat Rev Immunol* 2012;12:201-213.

226. Zhang X, Shi H, Wu J, Sun L, Chen C, Chen ZJ. Cyclic GMP-AMP containing mixed phosphodiester linkages is an endogenous high-affinity ligand for STING. *Mol Cell* 2013;51:226-235.

227. Thomsen MK, Nandakumar R, Stadler D, Malo A, Valls RM, Wang F, Reinert LS, et al. Lack of immunological DNA sensing in hepatocytes facilitates hepatitis B virus infection. *Hepatology* 2016;64:746-759.

228. Gerhardt E, Bruss V. Phenotypic mixing of rodent but not avian hepadnavirus surface proteins into human hepatitis B virus particles. *J Virol* 1995;69:01-08.

229. Dandri M, Schirmacher P, Rogler CE. Woodchuck hepatitis virus X protein is present in chronically infected woodchuck liver and woodchuck hepatocellular carcinomas which are permissive for viral replication. *J Virol* 1996;70:5246-5254.

230. Wieland SF. The Chimpanzee Model for Hepatitis B Virus Infection. *Cold Spring Harb Perspect Med* 2015;5.

231. Bukh J. A critical role for the chimpanzee model in the study of hepatitis C. *Hepatology* 2004;39:1469-1475.

232. Weber O, Schlemmer KH, Hartmann E, Hagelschuer I, Paessens A, Graef E, Deres K, et al. Inhibition of human hepatitis B virus (HBV) by a novel non-nucleosidic compound in a transgenic mouse model. *Antiviral Res* 2002;54:69-78.

233. Chisari F, Pinkert C, Milich D, Filippi P, McLachlan A, Palmiter R, Brinster R. A transgenic mouse model of the chronic hepatitis B surface antigen carrier state. *Science* 1985;230:1157-1160.

234. Yang PL, Althage A, Chung J, Chisari FV. Hydrodynamic injection of viral DNA: a mouse model of acute hepatitis B virus infection. *Proc Natl Acad Sci U S A* 2002;99:13825-13830.

235. Sprinzl MF, Oberwinkler H, Schaller H, Protzer U. Transfer of hepatitis B virus genome by adenovirus vectors into cultured cells and mice: crossing the species barrier. *J Virol* 2001;75:5108-5118.

236. Zeissig S, Murata K, Sweet L, Publicover J, Hu Z, Kaser A, Bosse E, et al. Hepatitis B virus-induced lipid alterations contribute to natural killer T cell-dependent protective immunity. *Nat Med* 2012;18:1060-1068.

237. Sandmann L, Ploss A. Barriers of hepatitis C virus interspecies transmission. *Virology* 2013;435:70-80.
238. Raney AK, Eggers CM, Kline EF, Guidotti LG, Pontoglio M, Yaniv M, McLachlan A. Nuclear covalently closed circular viral genomic DNA in the liver of hepatocyte nuclear factor 1 alpha-null hepatitis B virus transgenic mice. *J Virol* 2001;75:2900-2911.
239. Dandri M, Burda MR, Torok E, Pollok JM, Iwanska A, Sommer G, Rogiers X, et al. Repopulation of mouse liver with human hepatocytes and in vivo infection with hepatitis B virus. *Hepatology* 2001;33:981-988.
240. Lutgehetmann M, Bornscheuer T, Volz T, Allweiss L, Bockmann JH, Pollok JM, Lohse AW, et al. Hepatitis B virus limits response of human hepatocytes to interferon-alpha in chimeric mice. *Gastroenterology* 2011;140:2074-2083, 2083 e2071-2072.
241. Mercer DF, Schiller DE, Elliott JF, Douglas DN, Hao C, Rinfret A, Addison WR, et al. Hepatitis C virus replication in mice with chimeric human livers. *Nat Med* 2001;7:927-933.
242. Dorner M, Horwitz JA, Donovan BM, Labitt RN, Budell WC, Friling T, Vogt A, et al. Completion of the entire hepatitis C virus life cycle in genetically humanized mice. *Nature* 2013;501:237-241.
243. Lempp FA, Mutz P, Lipps C, Wirth D, Bartenschlager R, Urban S. Evidence that hepatitis B virus replication in mouse cells is limited by the lack of a host cell dependency factor. *J Hepatol* 2016;64:556-564.
244. Lempp FA, Qu B, Wang YX, Urban S. Hepatitis B Virus Infection of a Mouse Hepatic Cell Line Reconstituted with Human Sodium Taurocholate Cotransporting Polypeptide. *J Virol* 2016;90:4827-4831.
245. Maily L, Zeisel MB, Baumert TF. Towards novel immunocompetent animal models for hepatitis B virus infection. *Hepatology* 2017.
246. Nakabayashi H, Taketa K, Miyano K, Yamane T, Sato J. Growth of Human Hepatoma Cell Lines with Differentiated Functions in Chemically Defined Medium. *Cancer Reserch* 1982;42:3858-3863.
247. Sureau C, Romet-Lemonne JL, Mullins JI, Essex M. Production of hepatitis B virus by a differentiated human hepatoma cell line after transfection with cloned circular HBV DNA. *Cell* 1986;47:37047.
248. Lucifora J, Xia Y, Reisinger F, Zhang K, Stadler D, Cheng X, Sprinzl MF, et al. Specific and Nonhepatotoxic Degradation of Nuclear Hepatitis B Virus cccDNA. *Science* 2014;3436176:1221-1228.
249. Andersson TB, Kanebratt KP, Kenna JG. The HepaRG cell line: a unique in vitro tool for understanding drug metabolism and toxicology in human. *Expert opinion on drug metabolism & toxicology* 2012;8.
250. Gripon P, Rumin S, Urban S, Le Seyec J, Glaise D, Cannie I, Guyomard C, et al. Infection of a human hepatoma cell line by hepatitis B virus. *Proc Natl Acad Sci U S A* 2002;99:15655-15660.
251. Ndongo-Thiam N, Berthillon P, Errazuriz E, Bordes I, De Sequeira S, Trépo C, Petit M-A. Long-term propagation of serum hepatitis C virus (HCV) with production of enveloped HCV particles in human

HepaRG hepatocytes. *Hepatology* 2011;54:406-417.

252. Chen J, Wu M, Liu K, Zhang W, Li Y, Zhou X, Bai L, et al. New insights into hepatitis B virus biology and implications for novel antiviral strategies. *National Science Review* 2015;2:296-313.

253. Thomas D, Zoulim F. New challenges in viral hepatitis. *Gut* 2012;61 Suppl 1:i1-5.

254. Ploss A, Khetani SR, Jones CT, Syder AJ, Trehan K, Gaysinskaya VA, Mu K, et al. Persistent hepatitis C virus infection in microscale primary human hepatocyte cultures. *Proc Natl Acad Sci U S A* 2010;107:3141-3145.

255. Sivaraman A, Leach JK, Townsend S, Iida T, Hogan BJ, Stolz DB, Fry R, et al. A Microscale In Vitro Physiological Model of the Liver: Predictive Screens for Drug Metabolism and Enzyme Induction. *Current Drug Metabolism* 2005;6:569-591.

256. Iwamoto M, Watashi K, Tsukuda S, Aly HH, Fukasawa M, Fujimoto A, Suzuki R, et al. Evaluation and identification of hepatitis B virus entry inhibitors using HepG2 cells overexpressing a membrane transporter NTCP. *Biochem Biophys Res Commun* 2014;443:808-813.

257. Li W, Urban S. Entry of hepatitis B and hepatitis D virus into hepatocytes: Basic insights and clinical implications. *J Hepatol* 2016;64:S32-40.

258. Oehler N, Volz T, Bhadra OD, Kah J, Allweiss L, Giersch K, Bierwolf J, et al. Binding of hepatitis B virus to its cellular receptor alters the expression profile of genes of bile acid metabolism. *Hepatology* 2014;60:1483-1493.

259. Schieck A, Schulze A, Gahler C, Muller T, Haberkorn U, Alexandrov A, Urban S, et al. Hepatitis B virus hepatotropism is mediated by specific receptor recognition in the liver and not restricted to susceptible hosts. *Hepatology* 2013;58:43-53.

260. Baumert TF, Verrier ER, Nassal M, Chung RT, Zeisel MB. Host-targeting agents for treatment of hepatitis B virus infection. *Curr Opin Virol* 2015;14:41-46.

261. Verrier ER, Colpitts CC, Sureau C, Baumert TF. Hepatitis B virus receptors and molecular drug targets. *Hepatol Int* 2016;10:567-573.

262. Blanchet M, Sureau C, Labonte P. Use of FDA approved therapeutics with hNTCP metabolic inhibitory properties to impair the HDV lifecycle. *Antiviral Res* 2014;106:111-115.

263. Ko C, Park WJ, Park S, Kim S, Windisch MP, Ryu WS. The FDA approved drug irbesartan inhibits HBV-infection in HepG2 cells stably expressing sodium taurocholate co-transporting polypeptide. *Antivir Ther* 2015.

264. Kaneko M, Watashi K, Kamisuki S, Matsunaga H, Iwamoto M, Kawai F, Ohashi H, et al. A Novel Tricyclic Polyketide, Vanitaracin A, Specifically Inhibits the Entry of Hepatitis B and D Viruses by Targeting Sodium Taurocholate Cotransporting Polypeptide. *J Virol* 2015;89:11945-11953.

265. Dong Z, Ekins S, Polli JE. Structure-activity relationship for FDA approved drugs as inhibitors of the human sodium taurocholate cotransporting polypeptide (NTCP). *Mol Pharm* 2013;10:1008-1019.

266. Ferrari C. HBV and the immune response. *Liver Int* 2015;35 Suppl 1:121-128.

267. He J, Hao R, Liu D, Liu X, Wu S, Guo S, Wang Y, et al. Inhibition of hepatitis B virus replication by activation of the cGAS-STING pathway. *J Gen Virol* 2016;97:3368-3378.
268. Zou ZQ, Wang L, Wang K, Yu JG. Innate immune targets of hepatitis B virus infection. *World J Hepatol* 2016;8:716-725.
269. Wang J, Shen T, Huang X, Kumar GR, Chen X, Zeng Z, Zhang R, et al. Serum hepatitis B virus RNA is encapsidated pregenome RNA that may be associated with persistence of viral infection and rebound. *J Hepatol* 2016;65:700-710.
270. Lupberger J, Zeisel MB, Xiao F, Thumann C, Fofana I, Zona L, Davis C, et al. EGFR and EphA2 are host factors for hepatitis C virus entry and possible targets for antiviral therapy. *Nat Med* 2011;17:589-595.
271. Ladner SK, Otto MJ, Barker CS, Zaifert K, Wang GH, Guo JT, Seeger C, et al. Inducible Expression of Human Hepatitis B Virus (HBV) in Stably Transfected Hepatoblastoma Cells: a Novel System for Screening Potential Inhibitors of HBV Replication. *ANTIMICROBIAL AGENTS AND CHEMOTHERAPY* 1997;No. 8;p. 1715-1720.
272. Cui X, Luckenbaugh L, Bruss V, Hu J. Alteration of Mature Nucleocapsid and Enhancement of Covalently Closed Circular DNA Formation by Hepatitis B Virus Core Mutants Defective in Complete-Virion Formation. *J Virol* 2015;89:10064-10072.
273. Jinek M, Chylinski K, Fonfara I, Hauer M, Doudna JA, Charpentier E. A Programmable Dual-RNA-Guided DNA Endonuclease in Adaptive Bacterial Immunity. *Science* 2012;337:816-821.
274. Cong L, Ran FA, Cox D, Lin S, Barretto R, Habib N, Hsu PD, et al. Multiplex Genome Engineering Using CRISPR/Cas Systems. *Science* 2013;339:819-823.
275. Sanjana NE, Shalem O, Zhang F. Improved vectors and genome-wide libraries for CRISPR screening. *Nat Methods* 2014;11:783-784.
276. Laras A, Koskinas J, Dimou E, Kostamena A, Hadziyannis SJ. Intrahepatic levels and replicative activity of covalently closed circular hepatitis B virus DNA in chronically infected patients. *Hepatology* 2006;44:694-702.
277. Gao W, Hu J. Formation of hepatitis B virus covalently closed circular DNA: removal of genome-linked protein. *J Virol* 2007;81:6164-6174.
278. Lucifora J, Salvetti A, Marniquet X, Maily L, Testoni B, Fusil F, Inchauspe A, et al. Detection of the hepatitis B virus (HBV) covalently-closed-circular DNA (cccDNA) in mice transduced with a recombinant AAV-HBV vector. *Antiviral Res* 2017;145:14-19.
279. Subramanian A, Tamayo P, Mootha VK, Mukherjee S, Ebert BL, Gillette MA, Paulovich A, et al. Gene set enrichment analysis: a knowledge-based approach for interpreting genome-wide expression profiles. *Proc Natl Acad Sci U S A* 2005;102:15545-15550.
280. Farquhar MJ, Humphreys IS, Rudge SA, Wilson GK, Bhattacharya B, Ciaccia M, Hu K, et al. Autotaxin-lysophosphatidic acid receptor signalling regulates hepatitis C virus replication. *J Hepatol*

2017;66:919-929.

281. Stetson DB, Medzhitov R. Recognition of cytosolic DNA activates an IRF3-dependent innate immune response. *Immunity* 2006;24:93-103.
282. Ma F, Li B, Liu SY, Iyer SS, Yu Y, Wu A, Cheng G. Positive feedback regulation of type I IFN production by the IFN-inducible DNA sensor cGAS. *J Immunol* 2015;194:1545-1554.
283. Hui C, K., Lau GK. Immune system and hepatitis B virus infection. *J Clin Virol* 2005;34:44-48.
284. Xia T, Konno H, Ahn J, Barber GN. Deregulation of STING Signaling in Colorectal Carcinoma Constrains DNA Damage Responses and Correlates With Tumorigenesis. *Cell Rep* 2016;14:282-297.
285. Guo H, Jiang D, Zhou T, Cuconati A, Block TM, Guo JT. Characterization of the Intracellular Deproteinized Relaxed Circular DNA of Hepatitis B Virus: an Intermediate of Covalently Closed Circular DNA Formation. *Journal of Virology* 2007;81:12472-12484.
286. Hu MM, Liao CY, Yang Q, Xie XQ, Shu HB. Innate immunity to RNA virus is regulated by temporal and reversible sumoylation of RIG-I and MDA5. *J Exp Med* 2017;214:973-989.
287. Cui Y, Yu H, Zheng X, Peng R, Wang Q, Zhou Y, Wang R, et al. SENP7 Potentiates cGAS Activation by Relieving SUMO-Mediated Inhibition of Cytosolic DNA Sensing. *PLoS Pathog* 2017;13:e1006156.
288. Kim SJ, Khan M, Quan J, Till A, Subramani S, Siddiqui A. Hepatitis B virus disrupts mitochondrial dynamics: induces fission and mitophagy to attenuate apoptosis. *PLoS Pathog* 2013;9:e1003722.
289. Lahaye X, Satoh T, Gentili M, Cerboni S, Conrad C, Hurbain I, El Marjou A, et al. The capsids of HIV-1 and HIV-2 determine immune detection of the viral cDNA by the innate sensor cGAS in dendritic cells. *Immunity* 2013;39:1132-1142.
290. Wu G, Liu B, Zhang Y, Li J, Arzumanyan A, Clayton MM, Schinazi RF, et al. Preclinical characterization of GLS4, an inhibitor of hepatitis B virus core particle assembly. *Antimicrob Agents Chemother* 2013;57:5344-5354.
291. Brezillon N, Brunelle MN, Massinet H, Giang E, Lamant C, DaSilva L, Berissi S, et al. Antiviral activity of Bay 41-4109 on hepatitis B virus in humanized Alb-uPA/SCID mice. *PLoS One* 2011;6:e25096.
292. Bertoletti A, Ferrari C. Innate and adaptive immune responses in chronic hepatitis B virus infections: towards restoration of immune control of viral infection. *Gut* 2012;61:1754-1764.
293. Li W, Avey D, Fu B, Wu JJ, Ma S, Liu X, Zhu F. Kaposi's Sarcoma-Associated Herpesvirus Inhibitor of cGAS (KicGAS), Encoded by ORF52, Is an Abundant Tegument Protein and Is Required for Production of Infectious Progeny Viruses. *J Virol* 2016;90:5329-5342.
294. Aguirre S, Luthra P, Sanchez-Aparicio MT, Maestre AM, Patel J, Lamothe F, Fredericks AC, et al. Dengue virus NS2B protein targets cGAS for degradation and prevents mitochondrial DNA sensing during infection. *Nat Microbiol* 2017;2:17037.
295. Stetson DB, Ko JS, Heidmann T, Medzhitov R. Trex1 prevents cell-intrinsic initiation of autoimmunity. *Cell* 2008;134:587-598.
296. Cheng X, Xia Y, Serti E, Block PD, Chung M, Chayama K, Reherrmann B, et al. Hepatitis B virus

evades innate immunity of hepatocytes but activates cytokine production by macrophages. *Hepatology* 2017.

ANNEX

Hepatitis B virus evades cGAS sensing by genome encapsidation and repression of cGAS effector function

Seung-Ae Yim^{1,2,\$}, Eloi R. Verrier^{1,2,\$,*}, Laura Heydmann^{1,2}, Hussein El Saghire^{1,2}, Laurent Maily^{1,2}, Charlotte Bach^{1,2}, Sarah Durand^{1,2}, Julie Lucifora³, David Durantel³, Patrick Pessaux^{1,2,4}, Nicolas Manel^{5,6}, Mirjam Zeisel^{1,2}, Nathalie Pochet⁷, Catherine Schuster^{1,2,#,*} and Thomas F. Baumert^{1,2,4,#,*}

\$ SAY and ERV contributed equally to this work

CS and TFB contributed equally to this work

¹Université de Strasbourg, ²INSERM, Institut de recherche sur les maladies virales et hépatiques UMRS 1110, F-67000 Strasbourg, France; ³Inserm, U1052, Cancer Research Center of Lyon (CRCL), Université de Lyon (UCBL1), CNRS UMR_5286, Centre Léon Bérard, Lyon, France; ⁴Pôle Hépato-Digestif, Institut Hospitalo-Universitaire, Hôpitaux Universitaires de Strasbourg, Strasbourg, France; ⁵Immunity and Cancer Department, Institut Curie, PSL Research University, 75005 Paris, France; ⁶Inserm, U932, 75005 Paris, France; ⁷Program in Translational Neuro Psychiatric Genomics, Brigham and Women's Hospital, Harvard Medical School, Broad Institute of Massachusetts Institute of Technology and Harvard, Cambridge, MA 02142, USA;

***Corresponding authors:** Prof. Thomas F. Baumert, MD, e-mail: thomas.baumert@unistra.fr. Dr. Catherine Schuster, PhD, e-mail: catherine.schuster@unistra.fr. and Dr. Eloi R. Verrier, PhD, e-mail: e.verrier@unistra.fr.

Total character count: 3978 words (limit 4000); abstract 233 words (limit 250).

Key words: HBV, innate immune response, cGAS, immune evasion

Abstract

Background and aim: Chronic hepatitis B virus (HBV) infection is a major cause of liver disease and cancer worldwide. The mechanisms of viral genome sensing and the evasion of innate immune responses by HBV infection are still poorly understood. Recently, the cyclic GMP-AMP synthase (cGAS) was identified as a DNA sensor. In this study, we aimed to investigate the functional role of cGAS in sensing of HBV infection and elucidate the mechanisms of viral evasion.

Methods: We performed functional studies including loss- and gain-of-function experiments combined with cGAS effector gene expression profiling in an infectious cell culture model, primary human hepatocytes and HBV-infected humanized liver chimeric mice.

Results: cGAS is expressed in the human liver and primary human hepatocytes. In an HBV infectious cell culture model the cGAS-STING pathway exhibits antiviral activity against HBV infection including reduction of viral cccDNA levels. While naked relaxed-circular HBV DNA is sensed in a cGAS-dependent manner, packaging of the viral genome during infection abolishes host cell recognition of viral nucleic acids. In cell culture and humanized liver chimeric mice HBV infection suppresses both cGAS expression and function as shown by down-regulation of cGAS innate immune effector gene expression.

Conclusions: HBV exploits multiple strategies to evade sensing and antiviral activity of the cGAS-STING pathway. These results uncover a new mechanism of viral immune evasion. Restoration of immune sensing by cGAS-STING may provide an opportunity for immune-based antiviral therapies.

SUMMARY BOX

1. What is already known about this subject?

The mechanisms of viral genome sensing and the evasion of innate immune responses by HBV infection are still poorly understood. Recent studies suggested an antiviral activity of the DNA sensor cGAS against HBV. However, the detailed interactions between cGAS and HBV are still unknown.

2. What are the new findings?

Here, we showed that the cGAS-STING pathway exhibits antiviral activity against HBV infection including reduction of viral cccDNA levels even in absence of viral sensing by cGAS. Indeed, while naked HBV genomic DNA triggered the innate immune response in a cGAS-dependent manner, packaging of the viral genome during infection abolishes host cell recognition of viral nucleic acids, confirming the “stealth” nature of HBV. Moreover, we demonstrated that HBV suppresses the expression of both cGAS and cGAS-induced genes in cell culture and humanized liver chimeric mice, highlighting a new mechanism of immune evasion by HBV.

3. How might it impact on clinical practice in the foreseeable future?

These results uncover a new mechanism of viral immune evasion by HBV. Restoration of immune sensing by cGAS-STING may provide an opportunity for immune-based antiviral therapies.

Introduction

With more than 250 million chronically infected patients, hepatitis B virus (HBV) infection is a leading cause of liver disease and hepatocellular carcinoma world-wide[1-3]. Current antiviral therapies fail to provide complete cure[4-6]. HBV is a partially double-stranded DNA virus infecting human hepatocytes after initial attachment to HSPGs and its receptor NTCP (reviewed in[7]). Following uncoating, the viral nucleocapsid is released into the cytoplasm and the viral genome is imported into the nucleus through an unknown mechanism. The interaction between the HBV capsid and Nup153 suggests an interplay between the viral capsid and the nucleus import system, suggesting no release of the HBV genomic relaxed circular DNA (rcDNA) into the cytoplasm [8]. The viral genome is directly delivered in the nucleus where it is converted into a covalently closed circular DNA (cccDNA)[9]. This minichromosome serves as a template for both pregenomic RNA (pgRNA) and viral mRNA transcription. While recent studies suggested sensing of the pgRNA or other HBV RNAs by either MDA5[10] or RIG-I[11], the recognition of the viral nucleic acids by the regular Pattern Recognition Receptors (PRRs) still remains largely elusive. In general, HBV only marginally activates the innate immune response in cell culture models and *in vivo*[12-16], leading to the concept that HBV behaves as a “stealth” virus avoiding viral DNA and RNA detection[17]. On the other hand, other studies have suggested an active inhibition of the innate immune responses by HBV proteins, explaining the absence of strong activation of interferon (IFN) pathways after infection[18]. Consequently, the interaction of HBV and the innate immune system of hepatocytes, and specially the sensing of HBV DNA, is still only partially understood.

Foreign DNA recognition by cytosolic DNA sensors triggers an early antiviral innate immune response, including type I and type III IFN production[19]. Recently, the cyclic GMP-AMP (cGAMP) synthase (cGAS) was identified as a DNA sensor exhibiting an antiviral activity against a broad range of DNA and RNA viruses[20-22]. cGAS is encoded by *MB21D1* gene and directly binds to double-stranded DNAs inducing the production of cGAMP which is recognized by the

stimulator of IFN genes (STING, encoded by *TMEM173*) triggering the expression of type I IFN-stimulated genes (ISGs) through TBK1 activation[23-25].

The understanding of HBV-host interactions, including innate immune response after infection, has been impaired for long time by the absence of robust in vitro system for the study of viral infection[26]. The development of HBV-susceptible NTCP-overexpressing hepatoma cells, such as HepG2 cells, allows the study of the full life cycle in a robust and easy-to-use cell culture model[27, 28]. HepG2 cells are capable of mounting an efficient innate immune response after infection by hepatitis C virus[29]. Moreover, a recent study took advantage of HBV-infected HepG2-NTCP for studying the interaction between RIG-I and HBV RNA [11], suggesting that this cell line is suitable for the study of innate immune response after HBV infection.

In this study, we aimed to study the functional role of cGAS for the HBV life cycle and unravel the mechanisms of viral evasion using loss- and gain-of-function experiments combined with cGAS effector gene expression profiling in an infectious cell culture model and HBV-infected humanized chimeric mice.

MATERIAL AND METHODS

Human subjects. Human material including liver biopsies and liver tissue from patients undergoing surgical resection was obtained with informed consent from all patients. Respective protocols were approved by the Ethics Committee of the University Hospital of Basel, Switzerland (EKBB 13 December 2004) and University of Strasbourg Hospitals, France (CPP 10-17).

Cell lines and human hepatocytes. The sources for HEK 293T[30], HepG2[30], and HepG2-NTCP[31] cells have been described. Primary human hepatocytes (PHHs) were isolated and cultured as described[30]. The HepAD38 cell line (expressing the HBV genome, serotype ayw, genotype D) has been described[32].

Reagents and plasmids. DMSO, PEG 8000, Poly (I:C) and calf thymus DNA (a control dsRNA) were obtained from Sigma-Aldrich. The ECL reagent and Hyperfilms for Western blots were purchased from GE Healthcare. Transfections of DNA and Poly (I:C) at the indicated concentrations were performed using Lipofectamine 2000 (Invitrogen) and CalPhos Mammalian Transfection Kit (Clontech), according to the manufacturer's instructions. pReceiver-Lv151 plasmid was obtained from GeneCopoeia™. The lentiCas9-Blast and lentiGuide-Puro plasmids were gifts from Feng Zhang (Addgene # 52962 and #52963, respectively).

Small interfering RNAs for functional studies. Pools of ON-TARGET plus (Dharmacon) small interfering RNA (siRNA) targeting *MB21D1* (cGAS), *TMEM173* (STING), *TBK1*, and *IFI16* expression were reverse-transfected into HepG2-NTCP using Lipofectamine RNAi-MAX (Invitrogen) as described [30] according to manufacturer's instructions. Cells were harvested two days after transfection and gene expression was monitored using qRT-PCR.

Lentivirus production. Lentivirus particles were generated in HEK 293T cells by cotransfection of plasmids expressing the human immunodeficiency virus (HIV) gap-pol, the vesicular stomatitis virus glycoprotein (VSV-G) and either the human *MB21D1* full open reading frame (ORF) encoding plasmid, or the *MB21D1*-targeting single-guide RNA (sgRNA) encoding plasmids, or the Cas9 expressing plasmid in the ratio of 10:3:10. At 3 days after transfection, supernatants were collected and then pooled and cleared using 0.45µm pore filter.

Establishment of HepG2-NTCP-cGAS overexpressing cells. For the establishment of HepG2-NTCP cells overexpressing cGAS, HepG2-NTCP cells were plated and transduced with lentivirus encoding either the human *MB21D1* ORF or the EFGP ORF in pReceiver-Lv151 vector (GeneCopoeia™). After 3 days, transduced cells were selected with 200 µg/ml of neomycin

(G418). The cGAS-over-expressing- and control HepG2-NTCP cells were then further cultured in presence of G418 at 200 µg/ml.

Generation of MB21D1 knock-out cells. For the generation of MB21D1 knock-out cell lines, one *MB21D1*-targeting single-guide RNA (sgRNA) was designed using CRISPR Design Tool (Broad Institute: http://www.genome-engineering.org/crispr/?page_id=41). The sgRNA sequence targeting the exon 1 of *MB21D1* (sgcGAS 5'-CACCGCGGCCCCATTCTCGTACGG-3') was inserted into lentiGuide-Puro plasmid [33]. We first generated Cas9 expressing HepG2-NTCP cells after transduction of cells with the lentiCas9-Blast plasmid[33]. Cells were then selected with 6 µg/ml Blasticidin S for 10 days. HepG2-NTCP-Cas9 cells were then seeded in six-well plates at 50% confluency 24h prior to transduction with the sgcGAS-encoding plasmid. Subpopulations of cells were selected from the whole population and cultured independently. cGAS protein expression was controlled by Western blot. Finally, two cGAS deficient cell lines (cGAS_KO#1 and cGAS_KO#2) were selected for this study.

Analysis of gene expression using qRT-PCR. Gene expression was assessed by qRT-PCR. Total RNA was extracted using ReliaPrep™ RNA Miniprep Systems (Promega) and reverse transcribed into cDNA using Maxima First Strand cDNA Synthesis Kit (Thermo Scientific) according to the manufacturer's instructions. Gene expression was then quantified by qPCR using a CFX96 thermocycler (Bio-Rad). Primers and TaqMan® probes for *MB21D1* (cGAS), *TMEM173* (STING), *TBK1*, *IFI16*, *IFNB1*, and *GAPDH* mRNA detection were obtained from ThermoFisher (TaqMan® Gene expression Assay, Applied Biosystems). All values were normalized to *GAPDH* expression.

Protein expression. The expression of cGAS, STING and β-actin proteins was assessed by

Western blot. Cells were lysed in Glo lysis buffer (Promega) and protein concentration was determined using Bradford assay (Bio-Rad) following the manufacturer's instructions. Normalized cell lysates were ran on a 10-12% SDS-polyacrylamide gel (SDS-PAGE) by electrophoresis and transferred to polyvinylidene difluoride (PVDF) membrane using the Trans-Blot® Turbo™ Transfer System (Bio-Rad). Membranes were saturated with 5% milk PBS containing 0.1% tween. A polyclonal rabbit anti-cGAS antibody (HPA031700, Sigma), a polyclonal rabbit anti-STING antibody (19851-1-AP, Proteintech), and a monoclonal anti-β-actin (performed in parallel as a Western blot control) antibody (mAbcam8226, Abcam) were used for protein detection as described[31]. Quantification of protein expression was performed using ImageJ software.

Purification of HBV and infection of HepG2-NTCP cells. The purification of infectious recombinant HBV particles from the supernatant of HepAD38 cells as well as the HBV infection of HepG2-NTCP cells have been previously described[31, 32]. Briefly, HepG2-NTCP and derived cells were plated one day prior to incubation with HBV particles in presence of 4% PEG. 16 hour after HBV inoculation, cells were washed with PBS and then cultured in 2% DMSO primary hepatocyte maintenance medium (PMM) for ten days. HBV infection was assessed by quantification of HBV pgRNA using qRT-PCR using the following primers and probe as described[31, 34]: Forward primer: 5'-GGTCCCCTAGAAGAAGAACTCCCT-3'; reverse primer: 5'-CATTGAGATTCCCGAGATTGAGAT-3'; TaqMan® probe: 5'-[6FAM]-TCTCAATCGCCGCGTCGCAGA-[TAMRA]-3'. HBV infection was normalized to GAPDH expression. The expression of HBcAg in infected cells was detected by Western blot using a polyclonal rabbit anti-HBcAg antibody (B0586, Dako) as described above. Southern blot detection of HBV cccDNA was performed using DIG-labelled (Roche) specific probes as described [35]. Total DNA from HBV-infected cells was extracted using the previously described HIRT method [36]. *XhoI* digestion of DNA extracted from HBV-infected HepG2-NTCP-Cas9 cells was used as

a control. *XhoI* digestion of HBV DNA results in a single 3,2 kb band, which corresponds to a double stranded linear (dsl) DNA. DNA extracts were ran in an agarose gel for 24 h and then transferred to a Nylon membrane (Roche). Specific DIGlabelled probes for the detection of HBV and mitochondrial DNAs were synthesized using the PCR DIG Probe Synthesis Kit (Roche) and the primers indicated in Table S1. After probe hybridization on the membrane (DIG-easy Buffer, Roche), HBV and mitochondrial DNAs were detected using DIG Luminescent Detection Kit (Roche) according to manufacturer's instructions.

Extraction of HBV rcDNA from HBV infectious particles. HBV rcDNA was extracted from HBV preparations using QiaAMP DNA MiniKit protocol (Qiagen). PEG-precipitated cell supernatants from naive HepG2-NTCP cells were used as non-virion controls. The presence of HBV DNA was confirmed by PCR and quantified by qPCR using the following primers and probe[31] : forward primer 5'-CACCTCGCCTAATCATC-3', reverse primer 5'-GGAAAGAAGTCAGAAGGCA-3'; TaqMan probe 5'-[6FAM]-TGGAGGCTTCAACAGTAGGACATGAAC-[TAMRA]-3'. Copy number of HBV was determined using a standard curve. 1 µg or rcDNA or dsDNA (calf thymus DNA) were transfected in cells using Lipofectamine 2000 (Invitrogen) and CalPhos Mammalian Transfection Kit (Clontech) according to the manufacturer's instructions. Cells transfected with HepG2-NTCP control supernatants were used as a control. Three days after transfection, total RNA was extracted and purified as described above.

Transcriptomic analysis by digital multiplexed gene profiling using nCounter NanoString.

Transcriptomic analyses using nCounter NanoString were performed according to manufacturer's instructions. Specific probes for a set of cGAS-related genes (according to [22] and presented in Table S2) were obtained from the manufacturer. HepG2-NTCP cells were infected with HBV or transfected with Poly (I:C) (100ng) for two days. Alternatively, HepG2-NTCP-Cas9 and HepG2-

NTCP-KO_cGAS#2 cells were transfected with rcDNA (1µg) or dsDNA (calf thymus DNA, 1µg) for three days. Total RNA was then extracted and subjected to nCounter Digital Analyzer system (NanoString). cGAS-related genes were considered as an artificial gene set and the modulation of this gene set depending on the experimental conditions was determined through Gene Set Enrichment Analysis (GSEA [37]). False Discovery Rate (FDR) < 0.05 was considered statistically significant. Heatmaps illustrating the induction (red color) or repression (blue color) of the cGAS signature compared to control were designed using Morpheus software (Broad Institute of MIT and Harvard, Cambridge, MA, USA). The heatmap illustrating the induction (red color) or repression (blue color) of individual genes in mice were designed using GenePattern software (Broad Institute of MIT and Harvard, Cambridge, MA, USA).

HBV infection of human liver chimeric mice. Isolated PHH were transplanted into 3 week-old of uPA/SCID-bg mice by intrasplenic injection as described [38]. Transplantation of PHH into mice liver was assessed 4 weeks later by quantification of human serum albumin by ELISA (E80-129, Bethyl Laboratories). uPA-SCID were then infected with HBV and sacrificed 16 weeks after virus inoculation. HBV viral load in the mouse serum was determined by qPCR (Realtime HBV viral load kit, Abbott, by Laboratoire Schuh - groupement Bio67, Strasbourg) before sacrifice. Total liver RNA was extracted and gene expression was assessed by either qRT-PCR (MB21D1 expression) or nCounter Digital Analyzer system (NanoString) analysis (cGAS signature). All mice were kept in a pathogen-free housing facility. The experiments were carried out at the Inserm U1110 animal facility and the respective protocols were approved by the Ethics Committee of the University of Strasbourg Hospitals (number AL/02/19/08/12 and AL/01/18/08/1202014120416254981 and 02014120511054408).

FISH analyses. Fluorescence in situ hybridization (FISH) analyses were performed as

described[39, 40]. Briefly, liver samples were collected and then immediately embedded into optimal cutting temperature compound (OCT). OCT-embedded liver sections were cryosectioned (10 μ m) using a cryostat (Leica). Upon fixation with 4% formaldehyde at 4 °C, washing, and dehydration in ethanol, tissue sections were boiled at 90–95°C for 1 min in a pretreatment solution (Affymetrix-Panomics), followed by a 10 min digestion in protease QF (Affymetrix-Panomics) at 40°C. Sections were then hybridized using specific probe sets targeting HBV (target region nucleotides 483-1473 of HBV [Genotype D, GenBank V01460]) and human *MD21D1* (VA1-3013492-VC, Affymetrix-Panomics). Pre-amplification, amplification and detection of bound probes were performed according to the manufacturer's instructions. Finally, pictures were acquired by LSCM (LSM710, Carl Zeiss Microscopy) and Zen2 software.

Statistical Analysis. Each in vitro experiment (except digital multiplexed gene profiling) was performed at least three times in an independent manner. Statistical comparisons of the samples were performed using a two-tailed Mann-Whitney U test. For in vivo experiment, a two-tailed unpaired Student's t-test was performed for comparing gene expression from non-infected and HBV-infected mice. $p < 0.05$ (*), $p < 0.01$ (**), and $p < 0.001$ (***) were considered significant. Significant p values are indicated by asterisks in the figures. Each digital multiplexed gene profiling experiment was performed using three biological replicates per condition and the induction or repression of the gene set was analyzed using GSEA. FDR < 0.05 was considered statistically significant.

RESULTS

Expression of cGAS in human liver tissue, primary human hepatocytes and an infectious HBV cell culture model. Prior to its functional characterization, we studied cGAS/*MD21D1* expression in human liver tissues, hepatocytes, and HBV permissive cell lines. As shown in Figure

1A, *MB21D1* mRNA was slightly detectable in human liver biopsies using FISH, as recently reported[15]. However, cGAS protein expression was easily detectable in primary human hepatocytes (PHH) (Figure 1B). Since HBV infection of primary cells is highly variable and does not allow robust perturbation studies, we used an HBV infectious cell culture model based on differentiated hepatocyte-derived HepG2 cells overexpressing NTCP[31] – a key HBV entry factor[27, 28]. We first investigated cGAS protein expression in our cell-based models. As shown in Figure 1B, cGAS is robustly expressed in HepG2-NTCP. We validated the specificity of cGAS detection using a siRNA specifically targeting the *MD21B1* expression (sicGAS). Stimulation by Poly (I:C) or double-stranded DNA (dsDNA) transfection elicited *IFNB1* expression in HepG2-NTCP cells (Figure 1C-D), confirming that the model is suitable for functional studies related to innate immune responses. Moreover, cGAS protein expression was induced by both Poly (I:C) and dsDNA stimulation confirming an efficient IFN response through the upregulation of ISGs such as *MB21D1* after RNA or DNA stimulation (Figure 1C-D, lower panels).

The cGAS-STING pathway exhibits robust antiviral activity against HBV infection with reduction of cccDNA levels. To evaluate the antiviral activity of the cGAS-STING signaling pathway in HBV infection, we silenced the expression *MB21D1*, *TMEM173* (encoding the STING protein), *TBK1* and *IFI16* (encoding the gamma-interferon-inducible protein 16, another cytoplasmic DNA sensor able to directly activate STING [19]) in HepG2-NTCP cells prior to infection with HBV. As shown in Figure 2A-B, silencing of *MB21D1*, *TMEM173* and *TBK1* expression induced a marked increase in HBV infection. Notably, STING was detectable at the protein level in our model (Figure 2A, right panel). In contrast, the silencing of *IFI16* had no effect on HBV infection. Most importantly, CRISPR/Cas9-mediated KO or overexpression of cGAS protein resulted in a marked increase or decrease in HBV cccDNA levels – the key viral nucleic acid responsible for viral persistence (Figure 2D-E).

HBV evades cGAS sensing by genome encapsidation. We then investigated whether HBV was sensed in HBV permissive cells. To address this question, we infected HepG2-NTCP cells with recombinant HBV and studied the expression of *IFNB1* at early time points after HBV infection. HBV infection was assessed by qRT-PCR and immunofluorescence (Figure S1). As shown in Figure 3A, the lack of increase in *IFNB1* expression indicates poor or absent detection of HBV by cellular sensors. Since cGAS has been shown to induce the expression of a large set of innate effector genes (such as *OAS2* or *IFI44*, see[22]), the analysis of expression of a single effector gene such *IFNB1* may not be sufficient to evaluate cGAS sensing. Therefore, we designed a probe gene-set designated “cGAS signature” comprising genes modulated by cGAS activity and crucial innate immune genes described in[22] and in Table S2. We then infected HepG2-NTCP-Cas9 cells as well as HepG2-NTCP-KO_cGAS#2 with HBV and measured cGAS effector function at day 2 post infection by analysis of the signature using digital multiplexed gene profiling (nCounter NanoString) and GSEA-based analysis. Whereas Poly (I:C) transfection induced a marked modulation of cGAS effector gene expression (FDR = 0.004), no significant modulation of the cGAS signature was detected in HBV-infected samples, suggesting an absence of HBV sensing (Figure 3B), as illustrated by the expression of *IFNB1* and *IFI44* (Figure 3C).

As the HBV genome is packaged into the nucleocapsid[41], we investigated whether packaging shields virion DNA from cGAS recognition. We purified HBV genomic rcDNA from HBV infectious particles (Figure 3D, Figure S1) and transfected the naked viral genome into HepG2-NTCP cells. As shown in Figure 3E-F, a significant (FDR = 0.02) induction of the cGAS signature gene set (illustrated by *IFNB1* and *IFI44* expression Figure 3F) was observed after both rcDNA and dsDNA transfection, suggesting sensing of the naked HBV genome. Interestingly, this induction of the cGAS-related genes was no longer observed in HepG2-NTCP-KO_cGAS#2 cells, suggesting a cGAS-specific activation of innate immunity by both dsDNA and rcDNA transfection. Collectively,

these data suggest that HBV DNA is sensed by cGAS, but this sensing is impaired during HBV infection, probably due to the leaktight viral capsid.

HBV infection induces repression of cGAS and its effector gene expression in cell culture

and in liver chimeric mice. As several reports have suggested that HBV proteins can inhibit IFN-signaling pathways[18], we next investigated whether HBV infection interferes with the expression of cGAS-related gene expression. To address this question, we quantified *MB21D1*/cGAS mRNA and protein expression following HBV infection (Figure 4A-B). Interestingly, cGAS protein expression (Figure 4B) as well as the expression of *MB21D1*, *TMEM173*, and *TBK1* mRNA (Figure 4C) were significantly inhibited in HBV-infected cells. To confirm this observation in vivo, we then investigated the expression of human cGAS expression in HBV-infected human liver chimeric mice. Human liver chimeric mice repopulated with human hepatocytes were infected with serum-derived HBV (genotypes D and E). *MB21D1* was expressed at low but detectable levels in human hepatocytes of liver chimeric mice (Figure 4D). As shown in Figure 4E, *MB21D1* expression was significantly ($p = 0.013$) downregulated in HBV-infected mice compared to non-infected control mice, confirming our results in the cell culture model. Importantly, *MB21D1* expression levels did not correlate with HBV genotype (Table 1). An absent correlation of *MB21D1* expression with albumin (Table 1) rules out that differences in cGAS expression are due to different hepatocyte repopulation levels. To investigate whether HBV modulates cGAS effector function, we analyzed virus-induced changes on cGAS effector gene expression using gene expression profiling in three control mice and the three HBV-infected mice exhibiting the lowest levels of *MB21D1* expression (Table 1). As shown in Figure 4F, HBV infection resulted in a significant (FDR = 0.047) down-regulation of the expression of cGAS effector genes in human hepatocytes of liver chimeric mice. Taken together, our data suggest that HBV is not sensed by cGAS in vivo and at the same time represses expression of cGAS and its effector genes.

Table 1. cGAS expression in HBV-infected human liver chimeric mice. Levels of human albumin-, HBV viral load-, and *MB21D1* levels in liver tissue from HBV-infected and control mice are shown. *MB21D1* expression is normalized to *GAPDH* expression. The HBV genotype (Gt) is indicated. ***Bold: mice used for multiplexed gene profiling***

		Mouse	Albumin ($\mu\text{g/ml}$)	HBV (IU/ml)	<i>MB21D1</i> mRNA
Ctrl		6410	1280	-	1.40E-03
		6472	2720	-	1.40E-03
		6251	3240	-	2.30E-03
		6254	7870	-	1.90E-03
HBV	Gt E	4770	4200	2.9.E+07	1.30E-03
		4773	4800	1.5.E+08	1.70E-03
		4766	12760	3.6.E+06	3.20E-04
		4771	13120	6.2.E+05	3.70E-04
	Gt D	4846	2127	5.5.E+05	3.80E-04
		4847	10045	1.6.E+08	1.70E-04
		4848	1992	6.7.E+06	7.50E-04

DISCUSSION

The interaction between HBV and the innate immune system is a complex process still remaining elusive and controversial [17]. Collectively, our data demonstrate that (i) cGAS-STING pathway exhibits robust antiviral activity against HBV infection including reduction of viral cccDNA levels; (ii) naked HBV genomic rcDNA is sensed in a cGAS-dependent manner whereas packaging of the viral genome during infection abolishes host cell recognition of viral nucleic acids; (iii) HBV infection suppresses both cGAS expression and function in cell culture and humanized liver

chimeric mice as shown by down-regulation of cGAS innate immune effector gene expression.

The detection of HBV DNA by the cellular sensors within infected cells is poorly understood and remains controversial. In vitro and in vivo data strongly suggest that HBV behaves like a stealth virus unable to trigger any innate immune response[12, 13, 15]. Other studies have suggested that HBV-derived dsDNA fragments[42] and viral nucleocapsid destabilization and disassembly[43, 44] could induce innate immune responses. In our study, we observed that the exposure of the HBV genome led to the activation of the IFN response, supporting the observation that the HBV genome itself is recognized by the classical sensors, but this recognition is impaired during HBV infection due to packaging into the viral capsid. Interestingly, the capsid of HIV-1 also prevents the sensing of HIV cDNA by cGAS following reverse-transcription up to integration, whereas HIV-2 capsid may unmask the cDNA leading to a stronger sensing by cGAS and a lower pathogenicity of the strain[45].

Another explanation of this absence of sensing would be the lack a functional STING protein in hepatocyte, as it has been recently reported[46]. However, we detected STING at the protein level in our model and specific silencing of TMEM173 (STING) expression was associated with a significant increase in HBV infection (Figure 2). Moreover, rcDNA and dsDNA were sensed in a cGAS-dependent manner (Figure 3). Consequently, it is likely that STING is functionally active in our system.

Moreover, we show conclusive evidence that cGAS has antiviral activity against HBV infection including reduction of viral cccDNA. This finding extends a previous study showing that cGAS exhibited an antiviral activity against a broad range of RNA and DNA viruses[22] and two other studies showing that cGAS has anti-HBV activity targeting viral replication and assembly[42, 47]. Schoggins and colleagues have proposed that the expression of cGAS may be responsible for the establishment of a basal antiviral level in the cells through the activation of an unknown ligand. cGAS-depleted cells may then be more susceptible to viral infections through the

downregulation of the basal level of innate antiviral genes[22].

Given its antiviral function, cGAS is a target of choice for viruses in order to evade immune responses. It has been reported that the Kaposi's sarcoma-associated herpesvirus negatively regulated cGAS-dependent signaling pathway [48, 49]. In the same vein, HBV viral proteins have been shown to interfere with the JAK-STAT signaling pathway [18, 50]. Our data suggest that HBV can repress the expression of the cGAS and its related genes, such as *MB21D1*, *TMEM17* and *TBK1*. More interestingly, *MB21D1* expression was downregulated in the liver of HBV-infected mice, validating the relevance of these findings in vivo. It still needs to be determined whether HBV can directly target cGAS and cGAS-related factors for an active inhibition of this signaling pathway. A recent study elegantly demonstrated an active inhibition of cGAS pathway by Dengue virus through NS2B protein [51]. On the other hand, *MB21D1* (as a classical member of the ISGs [22]) downregulation may be the consequence of the global inhibition of the canonical IFN pathways by HBV [18]. Given the antiviral activity of the cGAS-signaling pathway against HBV including reduction of HBV cccDNA (Figure 2,[42, 47]) the viral-mediated restriction of *MB21D1* expression most likely plays an important role in HBV immune evasion.

Overall, we have identified viral encapsidation and active suppression of cGAS and its effectors as novel strategies of viral evasion. These findings advance our understanding of virus-innate immune factor interactions in the liver, and they open perspectives for novel therapeutic approaches i.e. restoration of immune sensing by cGAS-STING, for instance through capsid inhibitors may provide an opportunity to exploit the cGAS pathway for antiviral therapies.

ACKNOWLEDGMENTS. We thank F. Zhang (Broad Institute of MIT and Harvard, Cambridge, MA, USA) for lentiCas9-Blast and lentiGuide-Puro plasmids. We thank our colleagues C. Thumann, and M. Oudot for excellent technical support.

COMPETING INTERESTS. The authors declare no competing financial interests.

FUNDING. This work was supported by the European Union (ERC-AdG-2014-671231-HEPCIR, EU H2020-667273-HEPCAR, FP7 HepaMab, EU-InfectEra-HBVccc), The Agency Nationale de Recherches sur le Sida et les Hepatitis Virales (ANRS, 2015/1099), the Foundation ARC pour la Recherche sur le Cancer, (TheraHCC IHUARC IHU201301187) and a PhD fellowship of the Région d'Alsace, France. The work has been published under the framework of the LABEX ANR-10-LABX-0028_HEPSYS and benefits from funding from the state managed by the French National Research Agency as part of the Investments for the future program. E.R.V. was supported by an ANRS fellowship (2015/1099).

AUTHOR CONTRIBUTION. TFB initiated the study. TFB, ERV and CS designed and supervised research. SAY, LH, SD, LM, JL, TC and DD performed the experiments. SAY, ERV, LH, MZ, NP, CS and TFB analyzed the data. PP provided liver resections for PHH isolation. NM and NP made substantive intellectual contributions. ERV, SAY, CS and TFB wrote the paper.

References

1. El-Serag HB. Epidemiology of viral hepatitis and hepatocellular carcinoma. *Gastroenterology* 2012;142(6):1264-73 e1.
2. Trepo C, Chan HL, Lok A. Hepatitis B virus infection. *Lancet* 2014;384(9959):2053-63.
3. Zeisel MB, Lucifora J, Mason WS, *et al.* Towards an HBV cure: state-of-the-art and unresolved questions-report of the ANRS workshop on HBV cure. *Gut* 2015;64(8):1314-26.
4. Rehermann B, Nascimbeni M. Immunology of hepatitis B virus and hepatitis C virus infection. *Nat Rev Immunol* 2005;5(3):215-29.
5. Levrero M, Testoni B, Zoulim F. HBV cure: why, how, when? *Curr Opin Virol* 2016;18:135-43.
6. Gish R, Jia JD, Locarnini S, *et al.* Selection of chronic hepatitis B therapy with high barrier to resistance. *Lancet Infect Dis* 2012;12(4):341-53.
7. Verrier ER, Colpitts CC, Sureau C, *et al.* Hepatitis B virus receptors and molecular drug targets. *Hepatology international* 2016;10(4):567-73.
8. Schmitz A, Schwarz A, Foss M, *et al.* Nucleoporin 153 arrests the nuclear import of hepatitis B virus capsids in the nuclear basket. *PLoS Pathog* 2010;6(1):e1000741.
9. Nassal M. Hepatitis B virus cccDNA - viral persistence reservoir and key obstacle for a cure of chronic hepatitis B. *Gut* 2015;64(12):1972-84.
10. Lu HL, Liao F. Melanoma differentiation-associated gene 5 senses hepatitis B virus and activates innate immune signaling to suppress virus replication. *J Immunol* 2013;191(6):3264-76.
11. Sato S, Li K, Kameyama T, *et al.* The RNA sensor RIG-I dually functions as an innate sensor and direct antiviral factor for hepatitis B virus. *Immunity* 2015;42(1):123-32.
12. Wieland S, Thimme R, Purcell RH, *et al.* Genomic analysis of the host response to hepatitis B virus infection. *Proc Natl Acad Sci U S A* 2004;101(17):6669-74.
13. Wieland SF, Chisari FV. Stealth and cunning: hepatitis B and hepatitis C viruses. *J Virol*

2005;79(15):9369-80.

14. Fletcher SP, Chin DJ, Ji Y, *et al.* Transcriptomic analysis of the woodchuck model of chronic hepatitis B. *Hepatology* 2012;56(3):820-30.
15. Cheng X, Xia Y, Serti E, *et al.* Hepatitis B virus evades innate immunity of hepatocytes but activates macrophages during infection. *Hepatology* 2017.
16. Luangsay S, Gruffaz M, Isorce N, *et al.* Early inhibition of hepatocyte innate responses by hepatitis B virus. *J Hepatol* 2015;63(6):1314-22.
17. Ferrari C. HBV and the immune response. *Liver international : official journal of the International Association for the Study of the Liver* 2015;35 Suppl 1:121-8.
18. Bertoletti A, Ferrari C. Innate and adaptive immune responses in chronic hepatitis B virus infections: towards restoration of immune control of viral infection. *Gut* 2012;61(12):1754-64.
19. Chan YK, Gack MU. Viral evasion of intracellular DNA and RNA sensing. *Nature reviews Microbiology* 2016;14(6):360-73.
20. Gao D, Wu J, Wu YT, *et al.* Cyclic GMP-AMP synthase is an innate immune sensor of HIV and other retroviruses. *Science* 2013;341(6148):903-6.
21. Sun L, Wu J, Du F, *et al.* Cyclic GMP-AMP synthase is a cytosolic DNA sensor that activates the type I interferon pathway. *Science* 2013;339(6121):786-91.
22. Schoggins JW, MacDuff DA, Imanaka N, *et al.* Pan-viral specificity of IFN-induced genes reveals new roles for cGAS in innate immunity. *Nature* 2014;505(7485):691-5.
23. Xiao TS, Fitzgerald KA. The cGAS-STING pathway for DNA sensing. *Molecular cell* 2013;51(2):135-9.
24. Zhang X, Shi H, Wu J, *et al.* Cyclic GMP-AMP containing mixed phosphodiester linkages is an endogenous high-affinity ligand for STING. *Molecular cell* 2013;51(2):226-35.
25. Wu J, Sun L, Chen X, *et al.* Cyclic GMP-AMP is an endogenous second messenger in innate immune signaling by cytosolic DNA. *Science* 2013;339(6121):826-30.

26. Verrier ER, Colpitts CC, Schuster C, *et al.* Cell Culture Models for the Investigation of Hepatitis B and D Virus Infection. *Viruses* 2016;8(9).
27. Yan H, Zhong G, Xu G, *et al.* Sodium taurocholate cotransporting polypeptide is a functional receptor for human hepatitis B and D virus. *Elife* 2012;1:e00049.
28. Ni Y, Lempp FA, Mehrle S, *et al.* Hepatitis B and D viruses exploit sodium taurocholate co-transporting polypeptide for species-specific entry into hepatocytes. *Gastroenterology* 2014;146(4):1070-83.
29. Israelow B, Narbus CM, Sourisseau M, *et al.* HepG2 cells mount an effective antiviral interferon-lambda based innate immune response to hepatitis C virus infection. *Hepatology* 2014;60(4):1170-9.
30. Lupberger J, Zeisel MB, Xiao F, *et al.* EGFR and EphA2 are host factors for hepatitis C virus entry and possible targets for antiviral therapy. *Nat Med* 2011;17(5):589-95.
31. Verrier ER, Colpitts CC, Bach C, *et al.* A targeted functional RNAi screen uncovers Glypican 5 as an entry factor for hepatitis B and D viruses. *Hepatology* 2016;63(1):35–48.
32. Ladner SK, Otto MJ, Barker CS, *et al.* Inducible expression of human hepatitis B virus (HBV) in stably transfected hepatoblastoma cells: a novel system for screening potential inhibitors of HBV replication. *Antimicrob Agents Chemother* 1997;41(8):1715-20.
33. Sanjana NE, Shalem O, Zhang F. Improved vectors and genome-wide libraries for CRISPR screening. *Nature methods* 2014;11(8):783-4.
34. Laras A, Koskinas J, Dimou E, *et al.* Intrahepatic levels and replicative activity of covalently closed circular hepatitis B virus DNA in chronically infected patients. *Hepatology* 2006;44(3):694-702.
35. Lucifora J, Salvetti A, Marniquet X, *et al.* Detection of the hepatitis B virus (HBV) covalently-closed-circular DNA (cccDNA) in mice transduced with a recombinant AAV-HBV vector. *Antiviral Res* 2017; 145:14-19.

36. Gao W, Hu J. Formation of hepatitis B virus covalently closed circular DNA: removal of genome-linked protein. *J Virol* 2007;81(12):6164-74.
37. Subramanian A, Tamayo P, Mootha VK, *et al.* Gene set enrichment analysis: a knowledge-based approach for interpreting genome-wide expression profiles. *Proc Natl Acad Sci U S A* 2005;102(43):15545-50.
38. Farquhar MJ, Humphreys IS, Rudge SA, *et al.* Autotaxin-lysophosphatidic acid receptor signalling regulates hepatitis C virus replication. *J Hepatol* 2017;66(5):919-29.
39. Mailly L, Xiao F, Lupberger J, *et al.* Clearance of persistent hepatitis C virus infection in humanized mice using a claudin-1-targeting monoclonal antibody. *Nat Biotechnol* 2015;33(5):549-54.
40. Wieland S, Makowska Z, Campana B, *et al.* Simultaneous detection of hepatitis C virus and interferon stimulated gene expression in infected human liver. *Hepatology* 2014;59(6):2121-30.
41. Blondot ML, Bruss V, Kann M. Intracellular transport and egress of hepatitis B virus. *J Hepatol* 2016;64(1 Suppl):S49-59.
42. Dansako H, Ueda Y, Okumura N, *et al.* The cyclic GMP-AMP synthetase-STING signaling pathway is required for both the innate immune response against HBV and the suppression of HBV assembly. *The FEBS journal* 2016;283(1):144-56.
43. Cui X, Clark DN, Liu K, *et al.* Viral DNA-Dependent Induction of Innate Immune Response to Hepatitis B Virus in Immortalized Mouse Hepatocytes. *J Virol* 2015;90(1):486-96.
44. Cui X, Luckenbaugh L, Bruss V, *et al.* Alteration of Mature Nucleocapsid and Enhancement of Covalently Closed Circular DNA Formation by Hepatitis B Virus Core Mutants Defective in Complete-Virion Formation. *J Virol* 2015;89(19):10064-72.
45. Lahaye X, Satoh T, Gentili M, *et al.* The capsids of HIV-1 and HIV-2 determine immune detection of the viral cDNA by the innate sensor cGAS in dendritic cells. *Immunity*

2013;39(6):1132-42.

46. Thomsen MK, Nandakumar R, Stadler D, *et al.* Lack of immunological DNA sensing in hepatocytes facilitates hepatitis B virus infection. *Hepatology* 2016;64(3):746-59.

47. He J, Hao R, Liu D, *et al.* Inhibition of hepatitis B virus replication by activation of the cGAS-STING pathway. *J Gen Virol* 2016;97(12):3368-78.

48. Wu JJ, Li W, Shao Y, *et al.* Inhibition of cGAS DNA Sensing by a Herpesvirus Virion Protein. *Cell host & microbe* 2015;18(3):333-44.

49. Li W, Avey D, Fu B, *et al.* Kaposi's Sarcoma-Associated Herpesvirus Inhibitor of cGAS (KicGAS), Encoded by ORF52, Is an Abundant Tegument Protein and Is Required for Production of Infectious Progeny Viruses. *J Virol* 2016;90(11):5329-42.

50. Yu S, Chen J, Wu M, *et al.* Hepatitis B virus polymerase inhibits RIG-I- and Toll-like receptor 3-mediated beta interferon induction in human hepatocytes through interference with interferon regulatory factor 3 activation and dampening of the interaction between TBK1/IKKepsilon and DDX3. *J Gen Virol* 2010;91(Pt 8):2080-90.

51. Aguirre S, Luthra P, Sanchez-Aparicio MT, *et al.* Dengue virus NS2B protein targets cGAS for degradation and prevents mitochondrial DNA sensing during infection. *Nature microbiology* 2017;2:17037.

FIGURE LEGENDS

Figure 1: cGAS expression and function in the human hepatocytes and in a cell culture model for HBV infection.

(A) *MB21D1* mRNA expression in the human liver analyzed by FISH. Liver biopsies from an HBV-infected patient were stained using *MB21D1*-specific probes. (B) Detection of endogenous cGAS protein expression in different cellular models by Western blot. Cell lysates from Huh7.5.1, HepG2, HepG2-NTCP cells, and PHH from three independent donors were used. HepG2-NTCP cells were reverse transfected with a siRNA targeting *MB21D1* (siGAS) or a non-targeting siRNA control (siCtrl) two days before cGAS detection. β -actin was used as a Western blot control. Individual representative experiments are shown. (C-D) Poly (I:C) and dsDNA transfection induce *IFNB1* expression in HepG2-NTCP cells. HepG2-NTCP cells were transfected with 100 ng of Poly (I:C) (C) or calf thymus DNA at the indicated concentrations (D). *IFNB1* mRNA expression was quantified by qRT-PCR and cGAS protein expression was assessed by Western blot 72 h after transfection. Western blot individual experiments are shown. For qRT-PCR, data are expressed as means \pm SD relative *IFNB1* expression (log10) compared to Ctrl (set at 1) (C) and as means \pm SD % *IFNB1* expression compared to Ctrl (set at 100%) (D), from three independent experiments performed in triplicate.

Figure 2. Antiviral activity of cGAS results in reduction of HBV cccDNA.

(A, B) Silencing of cGAS-related gene expression increases HBV infection. siRNA targeting *MB21D1* (siGAS), *TMEM173* (siSTING), *TBK1* (siTBK1), *IFI16* (siIFI16) or a non-targeting siRNA (siCtrl) were reverse-transfected into HepG2-NTCP cells 2 days prior to HBV infection. Silencing efficacy was assessed by qRT-PCR 2 days after transfection (A, left panel). Results are expressed as means \pm SD % gene expression relative to siCtrl (set at 100%) from four independent experiments performed in technical duplicate. Alternatively, cGAS and STING silencing were assessed by

Western blot (A, right panel). One experiment is shown. HBV infection was assessed by quantification of HBV pgRNA by qRT-PCR 10 days after infection (B). Results are expressed as means \pm SD % HBV pgRNA expression relative to siCtrl (set at 100%) from four independent experiments performed in technical duplicate. (C) Knock-out (KO) of *MB21D1* gene increases HBV infection. *MB21D1* KO HepG2-NTCP cell lines were generated via CRISPR/Cas9 technology. The absence or presence of cGAS protein was controlled by Western blot (lower panel) in Cas9-expressing HepG2-NTCP cells (Cas9) and in different cell lines after transduction with the sgRNA targeting *MB21D1* (line-A, line-B, line-C, cGAS_KO#1 and cGAS_KO#2). One experiment is shown. cGAS_KO#1, cGAS_KO#2, and the control Cas9 cells were then infected with HBV and viral infection was assessed 10 days after infection as described above. Results are expressed as means \pm SD % HBV pgRNA expression relative to control cell line (Cas9, set at 100%) from three independent experiments performed in triplicate. (D) cGAS overexpression reduces HBV infection. HepG2-NTCP cells were transduced with lentivirus encoding either a control plasmid (Ctrl_ORF) or a plasmid encoding the full length *MB21D1* ORF (cGAS_OE). cGAS protein expression was assessed by Western blot (left panel). One experiment is shown. Cells were then infected with HBV and viral infection was assessed 10 days after infection as described above. Results are expressed as means \pm SD % HBV pgRNA expression relative to control cell line (Ctrl_ORF, set at 100%) from three independent experiments performed in triplicate. (E) Detection of HBV cccDNA by Southern blot. HepG2-NTCP-derived cGAS_KO- or cGAS_overexpressing cell lines were infected for 10 days with HBV. Total DNA from indicated HBV infected cells was extracted and HBV DNA were detected by Southern blot. Two different DNA ladders (L1 & L2) were used. *XhoI* digestion of DNA extracted from HBV-infected HepG2-NTCP-Cas9 cells was used as a control and resulted in a single 3.2 kb band (dsI HBV DNA). Mitochondrial DNA (mt DNA) was detected as a loading control. One experiment is shown.

Figure 3. cGAS-mediated sensing of naked HBV rcDNA and viral infection. (A) HBV infection does not induce *IFNB1* expression. HepG2-NTCP cells were infected with HBV or transfected with Poly (I:C) (100ng) and total RNA was extracted every day for 3 days. RNA extracted from non-infected or non-transfected cells was used as a control (Ctrl). *IFNB1* expression was then assessed by qRT-PCR. Results are expressed as means \pm SEM *IFNB1* relative expression (log10) compared to controls (Ctrl, both set at 1) from three independent experiments performed in triplicate (Poly (I:C) transfection) or four independent experiments performed at least in duplicate (HBV infection). (B-C) cGAS-related genes are not affected by HBV infection. HepG2-NTCP (NTCP), HepG2-NTCP-Cas9 (Cas9) and HepG2-NTCP-KO_cGAS#2 (Ko_cGAS #2) were infected with HBV. Alternatively, HepG2-NTCP cells (NTCP) were transfected with Poly (I:C) (100ng). Two days after infection or transfection, total RNA was extracted. Gene expression of cGAS signature gene set was then analyzed using multiplexed gene profiling. Results were analyzed by GSEA enrichment compared to non-transfected or non-infected controls (B) or by *IFNB1* and *IFI44* gene expression compared to non-transfected or non-infected controls (set at 1) (C). One experiment performed in triplicate is shown. (D-F) HBV genome exposure induced a cGAS-mediated innate immune response. HBV rcDNA was extracted from recombinant HBV virions. The presence of HBV DNA was confirmed by PCR (expected amplicon size: 148 bp, see Figure S1) and quantified by qPCR (D). HBV rcDNA (1 μ g) and positive control dsDNA (calf thymus DNA, 1 μ g) were transfected into HepG2-NTCP-Cas9 and HepG2-NTCP-KO_cGAS#2 cells. Three days after infection or transfection, total RNA was extracted. Gene expression of cGAS signature gene set was then analyzed using multiplexed gene profiling. Results were analyzed by GSEA enrichment compared to non-transfected control (E) or by *IFNB1* and *IFI44* gene expression compared to non-transfected control. One experiment in triplicate is shown.

Figure 4. HBV infection suppresses the expression of the cGAS-related genes *in vitro* and *in vivo*. (A-C) HepG2-NTCP cells were infected with HBV for 10 days. HBV infection was assessed by detection of HBV pgRNA by qRT-PCR (A, three experiments performed in triplicate are shown) and Western blot detection of HBcAg (B, one experiment is shown). cGAS protein expression was assessed 10 days after infection (B, one experiment is shown). Gene expression relative to non-infected control cells of *MB21D1*, *TMEM173* and *TBK1* were assessed by qRT-PCR at day 10 after infection (C). Results are expressed as means \pm SEM from three independent experiments performed in triplicate. (D-F) *MB21D1*- and cGAS-related gene expression is impaired in HBV-infected mice. uPA-SCID mice were infected with HBV for 16 weeks. Mice were then sacrificed and HBV infection was assessed by HBV RNA specific in situ hybridization (D) and quantification of HBV viral load in the serum (Table 1). Human *MB21D1* expression was detected in human hepatocytes by FISH from one HBV-infected mouse (D) and by qRT-PCR from 7 HBV-infected mice and 4 control mice (E). Results are expressed as the ratio *MB21D1* mRNA / *GAPDH* mRNA. All individual mice are presented as well as means \pm SD for each group (Mock- and HBV-infected mice). The expression of cGAS-related genes was analyzed using the nCounter NanoString in mice 6472, 6251, and 6254 (Mock-infected mice, Table 1) and 4766, 4771, and 4847 (HBV-infected mice, Table 1). A significant downregulation (FDR = 0.047) of the gene set was observed in HBV-infected mice compared to control mice. Individual Z-scores for the genes significantly modulated between the two groups according to GSEA analysis are presented. Negative Z-score (blue) and positive Z-score (red) correspond to repression and induction of the indicated genes, respectively.

Figure 1.

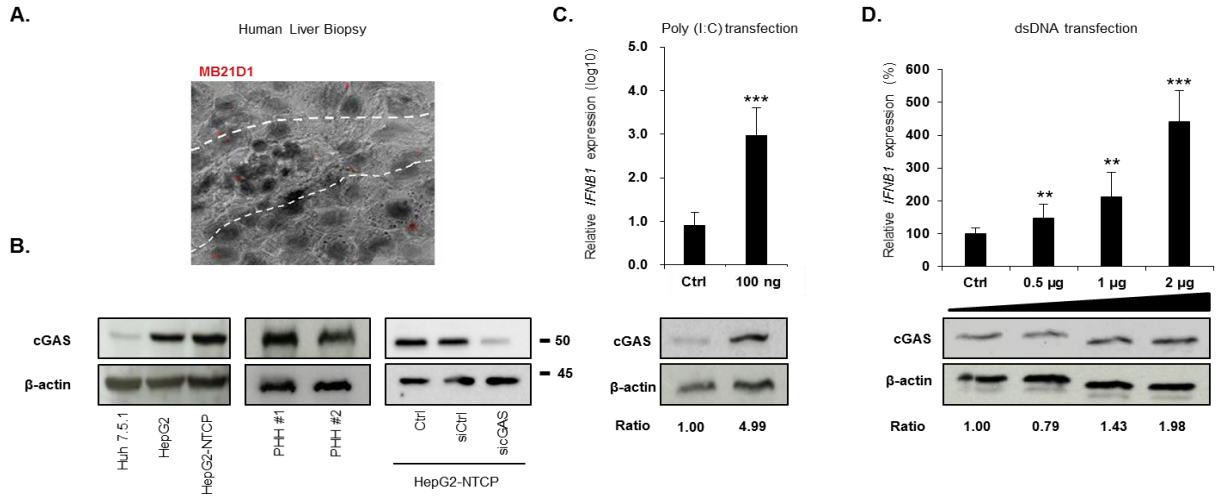


Figure 2.

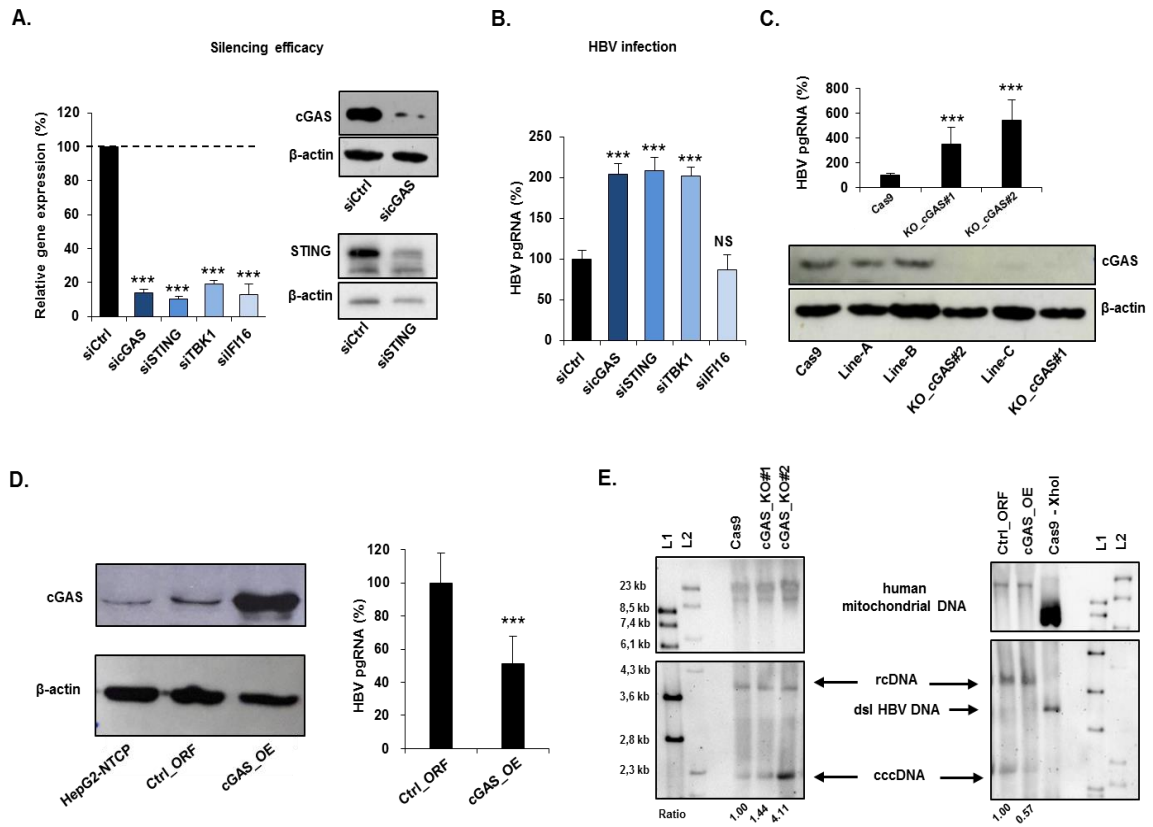


Figure 3.

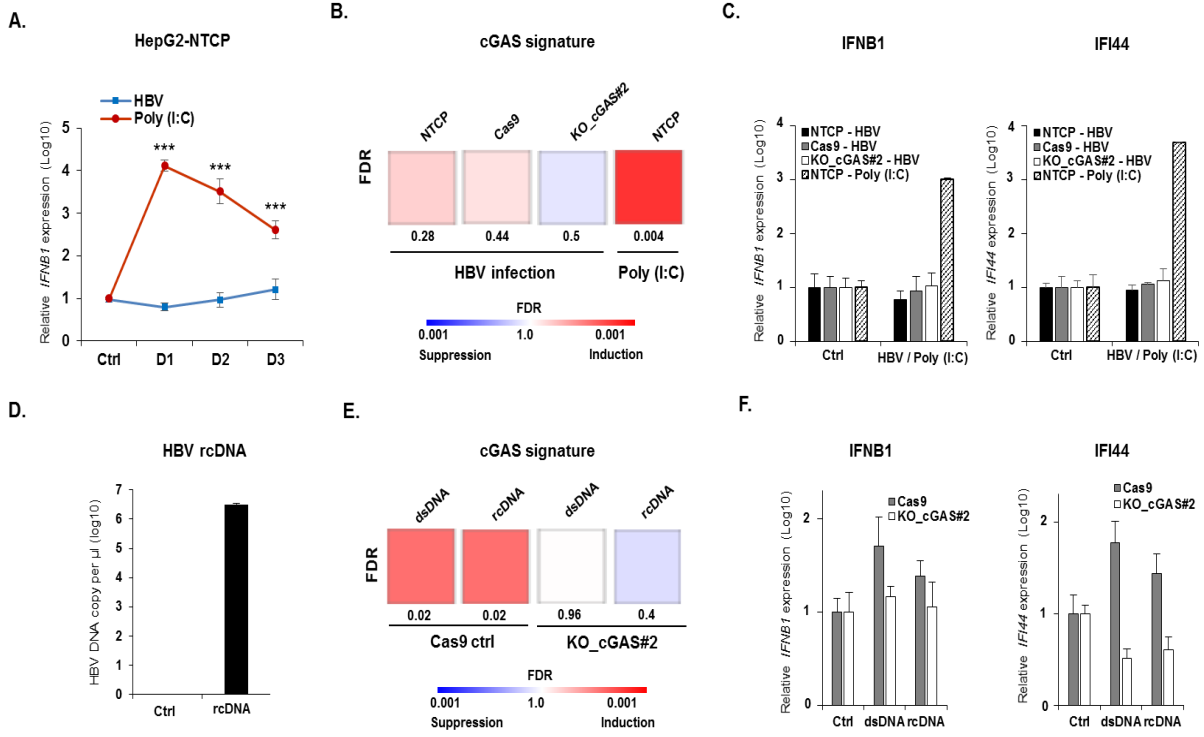
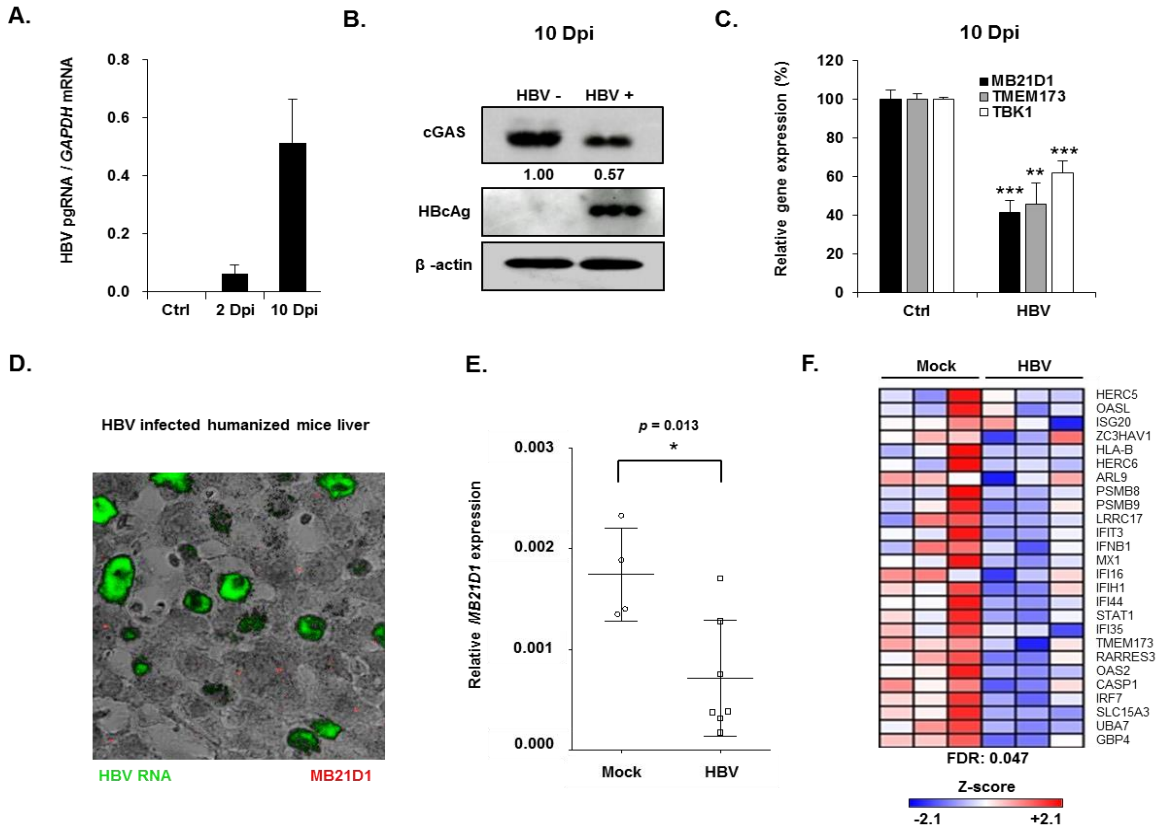


Figure 4.



Supplemental Figures

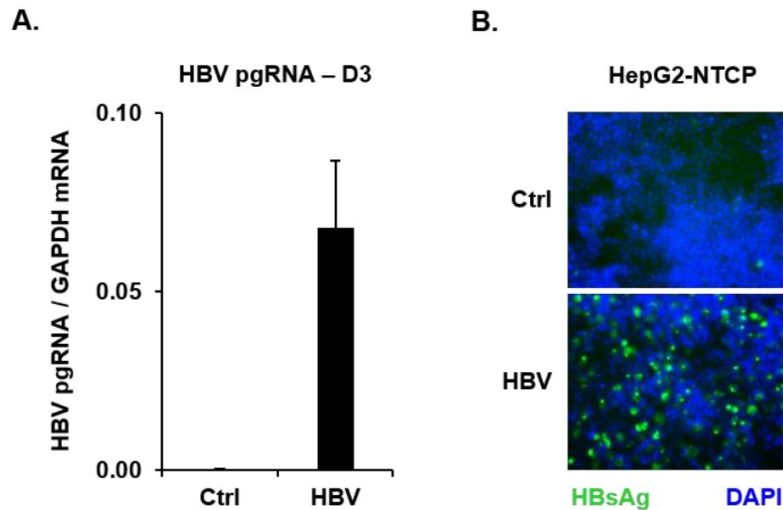


Figure S1: Control of HBV infection in HBV time course samples. HepG2-NTCP cells were infected with HBV. Three days after infection, total RNA was extracted and HBV infection was assessed by quantification of HBV pgRNA as described in the manuscript. Results are expressed as means \pm SEM HBV pgRNA / GAPDH mRNA from four independent experiments performed at least in duplicate (corresponding to the four experiments presented in Figure 3A). Alternatively, cells were infected for 10 days in HBV, and HBV infection was assessed by immunofluorescence using an anti-HBsAg antibody. One experiment (corresponding to independent experiment #2 from Figure 3A) is shown.

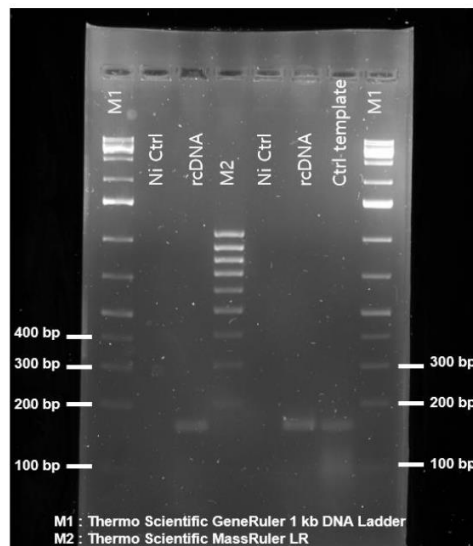


Figure S2: Detection of HBV DNA extracted from HBV infectious particles by PCR. HBV genomic DNA (rcDNA) was extracted from HBV virions. Extraction from naive HepG2-NTCP control supernatants was used as a control (Ctrl). HBV DNA standard preparation used as a template for the calculation of HBV DNA concentration was used as a positive control (Ctrl template). The presence of HBV DNA was controlled by PCR (expected band size: 148 base pairs [bp]). Two independent experiments are shown.

Tables S1: Specific probes used for the detection of HBV and Mitochondrial DNA by Southern blot [1].

Target	Name	Sequence
HBV	HBV-F1	TAGCGCCTCATTTTGTGGGT
	HBV-R1	CTTCCTGTCTGGCGATTGGT
	HBV-F2	TAGGACCCCTGCTCGTGTTA
	HBV-R2	CCGTCCGAAGGTTTGGTACA
	HBV-F3	ATGTGGTATTGGGGGCCAAG
	HBV-R3	GGTTGCGTCAGCAAACACTT
	HBV-F4	TGGAACCTTTTCGGCTCCTC
	HBV-R4	GGGAGTCCGCGTAAAGAGAG
	HBV-F6	TACTGCACTCAGGCAAGCAA
	HBV-R6	TGCGAATCCCACTCCGAAA
	HBV-F8	AGACGAAGGTCTCAATCGCC
	HBV-R8	ACCCACAAAATGAGGCGCTA
Mitochondrial DNA	Fw_huND1	CCCTACTTCTAACCTCCCTGTTCTTAT
	Rw_huND1	CATAGGAGGTGTATGAGTTGGTCGTA
	Fw_huND5	ATTTTATTTCTCCAACATACTCGGATT
	Rw_huND5	GGGCAGGTTTTGGCTCGTA
	Fw_huATP6	CATTTACACCAACCACCCAATC
	Rw-huATP6	CGAAAGCCTATAATCACTGTGCC

Tables S2: Specific probes of the cGAS signature gene set for multiplexed gene profiling analysis.

Gene	Accession Number	Target Sequence	Note
ATP5B	NM_001686.3	GAAATTCTGGTGACTGGTATCAAGGTTGTCGATCT GCTAGCTCCCTATGCCAAGGGTGGCAAAATTGGGC TTTTTGGTGGTGGTGGAGTTGGCAAGACTG	HG
BAG6	NM_001199698.1	CATTGATCACGGGGCTAGAAGAGTATGTGCGGGAG AGTTTTTCCTTGGTGCAGGTTCCAGCCAGGTGTGGA CATCATCCGGACAAACCTGGAATTTCTCCA	HG
NDUFA2	NM_001185012.1	ATGGGCTAGGCTTTAGGGTCCGCGGTTGGTCAGA CCGGAGCACTTGGCCTGAAGACCTGGAATTGGCG ACTTCGATATTAACAAGGATGGCGGCGGCCG	HG

ARL9	NM_206919.1	CAGATATCCATGAAGCTTTGGCATTATCTGAAGTGG GAAATGACAGGAAGATGTTCTTGTGGAACTAC CTGACTAAGAATGGCTCAGAGATACCCTC	Schoggins
CASP1	NM_001223.3	TGGAGACATCCCACAATGGGCTCTGTTTTATTGGA AGACTCATTGAACATATGCAAGAATATGCCTGTTCC TGTGATGTGGAGGAAATTTCCGCAAGG	Schoggins
CXCL16	NM_001100812.1	CCATGGGTTCCAGGAATTGATGAGCTGTCTTGATCT CAAAGAATGTGGACATGCTTACTCGGGGATTGTGG CCCACCAGAAGCATTACTTCCCTACCAGCC	Schoggins
CXCL8	NM_000584.2	ACAGCAGAGCACACAAGCTTCTAGGACAAGAGCC AGGAAGAAACCACCGGAAGGAACCATCTCACTGT GTGTAAACATGACTTCCAAGCTGGCCGTGGCT	Schoggins
HERC5	NM_016323.2	TGGGCTGCTGTTTACTTTTCGGTGCTGGAAAACATG GGCAACTTGGTCATAATTCAACACAGAATGAGCTAA GACCCTGTTTGGTGGCTGAGCTTGTGGG	Schoggins
HERC6	NM_001165136.1	TCCATCACCCAGATTTATACTTAGAGTCAGACGAAG TCGCCTGGTTAAAGATGCTCTGCGTCAATTAAGTC AAGCTGAAGCTACTGACTTCTGCAAAGTA	Schoggins
HLA-B	NM_005514.6	CCCTGAGATGGGAGCCGTCTTCCCAGTCCACCGT CCCCATCGTGGGCATTGTTGCTGGCCTGGCTGTC CTAGCAGTTGTGGTCATCGGAGCTGTGGTCGC	Schoggins
HLA-H	NR_001434.3	GAGCGGGAGGGGCCGGAGTATTGGGACCGGAAC ACACAGATCTGCAAGGCCCAAGCACGGACTGAAC GAGAGAACCTGCGGATCGCGCTCCGCTACTACA	Schoggins
IFI35	NM_005533.3	TGCCCTCTGCTTGCGGGCTCTGCTCTGATCACCTT TGATGACCCCAAAGTGGCTGAGCAGGTGCTGCAA CAAAGGAGCACACGATCAACATGGAGGAGT	Schoggins
IFI44	NM_006417.4	GATGAAAGAAAGATAAAAGGGGTCATTGAGCTCAG GAAGAGCTTACTGTCTGCCTTGAGAACTTATGAAC CATATGGATCCCTGGTTCAACAAATACGAA	Schoggins
IFIH1	NM_022168.2	GCTTGGGAGAACCCTCTCCCTTCTCTGAGAAAGAA AGATGTGCAATGGGTATTCCACAGACGAGAATTTTC CGCTATCTCATCTCGTGCTTCAGGGCCAGG	Schoggins
IFIT3	NM_001031683.2	CGCCTGCTAAGGGATGCCCTTCAGGCATAGGCA GTATTTTCTGTGAGCATCTGAGCTTGAGGATGGTA GTGAGGAAATGGGCCAGGGCGCAGTCAGCT	Schoggins
ISG20	NM_002201.5	AGCCCGCCGAGGGCTGCCCGCCTGGCTGTGTC AGACTGAAGCCCATCCAGCCCGTTCCGCAGGGA CTAGAGGCTTTTCGGCTTTTGGGACAGCAACTA	Schoggins
LRRC17	NM_001031692.1	CAGCACAACCAGATCAAAGTCTTGACGGAGGAAG TGTTCAATTACACACCTCTCTTGAGCTACCTGCGTC	Schoggins

		TTTATGACAACCCCTGGCACTGTACTTGTG	
MX1	NM_002462.2	GCCTTTAATCAGGACATCACTGCTCTCATGCAAGG AGAGGAAACTGTAGGGGAGGAAGACATTCGGCTG TTTACCAGACTCCGACACGAGTTCCACAAAT	Schoggins
OAS2	NM_016817.2	TGAAAAACAATTCGAGATCCAGAAGTCCCTTGAT GGGTTCCACCATCCAGGTGTTACAAAAATCAGAG AATCTCTTTCGAGGTGCTGGCCGCCTTCAA	Schoggins
OASL	NM_198213.1	GGCGTTTCTGAGCTGTTTCCACAGCTTCCAGGAG GCAGCCAAGCATCACAAAGATGTTCTGAGGCTGAT ATGGAAAACCATGTGGCAAAGCCAGGACCTG	Schoggins
PLCG2	NM_002661.2	GCTTGAAAATCTTACACCAGGAAGCGATGAATGCG TCCACGCCACCATTATCGAGAGTTGGCTGAGAAA GCAGATATATTCTGTGGATCAAACCAGAAG	Schoggins
PSMB8	NM_004159.4	ACTCACAGAGACAGCTATTCTGGAGGCGTTGTCAA TATGTACCACATGAAGGAAGATGGTTGGGTGAAAG TAGAAAGTACAGATGTCAGTGACCTGCTGC	Schoggins
PSMB9	NM_002800.4	TCAGGTATATGGAACCCTGGGAGGAATGCTGACTC GACAGCCTTTTGCCATTGGTGGCTCCGGCAGCAC CTTTATCTATGGTTATGTGGATGCAGCATAT	Schoggins
RARRES3	NM_004585.3	CTGACCCTCGTGCCCTGTCTCAGGCGTTCTCTAGA TCCTTTCTCTGTTTCCCTCTCTCGCTGGCAAAG TATGATCTAATTGAAACAAGACTGAAGGAT	Schoggins
SLC15A3	NM_016582.1	GCCGCTTCTTCAACTGGTTTTACTGGAGCATCAAC CTGGGTGCTGTGCTGTGCTGCTGGTGGTGGCGT TTATTCAGCAGAACATCAGCTTCTGCTGGG	Schoggins
TNFRSF1 B	NM_001066.2	CCCAGCTGAAGGGAGCACTGGCGACTTCGCTCTT CCAGTTGGACTGATTGTGGGTGTGACAGCCTTGG GTCTACTAATAATAGGAGTGGTGAAGTGTGTC	Schoggins
UBA7	NM_003335.2	GCGGGAGGATGGGTCCCTGGAGATTGGAGACACA ACAACCTTCTCTCGGTACTTGCCTGGTGGGGCTAT CACTGAAGTCAAGAGACCCAAGACTGTGAGA	Schoggins
UBE2L6	NM_004223.3	TGTTTCAAACCCTTCCATCCTGTTAGATTGCCA GTTCTGGGACCAGGCCTCAGACTGTGAAGTATAT ATCCTCCAGCATTCACTCCAGGGGGAGCC	Schoggins
ZC3HAV1	NM_020119.3	CTCCTTCTTACATCGTAGAAACATGGCATATAGGG CTAGAAGCAAGAGTAGAGATCGGTTCTTTCAGGGC AGCCAAGAATTTCTTGCCTCTGCTTCAGC	Schoggins
ZMYND15	NM_032265.1	CCTCAGAGCGGCCGACAACCTGCATGTCCTGGTAC TGCAATGCCTTCATCTTCCACCTGGTTTACAAGCCT GCTCAAGGGAGCGGGGCCCGCCCGGCGCCC	Schoggins

PMAIP1	NM_021127.2	CTAGTGTTTTTGCCGAAGATTACCGCTGGCCTACT GTGAAGGGAGATGACCTGTGATTAGACTGGGCGG CTGGGGAGAAACAGTTCAGTGCATTGTTGTT	Schoggins
GBP4	NM_052941.4	TTCTACAAGATATGCCATGGGCCTTTTCACAGGGG ACACAGGCTTCTTAAAACAACCCGGCTTCCTCACC CTATGTCCTTTATTTACAAAGCTGTGCTCC	Schoggins
TMEM173	NM_198282.1	CTGGCATGGTCATATTACATCGGATATCTGCGGCTG ATCCTGCCAGAGCTCCAGGCCCGGATTTCGAACCTTA CAATCAGCATTACAACAACCTGCTACGGG	STING
IFI16	NM_005531.1	ACGACTGAACACAATCAACTGTGAGGAAGGAGATA AACTGAAACTCACCAGCTTTGAATTGGCACCGAAA AGTGGGAATACCGGGGAGTTGAGATCTGTA	
IFNB1	NM_002176.2	ACAGACTTACAGTTACCTCCGAAACTGAAGATCT CCTAGCCTGTGCCTCTGGGACTGGACAATTGCTTC AAGCATTCTTCAACCAGCAGATGCTGTTTA	
IRF3	NM_001571.5	TCATGGCCCCAGGACCAGCCGTGGACCAAGAGGC TCGTGATGGTCAAGTTGTGCCACGTGCCTCAG GGCCTTGGTAGAAATGGCCCGGTAGGGGGTG	
IRF7	NM_001572.3	CGCAGCGTGAGGGTGTGTCTTCCCTGGATAGCAG CAGCCTCAGCCTCTGCCTGTCCAGCGCCAACAGC CTCTATGACGACATCGAGTGCTTCCTTATGGA	
STAT1	NM_139266.1	ACAGTGGTTAGAAAAGCAAGACTGGGAGCACGCT GCCAATGATGTTTTCATTTGCCACCATCCGTTTTTCAT GACCTCCTGTCACAGCTGGATGATCAATAT	
TBK1	NM_013254.2	ACCAGTCTTCAGGATATCGACAGCAGATTATCTCCA GGTGGATCACTGGCAGACGCATGGGCACATCAAG AAGGCACTCATCCGAAAGACAGAAATGTAG	

HG Housekeeping genes

Shoggins: cGAS-related genes described by Shoggins et al., [2]

Supplemental Material and Methods

Detection of HBV DNA by PCR. DNA was extracted using QiaAMP DNA MiniKit (Qiagen) following manufacturer's instructions. The presence of HBV DNA was confirmed by PCR the following primers (expected band size: 148 bp) [3] : forward primer 5'-CACCTCGCCTAATCATC-3', reverse primer 5'-GGAAAGAAGTCAGAAGGCA-3'.

Detection of HBV infection by immunofluorescence. HepG2-NTCP cells were infected with HBV for

10 days as described in the manuscript. 10 days after infection, cells were fixed and HBV infection was assessed by immunofluorescence as described [3] using an AF488-labelled anti-HBsAg antibody (1044/329, Bio-Techne).

Supplemental References

1. Lucifora J, Salvetti A, Marniquet X, *et al.* Detection of the hepatitis B virus (HBV) covalently closed-circular DNA (cccDNA) in mice transduced with a recombinant AAV-HBV vector. *Antiviral Res* 2017;145:14-19
2. Schoggins JW, MacDuff DA, Imanaka N, *et al.* Pan-viral specificity of IFN-induced genes reveals new roles for cGAS in innate immunity. *Nature* 2014;505(7485):691-5.
3. Verrier ER, Colpitts CC, Bach C, *et al.* A targeted functional RNAi screen uncovers Glypican 5 as an entry factor for hepatitis B and D viruses. *Hepatology* 2016;63(1):35–48.

Multimodal study of the interactions between the hepatitis B virus and the cyclic GMP-AMP synthase cGAS

RESUME: Le virus de l'hépatite B (HBV) est l'agent étiologique de l'hépatite B. Ce virus est responsable d'hépatite chronique B, de cirrhose et de cancer du foie au niveau mondial. L'absence d'activation de la voie Interféron (IFN) suite à l'infection par HBV est encore mal comprise. Récemment, le senseur cellulaire cytosolique GMP-AMP synthase (cGAS) a été décrit comme un senseur efficace de DNA double brin possédant également une activité antivirale envers des virus à ADN et à ARN. Le but de mes travaux de thèse a été de contribuer à la compréhension des relations existants entre le HBV et cGAS, à des stades précoces et tardifs de l'infection HBV en utilisant des expériences de perte- et gain-de fonction ainsi que du profilage génomique des gènes apparentés à cGAS dans un modèle cellulaire permissif au HBV. Mes travaux ont démontré (1) que cGAS exerce une forte activité antivirale envers le HBV incluant une réduction de la forme nucléaire du génome, le cccDNA; (2) alors que le rcDNA génomique nu est reconnu par la voie cGAS/STING et induit une réponse IFN efficace, la nucléocapside virale protège le DNA génomique viral et l'empêche d'être détecté par la réponse immunitaire innée; et (3) que l'infection par HBV diminue l'expression des acteurs de la voie cGAS-STING et des gènes impliqués dans la réponse immunitaire innée in vitro et in vivo. Ce dernier point met en lumière le rôle de cGAS dans un nouveau mécanisme d'échappement du HBV au système immunitaire inné dans les cellules hépatocytaires et dans ce mécanisme.

Mots-Clés: Virus de l'hépatite B (HBV) - Réponse immunitaire innée- Cytosolic GMP-AMP synthase (cGAS) – échappement immunitaire

ABSTRACT: Chronic hepatitis B virus (HBV) infection is a major cause of liver disease and cancer worldwide. The mechanisms of viral genome sensing and the evasion of innate immune responses by HBV infection are still poorly understood. Recently, the cyclic GMP-AMP synthase (cGAS) was identified as a DNA sensor. In this PhD work, we aimed to investigate the functional role of cGAS in sensing of HBV infection and elucidate the mechanisms of viral evasion. We performed functional studies including loss- and gain-of-function experiments combined with cGAS effector gene expression profiling in an HBV infection-susceptible cell culture model. Collectively, our data show that (1) the cGAS-STING pathway exhibits robust antiviral activity against HBV infection including reduction of viral cccDNA levels; (2) naked HBV genomic rcDNA is sensed in a cGAS-dependent manner whereas packaging of the viral genome during infection abolishes host cell recognition of viral nucleic acids; (3) HBV infection down-regulates the cGAS/STING pathway actors as well as innate immune effector gene expression in vitro and vivo. Overall, this work led to describing new aspects of the complex interaction between HBV and the DNA sensor cGAS in hepatocytes.

Key words: Hepatitis B virus (HBV), innate immune response, cytosolic GMP-AMP synthase (cGAS), immune evasion

Key words: HBV, innate immune response, cytosolic GMP-AMP synthase (cGAS), immune evasion

